Structure-activity relationship studies of anti-diabetic dioxidovanadium(V) benzimidazole complexes

submitted in fulfilment of the requirements for the degree of

Master of Science

in the School of Chemistry and Physics
at the University of KwaZulu-Natal

by

Patrick Mangundu

2022

Supervisor: Professor Irvin N. Booysen

As the candidate's supervisor I have approved this dissertation for submission:

Signed: _____[redacted]_____ Date: 13/07/2022

Table of Contents

Chapter 3

Synthesis and characterization of novel vanadium(V) benzimidazole analogues

Chapter 4

An investigation into the binding interactions of the vanadium benzimidazole complexes with relevant biomolecules

Chapter 5

Conclusion and Future Work

Declaration 1 - Plagiarism

I, Patrick Mangundu, declare that:

i. The research reported in this dissertation, except where otherwise indicated, is my original research.
ii. This dissertation has not been submitted for any degree or examination at any other university.
iii. This dissertation does not contain other persons' data, pictures, graphs or other information, unless specifically acknowledged as being sourced from other persons.
iv. This dissertation does not contain other persons' writing, unless specifically acknowledged as being sourced from other researchers. Where other written sources have been quoted, then:
    a) Their words have been re-written, but the general information attributed to them has been referenced.
    b) Where their exact words have been used, then their writing has been placed in italics and inside quotation marks and referenced.
v. This thesis does not contain text, graphics or tables copied and pasted from the internet, unless specifically acknowledged, and the source being detailed in the thesis and in the References sections.

Signed: [redacted]…… (Patrick Mangundu) Date: 13/07/2022

Signed: …[redacted]…….. (Prof. Irvin N. Booysen) Date: 13/07/2022

Declaration 2 - Research output and author contributions

Manuscript published:
Mangundu, P., Maharaj, S., Veale, C.G. and Booysen, I.N., 2022. Synthesis, characterization, biomolecular interaction, and in vitro glucose metabolism studies of dioxidovanadium (V) benzimidazole compounds. Polyhedron, p.115992.

I conducted the synthetic and characterization work whose results are reported herein in the Inorganic chemistry research laboratory at UKZN's Pietermaritzburg campus. Furthermore, photoluminescence titrations between the respective metal complexes and Bovine Serum Albumin were conducted by myself. I performed the data processing under the guidance of Prof Booysen's postdoctoral fellow, Dr Sanam Maikoo.

Under the mentorship and guidance of Dr Shantal Maharaj and I have evaluated the *in vitro* PTP-1B inhibitory activities of the metal complexes using different assays. She is a postdoctoral fellow under the supervision of Dr. Clint Veale, whom is an internal collaborator to my supervisor in the school. Data processing of the results for the *in vitro* inhibitory studies was done solely by Dr Maharaj. Subsequently, she further guided me in the conduction of the direct binding affinity experiments of the most active metal complex towards the Protein Tyrosine Phosphatase (PTP) 1B enzyme using fluorescence spectroscopy. The aforementioned data was then processed and discussed by me and checked by my supervisor.

The experimental work, data processing and discussion of the *in vitro* glucose metabolism studies were conducted by Dr Maharaj.

Signed: [redacted] (Patrick Mangundu) Date: 13/07/2022

Signed: _[redacted] (Dr Shantal Maharaj) Date: 13/07/2022

Signed: _[redacted] (Prof Irvin Noel Booysen) Date: 13/07/2022

Foreword

Other researchers' contribution to the results of this thesis is limited to that of the Declaration 2 – Research output and author contributions. Furthermore, I have adhered to all protocols listed in the Declaration 1 – Plagiarism.

Acknowledgements

I would like to express my gratitude to Prof Irvin N. Booysen for his supervision and patience during my research project. I am grateful to the following senior technicians:

- Mr Leigh Andre Hunter for X-ray data collection and crystal structure refinements.
- Mr Craig Douglas Grimmer for NMR spectral data collection.
- Mrs Caryl Janse van Rensburg for gathering of mass spectroscopy and elemental analysis data.

In addition, I would like to acknowledge the moral and technical support from my current and former members of our research group, including Dr S. Maikoo, MD. Makanyane, D. Moodley, KB. Kantize, SB. Shoba, T. Mapapiro and V. Ngwenya. I am thankful to the National Research Foundation (NRF) for awarding me a grant-holder linked NRF bursary and to the School of Chemistry and Physics at the University of KwaZulu-Natal's Pietermaritzburg campus for allowing me to use their facilities and instrumentation. More importantly, I am indebted to the sacrifices of my loved ones for their unwavering support throughout my studies.

Abbreviations

DM, diabetes mellitus

STZ, Streptozotocin

GI, gastrointestinal

Hobz, 2-hydroxyphenyl-1*H*-benzimidazole

py, pyridine

Hpybz, 2-pyridylbenzimidazole

BSA, bovine serum albumin

CT-DNA, calf-thymus deoxyribonucleic acid

PTP-1B, protein tyrosine phosphatase

AMPK, monophosphate activated protein kinase

Dipic, dipicolinic acid

BMOV, *bis*(maltolato)oxovanadium(IV)

BEOV, *bis*(ethylmaltolato)oxovanadium(IV)

acac, acetylacetone

GQD, graphene quantum dots

NMR, nuclear magnetic resonance

FTIR, fourier-transform infrared spectroscopy

d^6-DMSO, deuterated dimethyl sulfoxide

ESI, electron spray ionization

DFT, density functional theory

PES, potential energy surface

THF, tetrahydrofuran

terpy, terpyridine

bipy, bipyridine

phen, phenanthroline

Abstract

Organovanadium compounds have been widely investigated for the potential use in Diabetes Mellitus. However, most of these metal complexes has failed during studies using *in vivo* Streptozotocin (STZ)-diabetic rat models and human clinical trials. For candidate vanadium-based insulin enhancing agents to meet the stringent demands of the United States of America's Federal Agency of Food and Drug Administration, these metal complexes should be benign to healthy cells, should pose a target-specific biodistribution as well as illustrate optimal and prolonged control of blood-glucose levels.

In the first experimental chapter, the synthesis and characterization of new derivatives of the metal-based drugs (*viz. cis*-[VO_2(Hpybz)(pybz)] (**1**) (Hpybz = 2-pyridyl-1*H*-benzimidazole) and *cis*-[VO_2(obz)py] (**2**) (Hobz = 2-hydroxyphenyl-1*H*-benzimidazole) is described and discussed. The novel and potential metal-based anti-diabetic drugs, *cis*-[VO_2(Hmpybz)(mpybz)] (**3**) and *cis*-[VO_2(mobz)py] (**4**) constitute a structure-activity relationship study. The metal complexes were characterized *via* various spectroscopic techniques, high resolution mass spectrometry and structural elucidations were confirmed using single crystal X-ray analysis and elemental analysis.

In the second experimental chapter, the CT-DNA UV/Visible absorption spectroscopic titration studies of **1 - 4** were conducted. The results revealed that these metal complexes exhibit low binding affinities with intrinsic binding constants (K_b) in the order 10^3 M^{-1}. BSA emission spectroscopic titrations showed high BSA apparent association constants and quenching constants (K_a and K_{SV}) > 10^6 M^{-1}. The binding strengths of the individual metal complexes onto one of the key enzyme, Protein Tyrosine Phosphatase (PTP)-1B which is involved in insulin production were evaluated using fluorescence emission spectroscopy. Affinities of the pro-drugs **1** and **2** as well as their analogues towards Protein Tyrosine Phosphatase were monitored

using various physicochemical techniques. The *in vitro* inhibitory activities of **1** and **4** were classed as non-significant since they afforded relatively low PTP-1B inhibitory activities relative to the untreated enzyme (*viz*. basal/control agent). Compounds **2** and **3** showed significant PTP-1B inhibition activity when compared to the basal. However, compound **3** exhibited the most significant lowering of the in *vitro* PTP-1B enzymatic activity with binding strength K_b of 3.9×10^3 M^{-1} and affinity constant K_{SV} = 9.0×10^4 M^{-1}. The glycolytic flux assays flux proved that compounds 2 and 3 inhibit the rate of glycolysis based on the rate of the lactate products. The glucose consumption assays also revealed that via the potential inhibition of PTP1B, the glucose turnover is increased in HEK293T cells.

Keywords: vanadium, benzimidazole, diabetes mellitus, bovine serum albumin, protein tyrosine phosphatase, glucose metabolism

Chapter 1

Introduction

1.1 General background

Vanadium was first discovered by Andreś Manuel del Ríoy Fernandez in Mexico during 1801. Later, it was rediscovered in 1930 by a Swedish scientist named Nils Gabriel Sefstrom as an oxide.[1, 2] After nearly a century in 1927, vanadium metal of 99,7% purity was finally obtained by Marden and Rich.[3]

Vanadium is a steel-grey and rare transition element. In nature, it exists mainly as the ^{51}V (99.8 %) nuclide while the radioactive ^{50}V constitutes the remainder. Being a transition metal element, it exhibits variable oxidation states in its compounds found in ores such as sandstone, magnetite-ilmenite deposits, sedimentary iron ores and phosphate rock.[4] Even in ores such as mafic rocks, shales and rock phosphate, it is found in relatively small concentrations, making it a rare element. Traces of vanadium are also found in plants and as a co-factor, enhancing or in inhibiting enzymatic activities in humans and animals.[5]

The metal is a steel-grey transition element and despite having Vanadium has a body-centred cubic crystal structure, but it has a relatively high melting point of 1 910 ^{o}C. It is *d*-block metal with a valence electron configuration of [Ar]3$d^3$4s^2. Therefore, it has a maximum oxidation of +V.[6] In addition, variable valency is apparent from the palette of colours generated by vanadium compounds in solution.[7] Solution chemistry of vanadium predominately occurs in the +IV and +V oxidation states where oligomerization often occur.

Six- or five-coordinated vanadium compounds can readily undergo conformational change by hydrolysis to render the vanadates.[8] It is well established that the vanadate ion can serve as an active drug to enhance insulin levels for anti-diabetic therapy but there are challenges and research gaps to be tackled and closed, respectively before vanadium-based pro-drugs can be used routinely as anti-diabetic therapies. Vanadium complexes have been used for general catalysis, electrochemical fuel cells and energy storage.[9, 10]

1.2 Aim and motivation

Organovanadium compounds have been widely investigated for the potential use in Diabetes Mellitus (DM). However, the majority of these metal complexes have failed to go past the *in vivo* Streptozotocin (STZ)-diabetic rat models and human clinical trials.[11, 12] For a candidate vanadium-based insulin enhancing agents to meet the stringent demands of the United States of America's Federal Agency of Food and Drug Administration, these metal complexes should be benign to healthy cells, should pose a target-specific biodistribution as well as illustrate optimal and prolonged control of blood-glucose at optimal levels.

The objective of this research work is to address the aforementioned challenges of an earlier generation of vanadium-based anti-diabetic compounds. In particular, to conduct a structure-activity relationship study of the anti-diabetic metal-based drugs, *cis*-[VO_2(obz)py] (**1**) and *cis*-[VO_2(Hpybz)(pybz)] (**2**) as well as their novel derivatives. In addition, to explore the biomolecular affinities of the aforementioned metal complexes towards Bovine Serum Albumin (BSA), Calf-Thymus deoxyribonucleic acid (CT-DNA) and Protein Tyrosine Phosphatase (PTP)-1B. Furthermore, to compare *in vitro* glucose metabolic activities of the parent metal complexes and their new analogues.

The rationale behind the use of the *cis*-$[VO_2]^+$ core stems from its high coordination susceptibilities to a variety of chelators.[13, 14] Generally, the six-coordinate diamagnetic vanadium(V) complexes are typically more thermodynamically stable due to their d^0 electronic configurations than their corresponding five-coordinate paramagnetic vanadium(IV) complexes with d^1 electronic configurations which allows for the manipulation of their pharmacokinetics.[15] Moreover, research studies by a previous member from our research group on the parent compound, *cis*-$[VO_2(Hpybz)(pybz)]$ (**1**) enhances glucose metabolism in liver and skeletal muscle cells while the other parent compound, *cis*-$[VO_2(obz)py]$ (**2**) demonstrated that it can reduce blood-glucose levels in Streptozotocin (STZ)-diabetic rats. This provided an impetus to undertake this work. Compounds **3** and **4**, were synthesized from methods adopted for the synthesis of **1** in chapter 3 and **2** in chapter 3, respectively.

The benzimidazole motif's medicinal relevance has become significant in the numerous commercially available benzimidazole used as proton-pump inhibitors for lowering acid production for patients suffering from stomach ulcers.[16, 17] Benzimidazole-derived compounds have been shown to induce various medicinal applications which are due to their conducive stereo-electronic properties that facilitates binding into active sites of different biological activities. These benzimidazole-biological target interactions can be stabilized by classical hydrogen-bonding or *pi-pi* stacking short contacts.[18, 19]

The inherent attributes of benzimidazoles make them attractive pharmacophores for the design of dioxovanadium(V) benzimidazole compounds. Among these benzimidazole-containing pharmaceuticals includes Lansoprazole and Albendazole which are used as a proton-pump inhibitor and a deworming agent, respectively, see **Fig**. 1.1.[20, 21] In fact, these benzimidazole-containing drugs have been repurposed in anti-diabetic therapy. In particular, they could indirectly affect the adenosine 5′-monophosphate activated protein kinase (AMPK) pathway which in turn potentiates the reduction of blood glucose levels.[21]

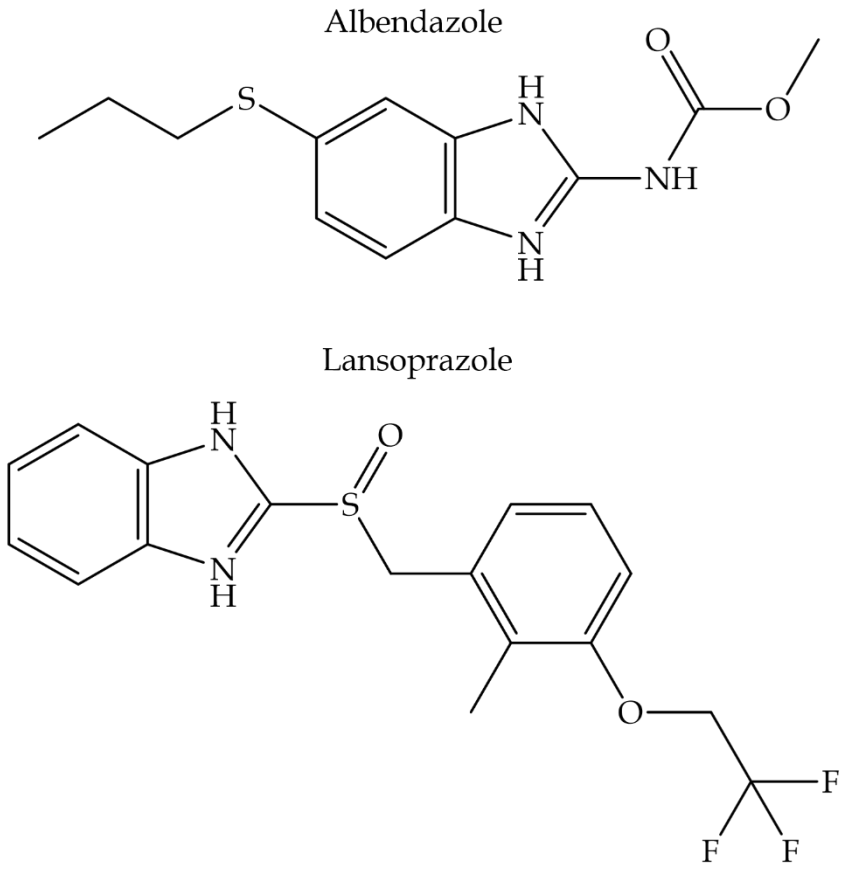

Figure 1.1: *Structures of selected benzimidazole-containing compounds which are used as anti-acid drugs and have shown to have anti-diabetic activities.*

1.3 Vanadium-based anti-diabetic agents

Serendipitous discovery of sodium metavanadate in the treatment of diabetes mellitus was in the late 1800s.[22] In particular, Lyonnet and his colleagues first reported the use of sodium metavanadate in phase 0 clinical trials where it was shown to slightly lower blood glucose levels.[23] The major setback in the use of metavanadate was the gastrointestinal intolerance which manifested in the form of vomiting, diarrhoea and desalivation as well as excessive hypoglycaemia. This led to its discontinued use which led to a permanent halt in the use of metavanadate.[24]

The pharmacological applications of vanadium compounds has evolved over the past century to include organovanadium derivatives some of which have that shown more therapeutic potential than the simple metal salts. Interestingly, a few of the later generation vanadium compounds were advanced to as far as Phase 1 clinical trials.[25] Several paramagnetic and diamagnetic vanadium derivatives of dipicolinic acid (H_2dipic) have shown diverse anti-diabetic profiles at the *in vivo* level, see **Fig**. 1.2.[26-28] The vanadium(V/IV) complexes of the ONO-H_2dipic chelator are used for the treatment of type II diabetes in cats.[29] Therefore, synergistic effects between this ligand and the vanadium(IV) and –(V) cores can lead to optimal hypoglyceamic activities in humans. Typically, mechanistic studies have shown that these metal complexes reacted with biological nucleophiles which may serve as intermediate reactive drugs.[30-32]

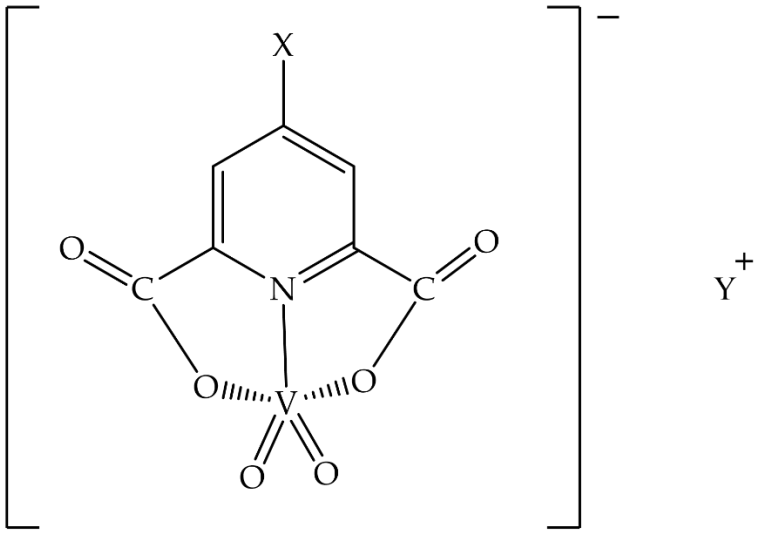

Figure 1.2: *Generic structure of the diamagnetic vanadium(V) dipicolinic acid compounds.*

The square bipyramidal vanadium(IV) compound, *bis*(maltolato)oxovanadium (BMOV) showed good efficacy *in vivo* response in STZ-diabetic rats, see **Fig**. 1.3.[33] However, GI tract discomfort led to the discontinued use of the compound, though it became the benchmark for drugs that were designed after it.[34] Subsequently, a more lipophilic analogue of BMOV was isolated and the resultant metal complex, *bis*-

(ethylmaltolato)oxovanadium(IV) (BEOV) completed phase I clinical trials where patients showed lower blood glucose levels. However, prolonged usage during phase IIA clinic trials led to renal complications in certain probands.[35] BEOV and BMOV are hypothesized to convert to vanadate which is the active specie that inhibits PTP-1B.[36] *Bis*(allixinate)oxovanadium(IV) compound showed a high *in vitro* insulin-mimetic activity after oral administrations and injections to mice suffering from type 1 diabetes, see **Fig**. 1.4.[37]

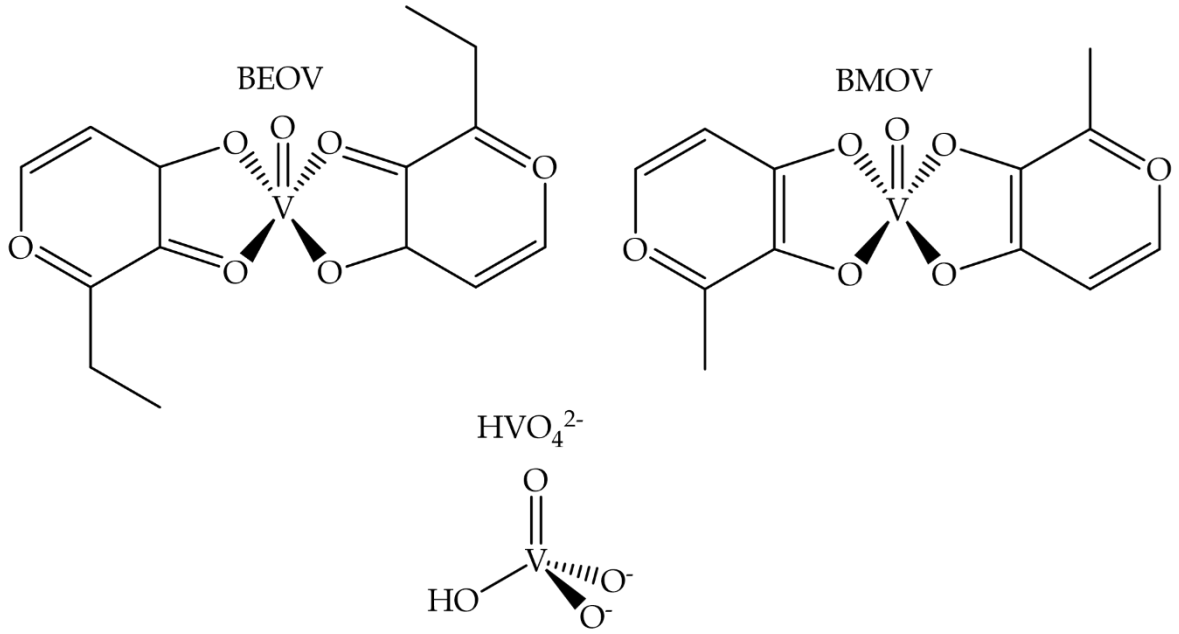

Figure 1.3: *Structures of bis(ethylmaltolato)oxovanadium(*IV*) (BEOV), bis(maltolato)oxovanadium(*IV*) (BMOV) and hydrogen vanadate that have been used as potential agents in diabetes therapy.*

This compound exhibited higher hypoglycaemic effect and residual time in tissues compared to the previous leading vanadium-based drug candidates, owing to its enhanced lipophilicity.[38] However, this vanadium(IV) compound caused disturbances in the GI tract optimal functions. In addition, identification of vanadium species in the stomach and bloodstream at the *in vivo* level, remains a major challenge to elucidate the mechanism of activity and to address inherent side effects of these drugs.[39] Current research studies have focused on the use of nanomaterial-based

platforms to ameliorate acute side effects.[40-42] One such compound GQD-PL1-V^V, where GQD (graphene quantum dots) and PL1 (PTP1B peptide mimic) has been explored and research findings showed that it enhanced anti-diabetic activity better than BMOV.[43]

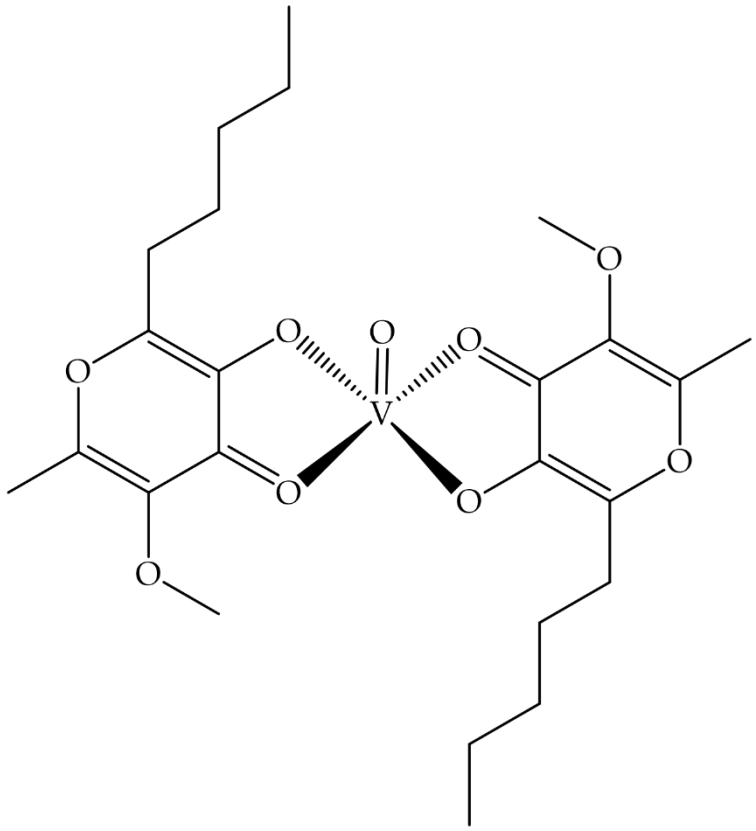

Figure 1.4: *Chemical structure of bis(allixinate)oxovanadium(IV).*

1.4 General chemistry of vanadium(V) species

1.4.1 Oxidation and reduction

Vanadium easily converts between oxidation states in the presence of atmospheric oxygen. In fact, its refinery via the salt roasting method makes use of aerial oxidation. In one process the insoluble slag containing traces of vanadium as V_2O_3 is oxidized into the water-soluble sodium metavanadate.[44] Another widely used extraction methods converts vanadium from vanadium-titanium magnetite concentrate by oxidising the magnetite to hematite and vanadium pentoxide.[45]

$$FeO(FeV)_2O_3 + O_2 \longrightarrow Fe_2O_3 + V_2O_5$$

Studies done on erythrocytes, fat cells and yeast have shown that under physiological conditions orthovanadate(V) is readily reduced to vanadyl(IV) ion, VO^{2+}.[46] However the VO^{2+} specie is only stable when coordinated to strong ligands under physiological conditions.

1.4.2 Disproportionation

Disproportionation of vanadium species has been noted in vanadium hexacarbonyl compounds in the presence of several oxygen and nitrogen Lewis bases.[47] However, the product of disproportionation varies with the type of Lewis base. For example, strong oxygen and nitrogen bases (py) affords $[V(py)_6]$, $[V(CO)_6]_2$ as the final product.[48]

$$3[V(CO)_6] + 6py \longrightarrow [V(py)_6]^{2+} + 2[V(CO)_6]^{-} + 6CO$$

1.4.3 Comproportionation

One classical example of comproportionation that occurs is the reaction between vanadium(III) and vanadium(V) to form vanadium(IV) see **Fig**. 1.5.[49]

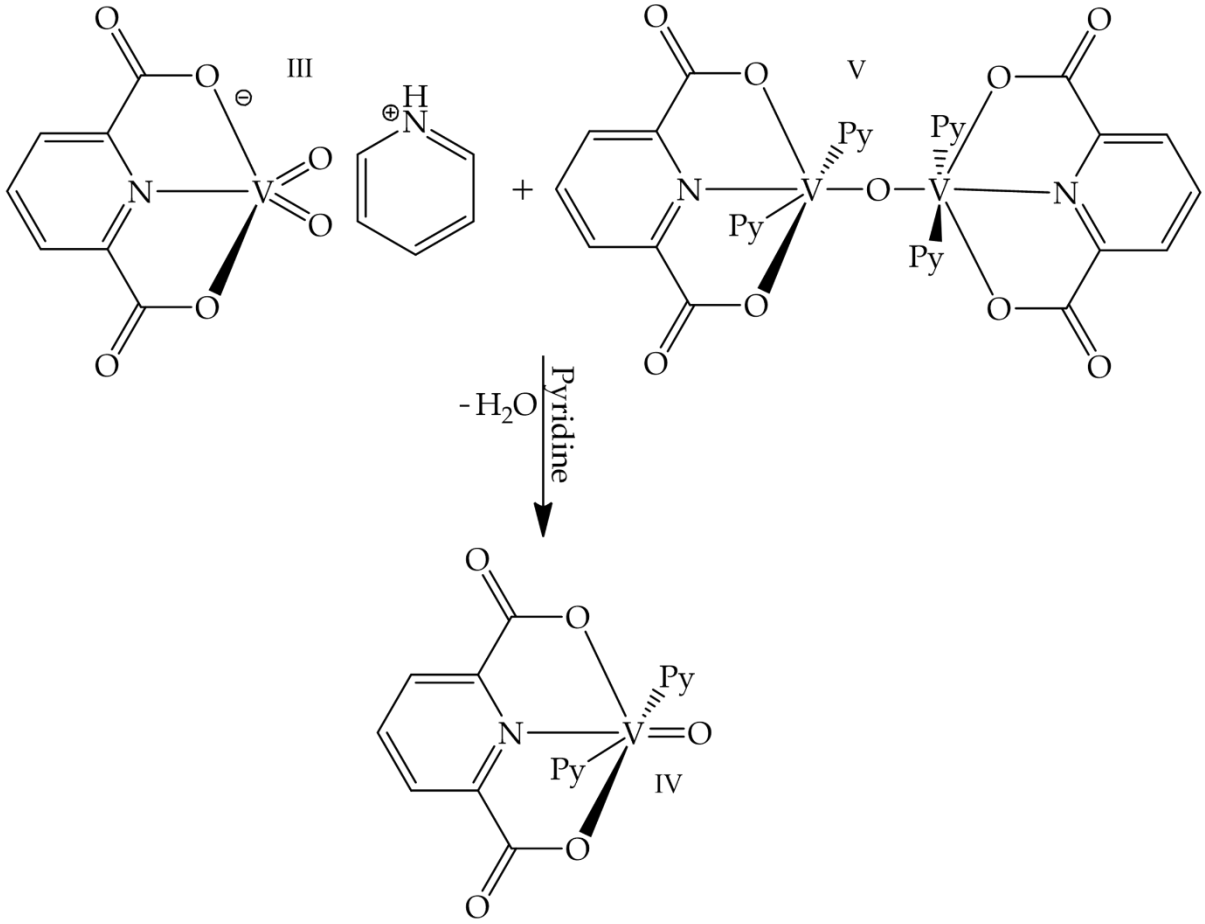

Figure 1.5: *Comproportionation reaction between vanadium(III) and vanadium(V) to form a vanadium(IV) compound.*

1.5 Coordination chemistry of vanadium(V)

The versatility of vanadium in its oxidation state of +V is portrayed in the diversity in the molecular geometries of its metal complexes. Also, the steric factors of the chelators can influence the molecular geometries of these diamagnetic metal compounds. Generally, charge neutrality of the *cis*-$[VO_2]^+$ core is attained through coordination to single mono-anionic chelators but dioxovanadium(V) complex salts are also known. The octahedral structures of *mono*-oxovanadium(V) complexes are typically reinforced by selected electronegative halides.[50]

1.5.1 Diamagnetic vanadium compounds with N, N-donor chelators

The bonding preference of vanadium(V) for neutral nitrogen donor atoms is illustrated by the following oxovanadium(V) compound: $[VO(OH)F_2(bipy)]$, where (terpy = 2,2′:6′,2″-terpyridine) and (bipy = 2,2′-bipyridyl).[51] $VOCl_3$ reacts with 1,10-phenanthroline (phen) to afford dark brown diamagnetic *mer*-$[VOCl_3(phen)]$ see **Fig**.1.6.[52] IR spectral data of these monomeric octahedral metal complexes exhibit characteristic dominant metal V=O bond vibrations at 968 and 973 cm^{-1}, respectively. Interestingly, high energy charge transfer bands originating from the oxo and halide co-ligands masked the low intensity metal based transitions.

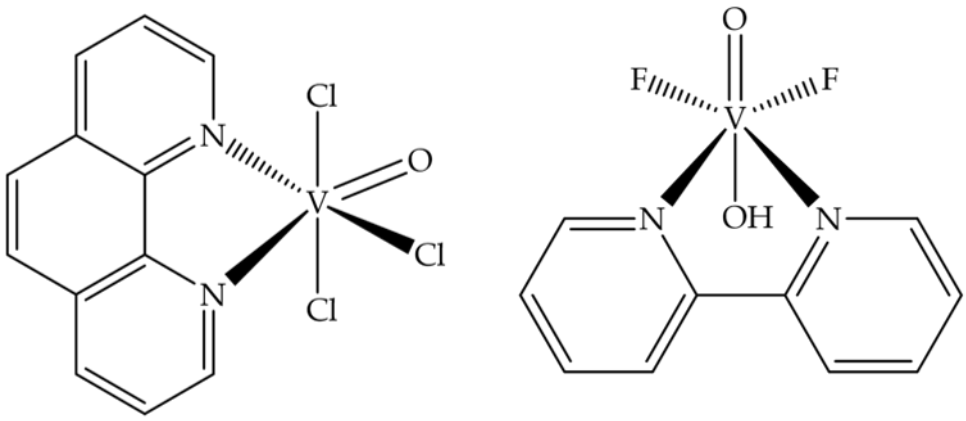

Figure 1.6: *Mono-oxovanadium(V) compounds with bidentate or tridentate pyridyl N-donor ligands.*

1.5.2 Vanadium compounds with benzimidazole-chelating ligands

Varying the stereo-electronic properties of benzimidazoles have led to vanadium complexes with diverse structural features. For instance, heterolyptic vanadium(IV) analogues, *cis*-$[VO(Hoa^{1/2})(bz)]$ (Hoa^1 = phenoxyacetohydroxamate, Hoa^2 = cinnamonhydroxamate and bz = benzimidazole) have displayed high cell viability in Hep2C cells which suggest that the metal complexes are essentially benign to living cells. These metal complexes show antifungal activities all be it moderate. This was

attributed to the free phenoxy and styrene groups enhancing their lipophilic characters and thereby promoting fungus cell permeability.[53]

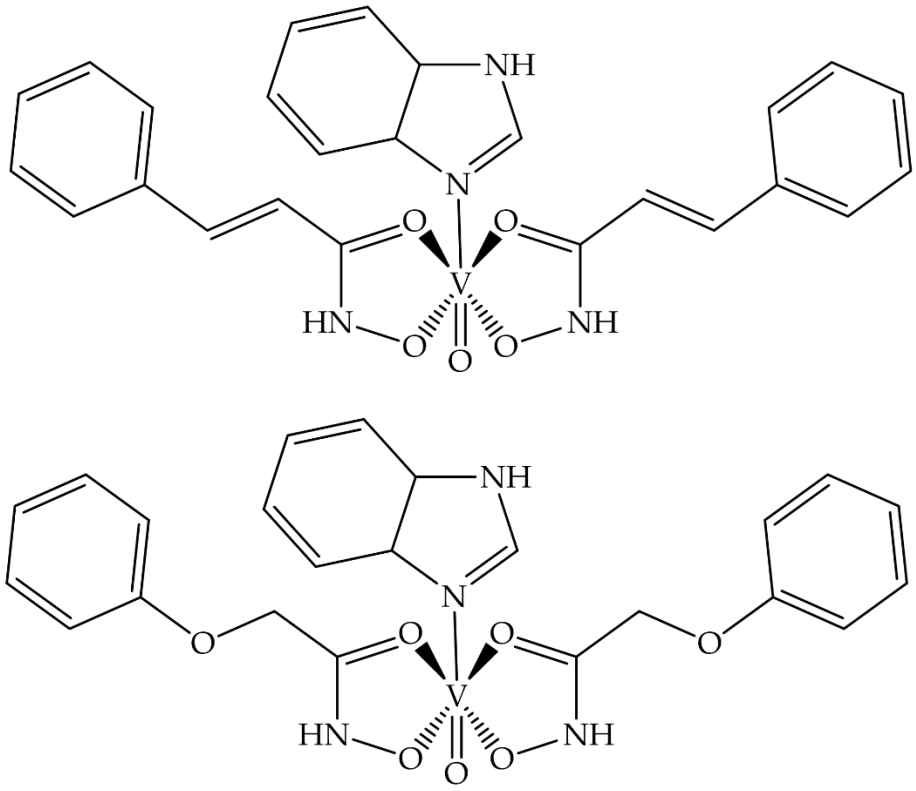

Figure 1.7: *Structures of heterolyptic oxovanadium(IV) benzimidazole compounds that have undergone antifungal studies.*

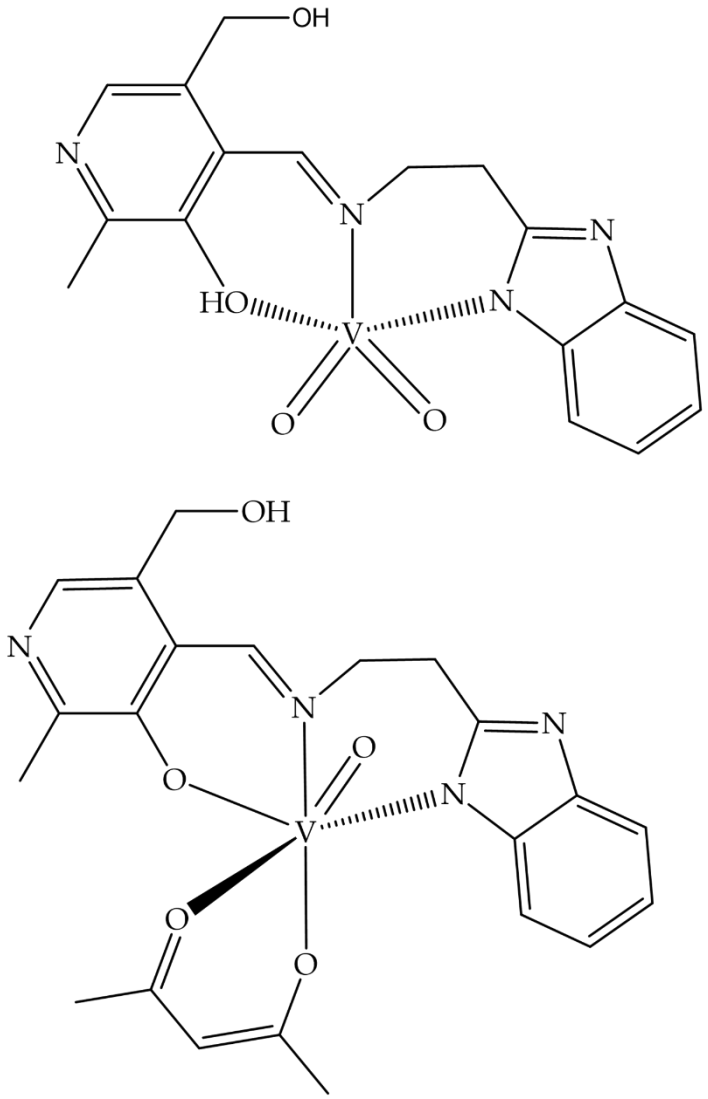

Figure 1.8: *Oxo and dioxovanadium compounds with benzimidazole Schiff base ligands.*

An ESR silent dioxovanadium(V) compound, *cis*-[VO_2(sal-aebmz)] (H-sal-aebmz = 4-(((2-(1*H*-benzimidazole)ethyl)imino)methyl)-5-(hydroxymethyl)-2-methylpyridin-3-ol) exhibited a singlet at -543 ppm, was synthesized from the paramagnetic vanadium(IV) compound, *cis*-[VO($ox_)$(sal-aebmz)] (H_2ox = oxalic acid). The oxidation reaction was catalyzed by the addition of potassium hydroxide. The aforementioned metal complex afforded an isotropic ESR spectrum in solution with a gauss value of 1.951.[54]

1.5.3 Stabilization of the cis-$[VO_2]^+$ core by other multidentate Schiff bases

The VO_2^+ motif has also showed unique coordination behaviour towards multidentate Schiff bases with variable donor atoms.[55, 56] This is illustrated in the reactivities of the nearly structurally identical pyridine-pyrimidine-pyrazole ligands *N*-[amino(pyridin-2-yl)methylidene]-5-methyl-1-(pyridin-2-yl)-1H-pyrazole-3-carbohydrazonic acid (PyPzOAP) and 1-(4,6-dimethylpyrimidin-2-yl)-5-methyl-N-[1-(pyridin-2-yl)ethylidene]-1H-pyrazole-3-carbohydrazide (PymPzCAP) which afforded mono and dinuclear oxovanadium compounds. Despite, the tridentate chelators having the same $N_{py\Lambda}O_{keto\Lambda}N_{amine}$ coordination mode, it is evident that the stereo electronic properties of the organic chelating ligands are different. The is also reflected in the emission properties of the ligands where PyPzOAP when excited at 280 emits at 377 nm while PymPzCAP shows no significant fluorescence emission.[56] The subtle differences in the stereo- electronic properties of the ligands is also reflected the differences in the emission properties of the cis-VO_2 complexes, $[VO_2Qx]$ (HQx = 4-bromo-6-[(2-phenylaminoethylimino)methyl]phenol) and $(\mu\text{-}O)_2[V(O)(Qy)]_2$ (HQy = 2-((2-(ethylamino)ethylimino)methyl)-4-chlorophenol) showed the same chemical reactivity as mentioned before. This was rationalised by DFT studies where the formation energy of the dimer in the mononuclear compound is -4.3 kcal mol^{-1} which is moderately smaller than the interaction energy (-3.7 kcal mol^{-1}) of the hydrogen bonded dimer of the dinuclear compound.[57]

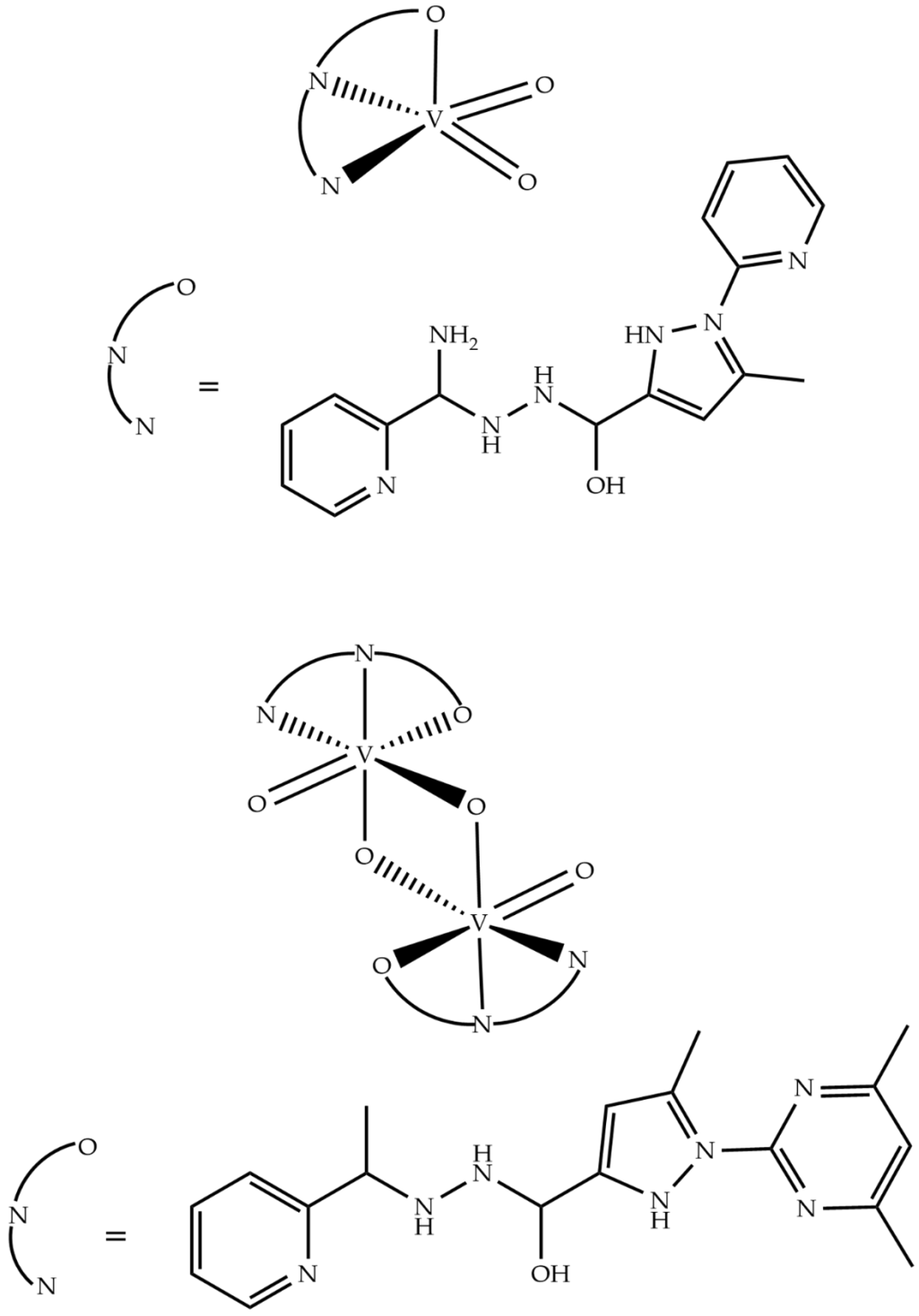

Figure 1.9: *Mono and dinuclear vanadium(V) compounds with fused N-heterocyclic rings.*

1.6 References

1. Rehder, D., The role of vanadium in biology. *Metallomics* **2015,** *7* (5), 730-742.
2. Del Carpio, E.; Hernández, L.; Ciangherotti, C.; Coa, V. V.; Jiménez, L.; Lubes, V.; Lubes, G., Vanadium: History, chemistry, interactions with α-amino acids and potential therapeutic applications. *Coordination Chemistry Reviews* **2018,** *372*, 117-140.
3. Gummow, B., Vanadium Mining and Cattle Health. **2005**.
4. Weeks, A. D., Mineralogy and geochemistry of vanadium in the Colorado Plateau. *Journal of the Less Common Metals* **1961,** *3* (6), 443-450.
5. Tripathi, D.; Mani, V.; Pal, R. P., Vanadium in biosphere and its role in biological processes. *Biological Trace Element Research* **2018,** *186* (1), 52-67.
6. Barceloux, D. G.; Barceloux, D., Vanadium. *Journal of Toxicology: Clinical Toxicology* **1999,** *37* (2), 265-278.
7. Morinville, A.; Maysinger, D.; Shaver, A., From Vanadis to Atropos: vanadium compounds as pharmacological tools in cell death signalling. *Trends in Pharmacological Sciences* **1998,** *19* (11), 452-460.
8. Rehder, D., Perspectives for vanadium in health issues. *Future Medicinal Chemistry* **2016,** *8* (3), 325-338.
9. Zhong, Y.; Xia, X.; Shi, F.; Zhan, J.; Tu, J.; Fan, H. J., Transition metal carbides and nitrides in energy storage and conversion. *Advanced Science* **2016,** *3* (5), 1500286.
10. Soloveichik, G. L., Regenerative fuel cells for energy storage. *Proceedings of the IEEE* **2014,** *102* (6), 964-975.
11. Willsky, G. R.; Chi, L.-H.; Godzala III, M.; Kostyniak, P. J.; Smee, J. J.; Trujillo, A. M.; Alfano, J. A.; Ding, W.; Hu, Z.; Crans, D. C., Anti-diabetic effects of a series of vanadium dipicolinate complexes in rats with streptozotocin-induced diabetes. *Coordination Chemistry Reviews* **2011,** *255* (19-20), 2258-2269.
12. Poucheret, P.; Verma, S.; Grynpas, M. D.; McNeill, J. H., Vanadium and diabetes. *Molecular and Cellular Biochemistry* **1998,** *188* (1), 73-80.
13. Maurya, M. R.; Haldar, C.; Kumar, A.; Kuznetsov, M. L.; Avecilla, F.; Costa Pessoa, J., Vanadium complexes having $[VO]^{2+}$, $[VO]^{3+}$ and $[VO_2]^{+}$ cores with hydrazones of 2,6-diformyl-4-methylphenol: synthesis, characterization, reactivity, and catalytic potential. *Dalton Trans* **2013,** *42* (33), 11941-62.
14. Mir, J.M., Maurya, R.C., Vishwakarma, P.K., Rajak, D.K., Malik, B.A., Jaget, P.S. and Bohre, P., 2017. Synthesis and Conjoint Experimental-DFT Characterization of Some Pyrazolone Functionalized Dioxovanadium(V) Schiff Base Complexes. J Theor Comput Sci, 4(152), p.3.
15. Niemann, A.; Bossek, U.; Haselhorst, G.; Wieghardt, K.; Nuber, B., Synthesis and characterization of six-coordinate nitrido complexes of vanadium(V), chromium (V), and manganese(V). Isolation of a dinuclear, mixed-valent μ-nitrido chromium (III)/chromium(V) species. *Inorganic Chemistry* **1996,** *35* (4), 906-915.
16. Peng, C. C.-H.; Tu, Y.-K.; Lee, G. Y.; Chang, R. H.-E.; Huang, Y.; Bukhari, K.; Tsai, Y.-C.; Fu, Y.; Huang, H.-K.; Munir, K. M., Effects of proton pump inhibitors on glycemic control and incident diabetes: A systematic review and meta-analysis. *The Journal of Clinical Endocrinology & Metabolism* **2021,** *106* (11), 3354-3366.
17. Zhang, H.-J.; Zhang, X.-H.; Liu, J.; Sun, L.-N.; Shen, Y.-W.; Zhou, C.; Zhang, H.-W.; Xie, L.-J.; Chen, J.; Liu, Y., Effects of genetic polymorphisms on the

pharmacokinetics and pharmacodynamics of proton pump inhibitors. *Pharmacological Research* **2020,** *152*, 104606.
18. Hernández-Romero, D.; Rosete-Luna, S.; López-Monteon, A.; Chávez-Piña, A.; Pérez-Hernández, N.; Marroquín-Flores, J.; Cruz-Navarro, A.; Pesado-Gómez, G.; Morales-Morales, D.; Colorado-Peralta, R., First-row transition metal compounds containing benzimidazole ligands: An overview of their anticancer and antitumor activity. *Coordination Chemistry Reviews* **2021,** *439*.
19. Babkov, D. A.; Zhukowskaya, O. N.; Borisov, A. V.; Babkova, V. A.; Sokolova, E. V.; Brigadirova, A. A.; Litvinov, R. A.; Kolodina, A. A.; Morkovnik, A. S.; Sochnev, V. S.; Borodkin, G. S.; Spasov, A. A., Towards multi-target antidiabetic agents: Discovery of biphenyl-benzimidazole conjugates as AMPK activators. *Bioorg Med Chem Lett* **2019,** *29* (17), 2443-2447.
20. Benchamana, A.; Mori, H.; MacDougald, O. A.; Soodvilai, S., Regulation of adipocyte differentiation and metabolism by lansoprazole. *Life Sciences* **2019,** *239*, 116897.
21. Dik, B.; Coşkun, D.; Bahçivan, E.; Üney, K., Potential antidiabetic activity of benzimidazole derivative albendazole and lansoprazole drugs in different doses in experimental type 2 diabetic rats. *Turkish Journal of Medical Sciences* **2021,** *51* (3), 1579-1586.
22. Goldfine, A. B.; Patti, M.-E.; Zuberi, L.; Goldstein, B. J.; LeBlanc, R.; Landaker, E. J.; Jiang, Z. Y.; Willsky, G. R.; Kahn, C. R., Metabolic effects of vanadyl sulfate in humans with non—insulin-dependent diabetes mellitus: in *vivo* and in *vitro* studies. *Metabolism* **2000,** *49* (3), 400-410.
23. Thompson, K. H.; Orvig, C., Vanadium in diabetes: 100 years from Phase 0 to Phase I. *Journal of Inorganic Biochemistry* **2006,** *100* (12), 1925-1935.
24. Scior, T.; Guevara-García, A.; Bernard, P.; Do, Q.-T.; Domeyer, D.; Laufer, S., Are vanadium compounds drugable? Structures and effects of antidiabetic vanadium compounds: a critical review. *Mini Reviews in Medicinal Chemistry* **2005,** *5* (11), 995-1008.
25. Crans, D. C.; Henry, L.; Cardiff, G.; Posner, B. I., Developing vanadium as an antidiabetic or anticancer drug: A clinical and historical perspective. *Met. Ions Life Sci* **2019,** *19*, 203-230.
26. Crans, D. C.; Mahroof-Tahir, M.; Johnson, M. D.; Wilkins, P. C.; Yang, L.; Robbins, K.; Johnson, A.; Alfano, J. A.; Godzala III, M. E.; Austin, L. T., Vanadium (IV) and vanadium (V) complexes of dipicolinic acid and derivatives. Synthesis, X-ray structure, solution state properties: and effects in rats with STZ-induced diabetes. *Inorganica Chimica Acta* **2003,** *356*, 365-378.
27. Celestine, M. J.; Bullock, J. L.; Boodram, S.; Rambaran, V. H.; Holder, A. A., Interesting properties of p-, d-, and f-block elements when coordinated with dipicolinic acid and its derivatives as ligands: their use as inorganic pharmaceuticals. *Reviews in Inorganic Chemistry* **2015,** *35* (2), 57-67.
28. Bergeron, A.; Kostenkova, K.; Selman, M. O.; Murakami, H. A.; Owens, E.; Haribabu, N.; Arulanandam, R.; Diallo, J.-S.; Crans, D. C., Enhancement of oncolytic virotherapy by vanadium(V) dipicolinates. *BioMetals* **2019,** *32*, 545-561.

29. Hernández, L.; Araujo, M. L.; Madden, W.; Del Carpio, E.; Lubes, V.; Lubes, G., Vanadium complexes with polypyridyl ligands: Speciation, structure and potential medicinal activity. *Journal of Inorganic Biochemistry* **2022**, 111712.
30. Sanna, D.; Buglyó, P.; Nagy, S.; Perdih, F.; Palomba, J.; Ugone, V.; Garribba, E., Interaction of Vanadium(V) complexes formed by picolinic and pyrazinecarboxylic acid derivatives with red blood cells. *Polyhedron* **2022,** *212*, 115590.
31. Mihajlović-Lalić, L. E.; Poljarević, J.; Grgurić-Šipka, S., Metal complexes with α-picolinic acid frameworks and their antitumor activity. *Inorganica Chimica Acta* **2021,** *527*, 120582.
32. Hakimi, M.; Kukovec, B. M.; Rezvaninezhad, M.; Schuh, E.; Mohr, F., Preparation, structural and spectroscopic characterization of vanadium (IV) and vanadium (V) complexes with dipicolinic acid. *Zeitschrift für Anorganische Und allgemeine Chemie* **2011,** *637* (14-15), 2157-2162.
33. Thompson, K. H.; Lichter, J.; LeBel, C.; Scaife, M. C.; McNeill, J. H.; Orvig, C., Vanadium treatment of type 2 diabetes: a view to the future. *Journal of Inorganic Biochemistry* **2009,** *103* (4), 554-558.
34. Thompson, K. H.; Orvig, C., Design of vanadium compounds as insulin enhancing agents. *Journal of the Chemical Society, Dalton Transactions* **2000,** (17), 2885-2892.
35. Jakusch, T.; Kiss, T., In *vitro* study of the antidiabetic behavior of vanadium compounds. *Coordination Chemistry Reviews* **2017,** *351*, 118-126.
36. Bordbar, A.-K.; Creagh, A. L.; Mohammadi, F.; Haynes, C. A.; Orvig, C., Calorimetric studies of the interaction between the insulin-enhancing drug candidate bis (maltolato) oxovanadium(IV)(BMOV) and human serum apo-transferrin. *Journal of Inorganic Biochemistry* **2009,** *103* (4), 643-647.
37. Treviño, S.; Díaz, A.; Sánchez-Lara, E.; Sanchez-Gaytan, B. L.; Perez-Aguilar, J. M.; González-Vergara, E., Vanadium in biological action: chemical, pharmacological aspects, and metabolic implications in diabetes mellitus. *Biological Trace Element Research* **2019,** *188* (1), 68-98.
38. Adachi, Y.; Yoshida, J.; Kodera, Y.; Katoh, A.; Takada, J.; Sakurai, H., Bis (allixinato) oxovanadium(IV) complex is a potent antidiabetic agent: studies on structure− activity relationship for a series of hydroxypyrone− vanadium complexes. *Journal of Medicinal Chemistry* **2006,** *49* (11), 3251-3256.
39. Niu, X.; Xiao, R.; Wang, N.; Wang, Z.; Zhang, Y.; Xia, Q.; Yang, X., The molecular mechanisms and rational design of anti-diabetic vanadium compounds. *Current Topics in Medicinal Chemistry* **2016,** *16* (8), 811-822.
40. Huang, L.; Zhu, W.; Zhang, W.; Chen, K.; Wang, J.; Wang, R.; Yang, Q.; Hu, N.; Suo, Y.; Wang, J., Layered vanadium(IV) disulfide nanosheets as a peroxidase-like nanozyme for colorimetric detection of glucose. *Microchimica Acta* **2018,** *185* (1), 1-8.
41. Rauf, S.; Hayat Nawaz, M. A.; Badea, M.; Marty, J. L.; Hayat, A., Nano-engineered biomimetic optical sensors for glucose monitoring in diabetes. *Sensors* **2016,** *16* (11), 1931.
42. Liu, Y.; Zeng, S.; Ji, W.; Yao, H.; Lin, L.; Cui, H.; Santos, H. A.; Pan, G., Emerging Theranostic Nanomaterials in Diabetes and Its Complications. *Advanced Science* **2022,** *9* (3), 2102466.

43. Feng, B.; Dong, Y.; Shang, B.; Zhang, B.; Crans, D. C.; Yang, X., Convergent Protein Phosphatase Inhibitor Design for PTP1B and TCPTP: Exchangeable Vanadium Coordination Complexes on Graphene Quantum Dots. *Advanced Functional Materials* **2022,** *32* (5), 2108645.
44. Wang, Z.-h.; Zheng, S.-l.; Wang, S.-n.; Biao, L.; Wang, D.-w.; Hao, D.; Zhang, Y., Research and prospect on extraction of vanadium from vanadium slag by liquid oxidation technologies. *Transactions of Nonferrous Metals Society of China* **2014,** *24* (5), 1273-1288.
45. Li, R.; Liu, T.; Zhang, Y.; Huang, J.; Xu, C., Efficient extraction of vanadium from vanadium–Titanium magnetite concentrate by potassium salt roasting additives. *Minerals* **2018,** *8* (1), 25.
46. Chasteen, N. D.; Grady, J. K.; Holloway, C. E., Characterization of the binding, kinetics, and redox stability of vanadium(IV) and vanadium(V) protein complexes in serum. *Inorganic Chemistry* **1986,** *25* (16), 2754-2760.
47. Richmond, T. G.; Shi, Q.-Z.; Trogler, W. C.; Basolo, F., Mechanism of Lewis base induced disproportionation of vanadium hexacarbonyl. *Journal of the Chemical Society, Chemical Communications* **1983,** (12), 650-652.
48. Richmond, T. G.; Shi, Q. Z.; Trogler, W. C.; Basolo, F., Kinetics and mechanism of Lewis-base-induced disproportionation of vanadium hexacarbonyl and its phosphine-substituted derivatives. *Journal of the American Chemical Society* **1984,** *106* (1), 76-80.
49. Langeslay, R. R.; Kaphan, D. M.; Marshall, C. L.; Stair, P. C.; Sattelberger, A. P.; Delferro, M., Catalytic applications of vanadium: a mechanistic perspective. *Chemical Reviews* **2018,** *119* (4), 2128-2191.
50. Thompson, K. H.; Orvig, C., Coordination chemistry of vanadium in metallopharmaceutical candidate compounds. *Coordination Chemistry Reviews* **2001,** *219*, 1033-1053.
51. Chang, Y.-P.; Furness, L.; Levason, W.; Reid, G.; Zhang, W., Complexes of vanadium (IV) oxide difluoride with neutral N-and O-donor ligands. *Journal of Fluorine Chemistry* **2016,** *191*, 149-160.
52. Beard, C. D.; Barrie, R. J.; Evans, J.; Levason, W.; Reid, G.; Spicer, M. D., Synthesis and Properties of Complexes of Vanadium(V) Oxide Trichloride with Nitrogen-and Oxygen-Donor Ligands. Wiley Online Library: 2006.
53. Hernández-Romero, D.; Rosete-Luna, S.; López-Monteon, A.; Chávez-Piña, A.; Pérez-Hernández, N.; Marroquín-Flores, J.; Cruz-Navarro, A.; Pesado-Gómez, G.; Morales-Morales, D.; Colorado-Peralta, R., First-row transition metal compounds containing benzimidazole ligands: An overview of their anticancer and antitumor activity. *Coordination Chemistry Reviews* **2021,** *439*, 213930.
54. Maurya, M. R.; Bisht, M.; Kumar, A.; Kuznetsov, M. L.; Avecilla, F.; Pessoa, J. C., Synthesis, characterization, reactivity and catalytic activity of oxidovanadium (IV), oxidovanadium(V) and dioxidovanadium(V) complexes of benzimidazole modified ligands. *Dalton Transactions* **2011,** *40* (26), 6968-6983.
55. Sumrra, S. H.; Ibrahim, M.; Ambreen, S.; Imran, M.; Danish, M.; Rehmani, F. S., Synthesis, spectral characterization, and biological evaluation of transition metal complexes of bidentate N, O donor Schiff bases. *Bioinorganic Chemistry and Applications* **2014,** *2014*.

56. Mandal, T. N.; Roy, S.; Gupta, S.; Paul, B. K.; Butcher, R. J.; Rheingold, A. L.; Kar, S. K., Syntheses, characterization, X-ray crystal structures and emission properties of five oxovanadium(V) complexes with pyridyl/pyrimidyl–pyrazole derived ditopic ligands. *Polyhedron* **2011,** *30* (9), 1595-1603.
57. Thakur, S.; Drew, M. G.; Franconetti, A.; Frontera, A.; Chattopadhyay, S., Analysis of energies of halogen and hydrogen bonding interactions in the solid state structures of vanadyl Schiff base complexes. *RSC Advances* **2019,** *9* (9), 4789-4796.

Chapter 2

Experimental

2.1 Handling of vanadium

All undertaken reactions were done in the fume hood and the standard laboratory procedures and precautions on the proper handling of reagents, solvents and glassware were observed at all times. This included the handling of the vanadium precursors, the syntheses of the dioxovanadium(V) complexes up to their characterization. Exposure to the vapours of vanadium metal salts its coordination compounds can lead to adverse health problems or death.[1, 2]

2.2 Materials

2.2.1 Metal precursor

Ammonium metavanadate (NH_4VO_3) of 98% purity was purchased from Sigma-Aldrich and was used without any further purification.

2.2.2 Ligands

Organic chemicals listed below in **Table 2.1** were procured from Sigma-Aldrich and used without further purification. High purity analytical grade solvents and other common laboratory chemicals were used without further modification.

Table 2.1: *List of chemicals attained from Sigma-Aldrich.*

Name	**Purity**
2-(pyridyl)-1*H*-benzimidazole (Hpybz)	97%
2-hydroxyphenyl-1*H*-benzimidazole (Hobz)	95%
4-methyl-2-pyridyl-1*H*-benzimidazole (Hmpybz)	99%
2-(5, 6-dimethyl-2-benzimidazolyl)phenol (mobz)	99%

2.2.3 Synthesis of selected vanadium compounds

The metal compounds *cis*-[VO_2(Hpybz)(pybz)] (**1**) and *cis*-[VO_2(obz)py] (**2**) were synthesized according to a previously reported method. The purities of these dioxidovanadium(V) compounds were confirmed by various physicochemical techniques eg nuclear magnetic resonance (NMR) and mass spectroscopy.

2.3. Instrumentation

2.3.1. Conventional

An Agilent Cary 630 spectrometer controlled via the Agilent Microlab PC 5.1.22 and the accompanying Resolution Pro 5.0.0.395 software was used to collect and process the FTIR (Fourier-transform infrared spectroscopy) data. The data was collected using ATR Diamond-1 Bounce with 30 background scans and 30 sampling scans in the range 4000 – 650 cm^{-1} with a resolution of 4 cm^{-1}. Nuclear Magnetic Resonance (NMR) spectroscopy was done using a Varian 500 MHz spectrometer. Both the free ligands and their corresponding metal complexes were dissolved in deuterated dimethyl sulfoxide (d^6-DMSO) before being run on the instrument. The melting points were obtained using a Stuart SMP3 machine. The electronic properties of the metal complexes were explored using an Agilent Cary 60 UV-Vis Spectrophotometer. The compounds' mass spectra were collected by the direct injection of the samples into a Shimadzu LCMS-2020 analyser with an Electron Spray Ionization (ESI) source and done in the positive and negative modes. A Thermo Scientific Flash 2000 Organic Elemental CHNS-O Analyser was used to determine the elemental composition of the metal complexes. The ELGA PURELAB Ultra was used to purify the ultrapure water (to have a resistivity of 18.2 MΩ cm^{-1}) which was used for the laboratory work. The SpectraMax ABS Plus microplate reader was used for all the plate reading experiments.

2.3.2 X-ray crystallography

Crystallographic data of the novel metal complexes was collected using a Bruker APEX-II CCD diffractometer which has an Oxford Instruments Cryojet at 101 K and Inocoatec Cu Kα (λ = 1.54178 Å) radiation. This instrument was operated at 30 W and a crystal-to-detector distance of 40 mm. In addition, 0.50^{o} frame widths were applied using APEX2.[3] The program SAINT was utilised to reduce the data using outlier rejection, scan speed scaling, as well as standard Lorentz and polarization correction factors. A SADABS semi-empirical multi-scan absorption correction was applied to the data.[4] All structures were solved *via* direct methods, SHELX and WinGX.[5, 6]

2.4 References

1. Ghosh, S. K.; Saha, R.; Saha, B., Toxicity of inorganic vanadium compounds. *Research on Chemical Intermediates* **2015,** *41* (7), 4873-4897.
2. Fatola, O. I.; Olaolorun, F. A.; Olopade, F. E.; Olopade, J. O., Trends in vanadium neurotoxicity. *Brain Research Bulletin* **2019,** *145*, 75-80.
3. APEX, B., SAINT and SADABS Bruker AXS Inc. *Madison, WI, USA* **2009**.
4. Blessing, R. H., An empirical correction for absorption anisotropy. *Acta Crystallographica Section A: Foundations of Crystallography* **1995,** *51* (1), 33-38.
5. Farrugia, L. J., WinGX and ORTEP for Windows: an update. *Journal of Applied Crystallography* **2012,** *45* (4), 849-854.
6. Sheldrick, G. M., A short history of SHELX. *Acta Crystallographica Section A: Foundations of Crystallography* **2008,** *64* (1), 112-122.

Chapter 3

Synthesis and characterization of novel vanadium(V) benzimidazole analogues

3.1 Introduction

The interest in developing new metal-based anti-diabetic compounds has grown exponentially due to the optimal insulin mimetic activities of a diverse spectrum of vanadium compounds.[1, 2] Vanadium compounds portray affinities to different biological targets synonymous with diabetes pathogenesis, including phosphatases and enzymes involved in gluconeogenesis. In particular, vanadium precursor and active drugs can serve as cofactors which bind to the aforementioned biological targets and in the process may lead to inhibiting of key enzymes.[3, 4] One such example is where organovanadium compounds can undergo bioconversion to an active specie, vanadate which mimics the stereo-electronic features of phosphate and thus can inhibit the phosphorylation of protein tyrosine phosphatase (PTP). Subsequently, the blood glucose levels are regulated due to the preservation of insulin.[5, 6]

However, there are several key requirements that a vanadium-based anti-diabetic drug must meet before it can be widely administered. Firstly, the metallo-drug must be compatible with oral administration in contrast to methods such as the uncomfortable insulin injections and the associated requirement for regular blood glucose monitoring. In addition, the potential metallopharmaceutical must be chemically stable under the acidic conditions of the gastrointestinal (GI) tract, diffuse actively or otherwise through the lipophilic GI membrane into the bloodstream where it is biotransformed to the vanadate ion.[7, 8]

The design strategy entailed the isolation of dioxovanadium(V) coordination compounds containing benzimidazole ligands. The rationale for including benzimidazole chelators into the coordination spheres of dioxovanadium(V)

compounds was to render robustness at the low pH values of the GI tract. The coordination of the strong N, N benzimidazole based ligands (bidentate chelates) to the VO_2^{2+} core was meant to provide the chemical stabilization required to present the pharmaceuticals in a less reactive form than the metavanadate anion in the acidic GI, and also to facilitate their absorption into the blood stream via the lipophilic cell membranes of the epithelial cells of the GI.[9, 10]

Recent studies have illustrated that the vanadium heterocyclic complexes: cis-[VO2(Hpybz)(pybz)] (**1**) {Hpybz = 2-pyridylbenzimidazole} and *cis*-[VO_2(obz)py] (**2**) {Hobz = 2-hydroxyphenyl-1*H*-benzimidazole and py = pyridine} exhibited optimal hepato-, cardioprotective and haematitic effects accompanied with negligible cytotoxicity.[11, 12] Similarly, derivatives of **1** including the binuclear (*μ*-O)[VO(Hpybz)(pybz).VO(Hpybz)(acac)] and monomeric [$VO(Hpbyz)_2SO_4$].H_2O showed hypoglycaemic effects in Chang and C2C12 cell lines.[13, 14] These research findings provide the impetus to trends in the affinities and activity of dioxovanadium(V) as their microstructures were changed.

3.2 Experimental

*3.2.1 Synthesis of cis-[VO_2(Hmpybz)(mpybz)] (**3**), {Hmpybz = 2-(4-methyl-2-pyridyl-1H) -benzimidazole}*

A solution of 0.100 g of NH_4VO_3 (0.855 mmol) in 5 cm^3 of ultrapure water was added to 0.389 g of 2-(4-methyl-2-pyridyl-1*H*-benzimidazole) (Hmpybz) (1.86 mmol) in 20 cm^3 of pyridine. Thereafter, the reaction mixture was heated to reflux for 6 hours. The precipitate was filtered and dried under vacuum. Afterwards, the precipitate was dissolved in a pyridine:THF (7:3, *v:v*) mixture and the solution was layered with hexane. From the slow diffusion of hexane into the solvent mixture, yellow needles grew which were suitable for single crystal X-ray analysis. Yield = 67 %, m.p. = 225.9 – 231.8 °C. IR(ν_{max}/cm^{-1}): ν(N-H) 3048 w; ν(C=N) 1615 s; ν(*cis-*$[VO_2]^+$) 881 vs br. ^{1}H NMR (δ, ppm) 13.00 (br, s, 1H, *N5H*); 8.59 (d, 1H, *H6*); 8.20 (s, 1H, *H14*); 8.10 (s, 2H, *H4*, *H13)*; 7.89 (d, 2H, *H3*, *H12*); 7.80 (d, 2H, *H2*, *H11*); 7.22 (dd, 2H, *H9*, *H17*); 7.07 (d, 2H, *H7*, *H15*); 6.88 (d, 2H, *H8*, *H16*); 2.33 (s, 6H, *H1*, *H10*). ^{51}V NMR (δ, ppm) -589. UV-Vis (DMSO, (λ_{max} (ε, $M^{-1}cm^{-1}$))): 324 nm (3800, sh), 310 nm (4910), 299 nm (4340, sh). MS ESI$^+$ TOF (*m/z*): Calcd. for $C_{26}H_{25}N_6O_4V$: 500.43, Found: 501.13 $[M+H]^+$, 502,13 $[M+2H]^+$. $]^+$. Anal. Calcd. for $C_{26}H_{25}N_6O_4V$ (%): C, 58.21; H, 4.70; N, 15.67. Found: C, 58.08; H, 3.38; N, 15.38.

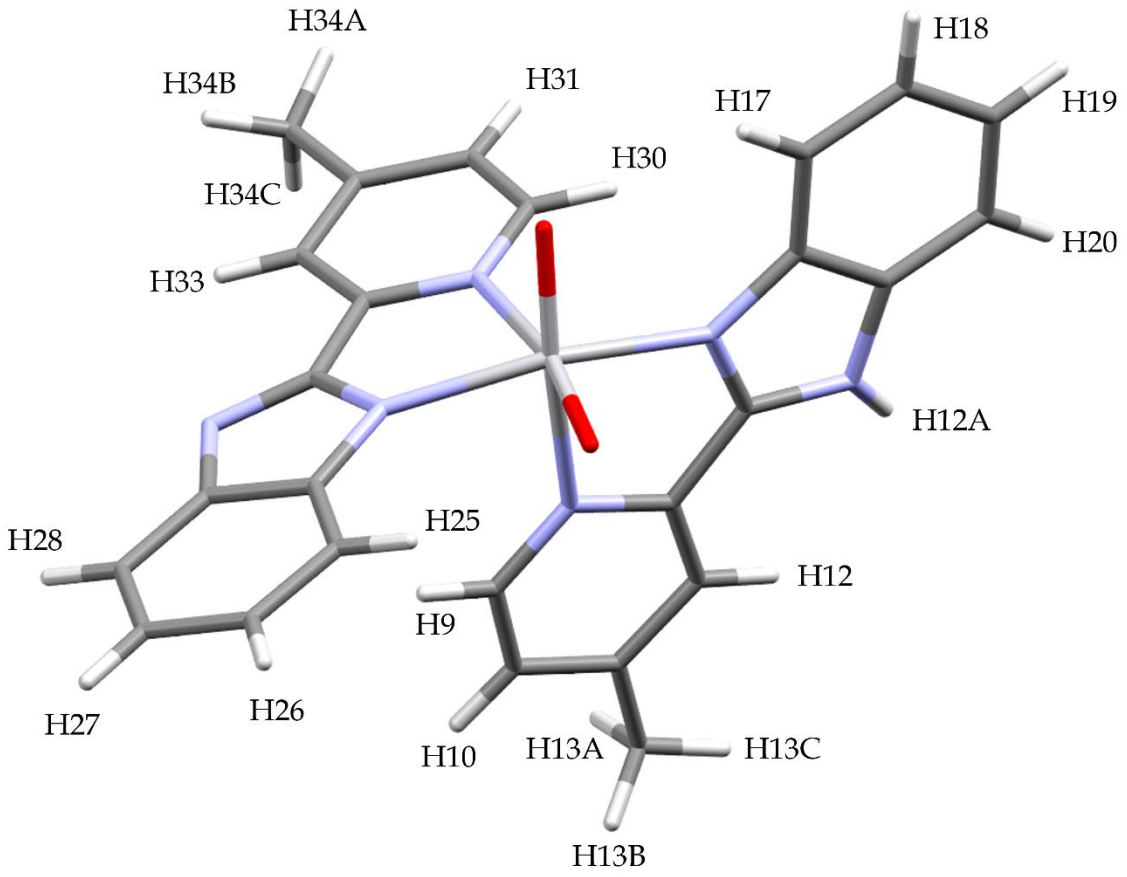

Figure 3.1: *Proton numbering scheme of* ***3.***

*3.2.2 Synthesis of cis-[VO_2(mobz)py] (**4**), {mobz = 2-(5,6-dimethyl-2-benzimidazolyl)phenol}*

An equimolar reaction of NH_4VO_3 (0.100 g, 0.86 mmol) in 5 cm^3 of ultrapure water with 2-(5,6-dimethyl-2-benzimidazolyl)phenol (0.389 g, 1.63 mmol) in 20 cm^3 of pyridine was performed by heating the aforementioned solution until reflux for 12 hours. Subsequently, the reaction mixture was cooled to room temperature and a yellow precipitate was collected by vacuum filtration. Similarly, the precipitate was dissolved in the pyridine:THF (7:3, *v:v*) mixture followed by layering with hexane. From the slow diffusion of hexane into the solvent mixture, yellow needles were grown that were suitable for single crystal X-ray analysis. Yield = 80 %, m.p. = 132.4 – 133.8 °C. IR(ν_{max}/cm^{-1}): ν(N-H) 3196 w; ν(C=N) 1643 w; ν(*cis-*$[VO_2]^+$) 915 s. ^{1}H NMR (δ, ppm) 13.26 (br, s, 1H, *N5H*); 8.58 (d, 2H, *H10*, *H14*); 8.29 (s, 1H, *H4*); 8.04 (dd, 1H, *H9*); 7.79 (t, 1H, *H8*); 7.40 (m, 3H, *H11*, *H12*, *H13*); 7.32 (s, 1H, *H3*); 7.03 (d, 1H, *H6*); 6.91

(t, 1H, *H7*); 2.42 (s, 3H, *H1*); 2.37 (s, 3H, *H2*). ^{51}V NMR (δ, ppm) -513. UV-Vis (DMSO, (λ_{max} (ε, $M^{-1}cm^{-1}$))): 324 nm (4770), 310 nm (6160), 299 nm (5540). MS ESI+ TOF (m/z): Calcd. for $C_{20}H_{18}N_3O_3V$: 399.08, Found: 320.03 [M-C_5H_5N-H]-. Anal. Calcd. for $C_{20}H_{18}N_3O_3V$ (%): C, 60.16; H, 4.54; N, 10.52. Found: C, 59.39; H, 3.29; N, 10.45.

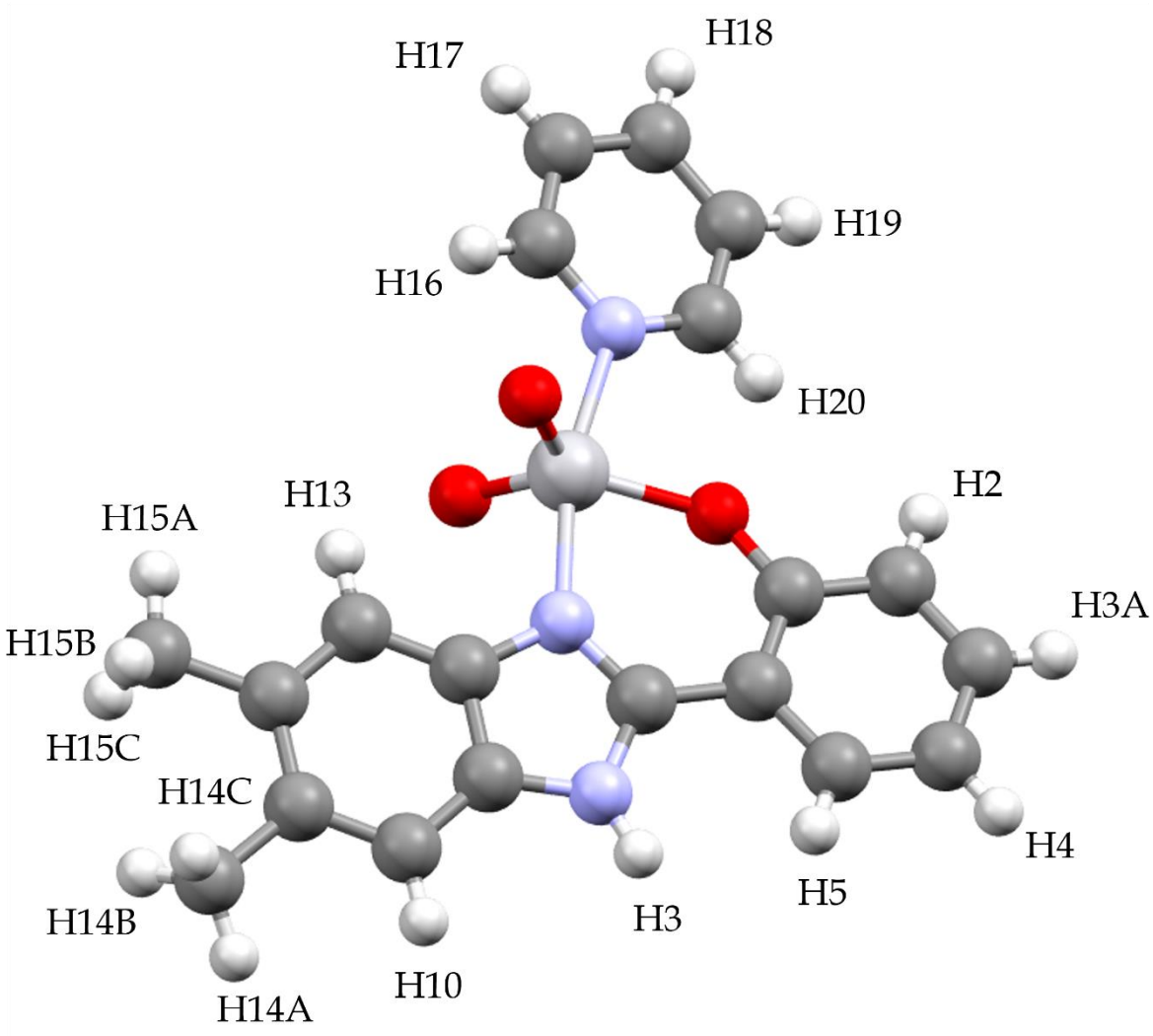

Figure 3.2: *Proton numbering scheme of* ***4****.*

3.3 Results and discussion

3.3.1 Synthesis and spectral characterization

The dioxidovanadium(V) compounds, *cis*-[VO_2(Hpybz)(pybz)] (**1**) and *cis*-[VO_2(obz)py] (**2**) and were successfully resynthesized and purified and the latter has been confirmed by various physicochemical techniques. As per the design strategy, the synthetic procedures of **1** and **2** were adopted to isolate **3** and **4**, respectively. Equimolar coordination reactions between ammonium metavanadate and Hmpybz, and mobz in a hot methanol/water mixture (volume:volume ratio = 1:1), yielded the yellow distorted octahedral dioxidovanadium(V) complexes: *cis*-[VO_2(Hmpybz)(mpybz)] (**3**) and distorted trigonal bi-pyramidal *cis*-[VO_2(mobz)py] (**4**), respectively. The same coordination mode has been adopted by other heterocyclic chelators towards the acidic dioxovanadium(V) core.[15-17]

Spectroscopic characterization data provided insight into the structural features of the respective metal compounds. In particular, the solid-state infrared spectra revealed common common strong absorption bands appearing at 881 cm-1 and 915 cm-1 for **3** and **4**, respectively, see **Figs**. 3.3 and 3.4. The respective vibrations are attributed to the vibration of the C=O bonds of the *cis-*$[VO_2]^+$.[18, 19] The amide bonds of the free-ligand, Hmpybz and its corresponding chelated form in **3** (3048 cm^{-1}) stretches essentially at the same stretching frequency, while there is only one broad band for **3** within the range new broad and medium intensity vibrational band appears at 3334 cm^{-1} (in **3**) which is ascribed to the bending mode of the N-H bond. In the case of **4**, a high energy is required to vibrate the N-H bond of the mobz chelator compared to its free ligand. The υ(C=N) bonds of **3** vibrate at the same frequencies as the corresponding signals of the free ligand while the pyridyl (at 1567 cm^{-1}) and benzimidazolium (at 1647 cm^{-1}) vibrational bands are found at different positions in the IR spectrum of **4**.

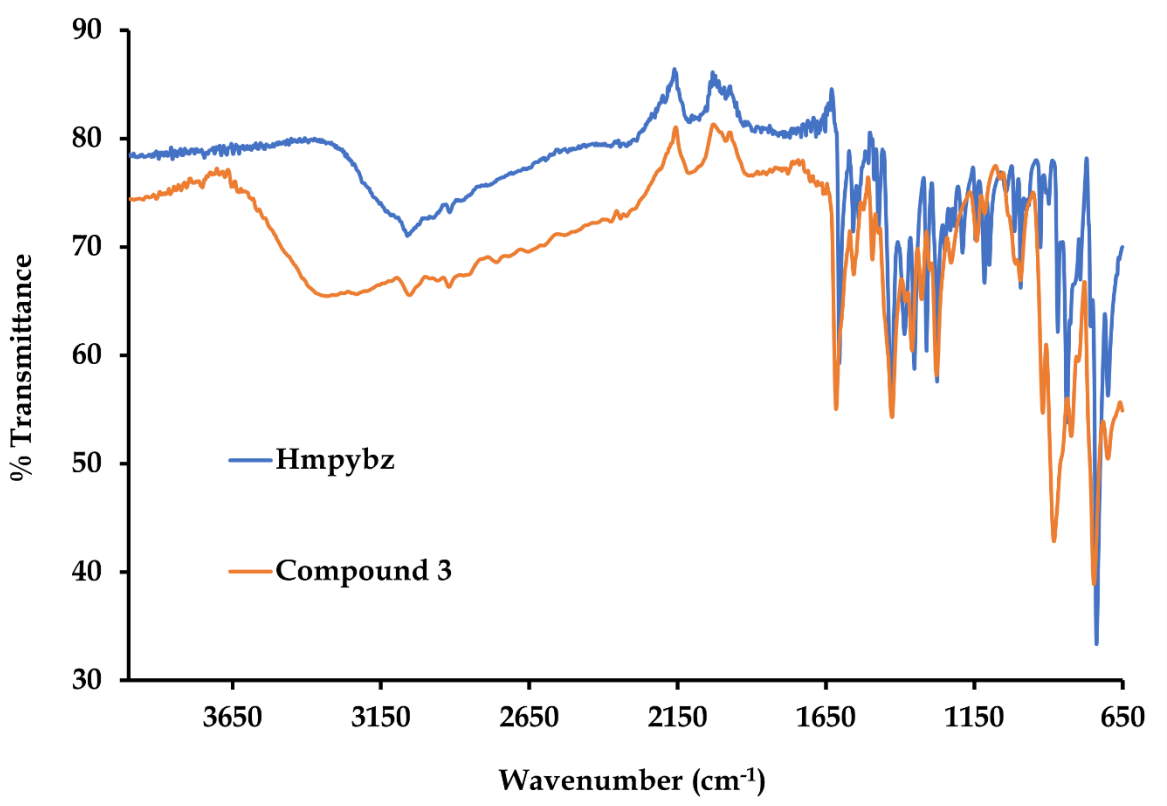

Figure 3.3: *Overlay IR spectra of the free ligand, Hmpybz and its corresponding metal complex, cis-[VO_2(Hmpybz)(mpybz)] (**3**) in the range of 4000 and 650 cm^{-1}. The intense band at 881 cm^{-1} is assigned to the cis-[VO_2]$^+$ stretching frequency.*

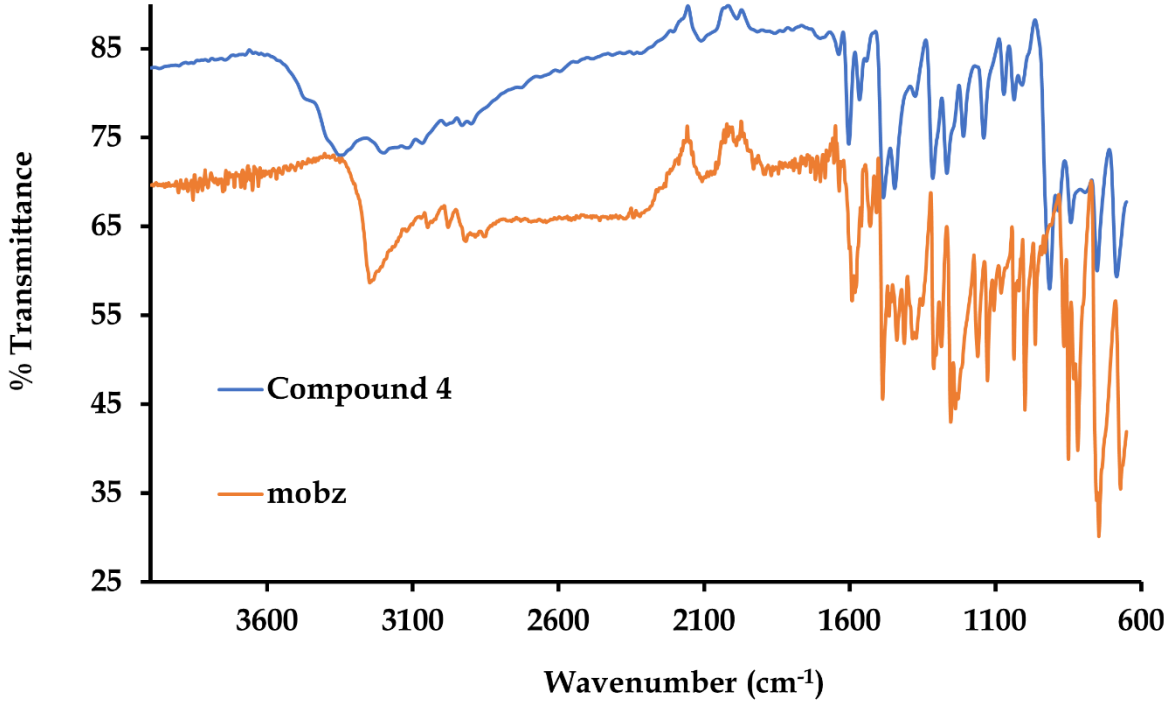

Figure 3.4: *IR spectra of cis-[VO_2(mobz)(py)] (**4**) (mobz = 2-(5-6 dimethyl-2-pyridine)-1H-*

benzimidazolyl) and its free ligand mobz in the range of 4000 and 650 cm^{-1}. The intense and broad band at 915 cm^{-1} is assigned to the cis-$[VO_2]^+$ stretching frequency.

The ground state electronic spectra of **3** mimic those of its free ligand whereas blue-shifting of **4**'s π→π* intra-ligand transitions occur relative to those of the free ligand, see **Figs**. 3.5 and 3.6. Furthermore, a charge transfer shoulder is found at 350 nm in the UV-Vis spectrum of **4**, which is attributed to the electron density redistribution from the phenolate moiety of mobz to the acidic vanadium centre in its oxidation number +V. As with all the metal compounds which contain vanadium centres with an empty *d*-shell, no metal-based electronic transitions are observed.

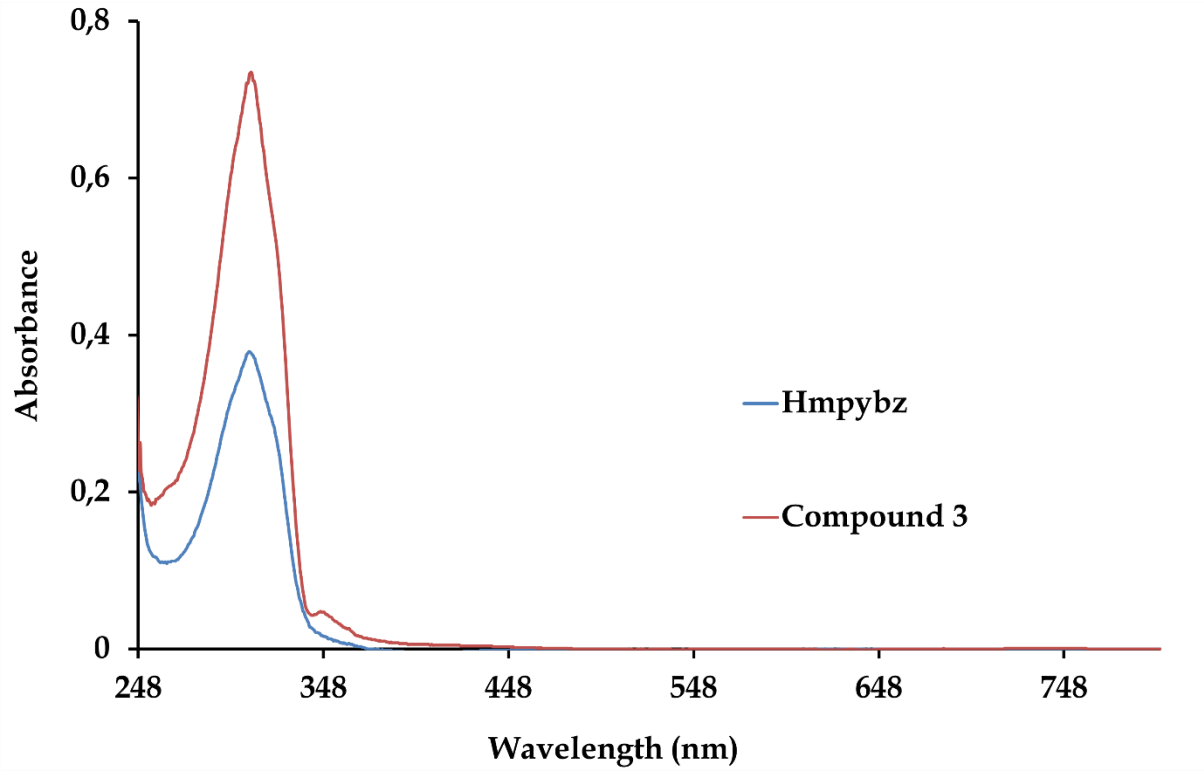

Figure 3.5: *Overlay UV-Vis spectra of compound* ***3*** *and its free ligand, Hmpybz.*

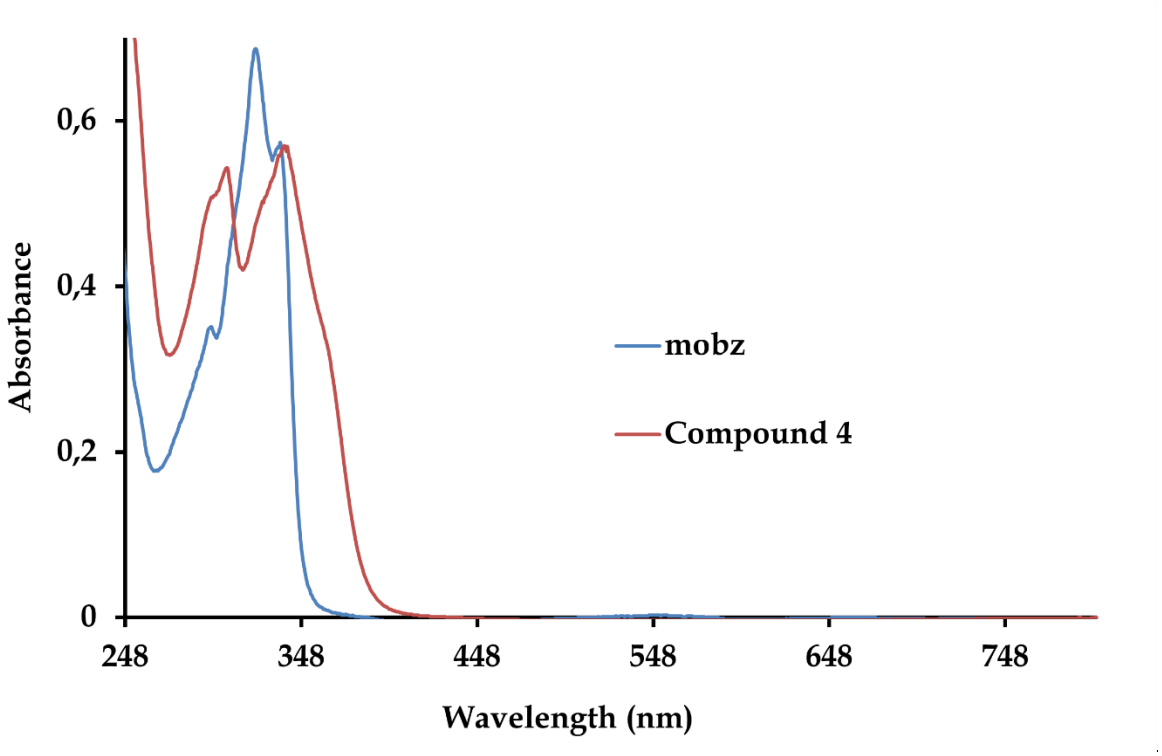

Figure 3.6: *Overlay UV-Vis spectra of compound* **4** *and its free ligand, mobz.*

Mutual broad singlets are observed downfield relative to the aromatic peaks, in the proton NMR spectra of the respective metal compounds see **Figs**. 3.7 and 3.9. The broadness could be accounted to the long relaxation times of the proton spins due to hydrogen-bonding in solution. It is evident that more aromatic signals occur in the proton spectra of **3** compared to those of the relating free ligand. In fact, several proton peaks associated with the protonated and unprotonated forms of the chelator coalesce. For instance, a doublet of doublets is observed at 7.22 ppm in the proton spectrum of **3** which is associated with the *H9* and *H17* protons. In contrast, and as expected the aliphatic protons are significantly shielded. The ^{51}V NMR singlets of the respective compounds are observed in -513 ppm to -598 ppm range.[20]

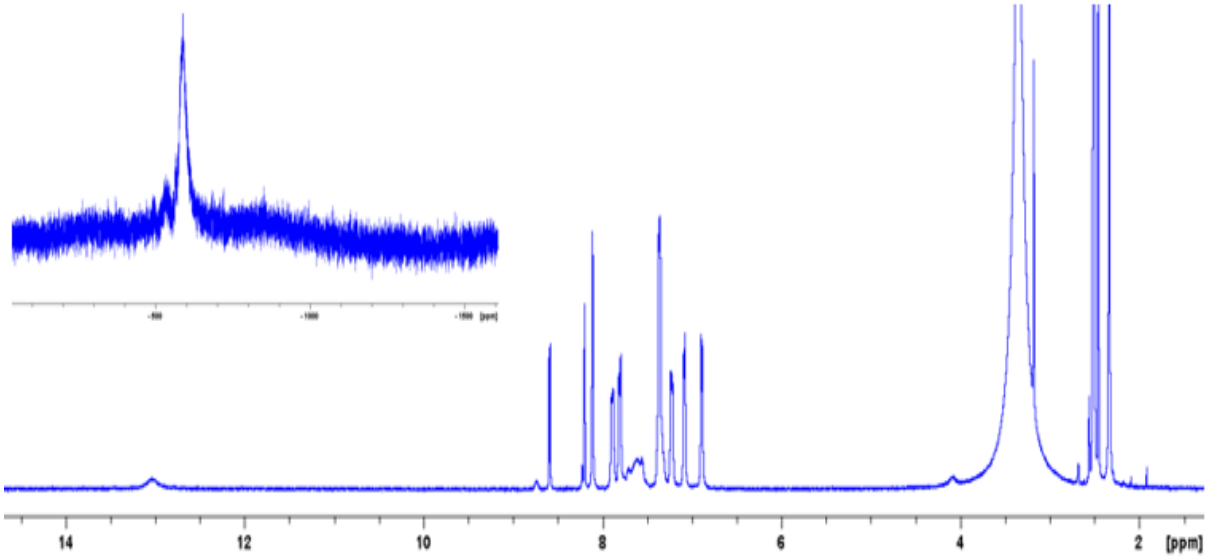

Figure 3.7: *^{1}H NMR spectrum of cis-[VO_2(Hmpybz)(mpybz)] (**3**) where the benzimidazolium proton (i.e. N-H signal) is the most de-shielded and the series of signals found upfield between 6.5-9 ppm are ascribed to the aromatic protons.* ***Inset:*** *The signal at -589.0 ppm in the ^{51}V NMR confirms the presence of the vanadium(V) centre.*

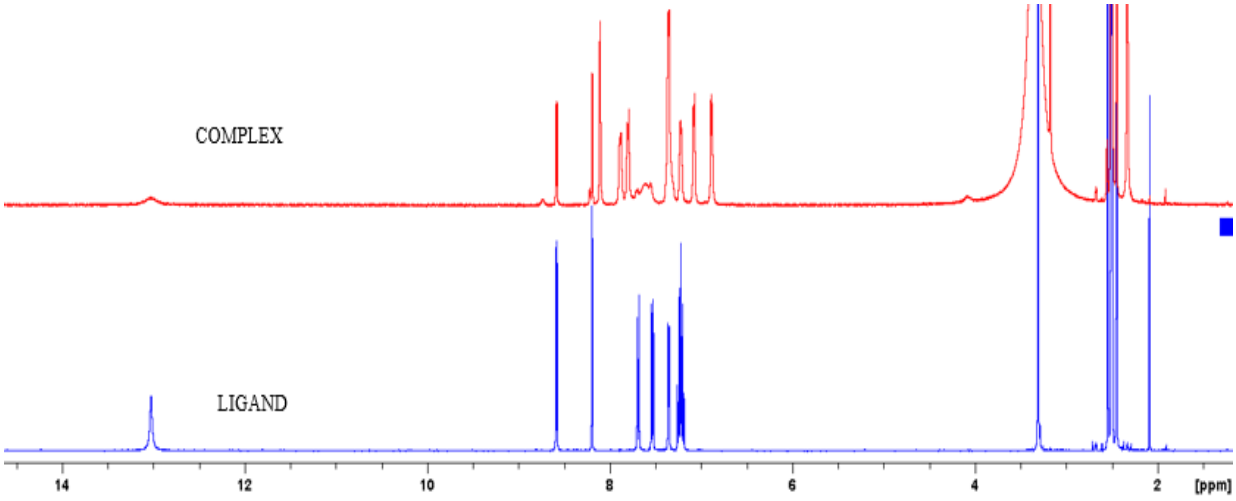

Figure 3.8: *Overlay ^{1}H NMR spectrum of cis-[VO_2(Hmpybz)(mpybz)] (**3**) and its free-ligand Hmpybz.*

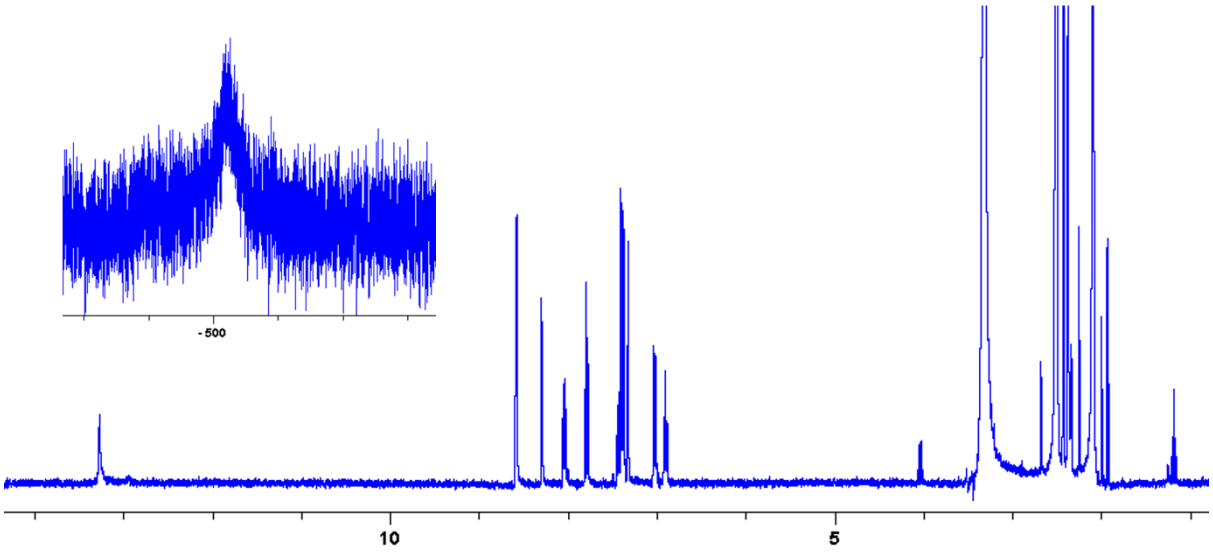

Figure 3.9: *^{1}H NMR spectrum of cis-[VO_2(mobz)(py)] (**4**) (mobz = 2-(5-6 dimethyl-2-pyridine)-1H-benzimidazolyl) where the benzimidazolium proton (i.e. N-H signal) is the most de-shielded and the series of signals found upfield between 6.5-9 ppm are ascribed to the aromatic protons.* ***Inset:*** *The signal at -519.4 ppm in the ^{51}V NMR confirms the presence of the vanadium(V) metal center.*

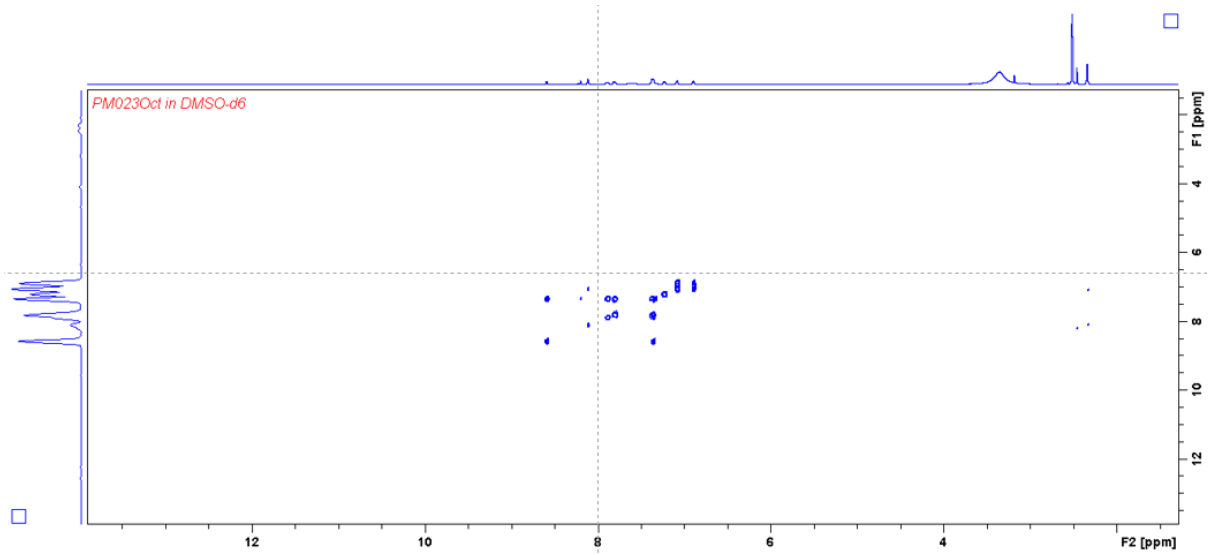

Figure 3.10: *Two-dimensional COSY NMR spectrum of the metal complex, cis-[VO_2(Hmpybz)(mpybz)] (**3**).*

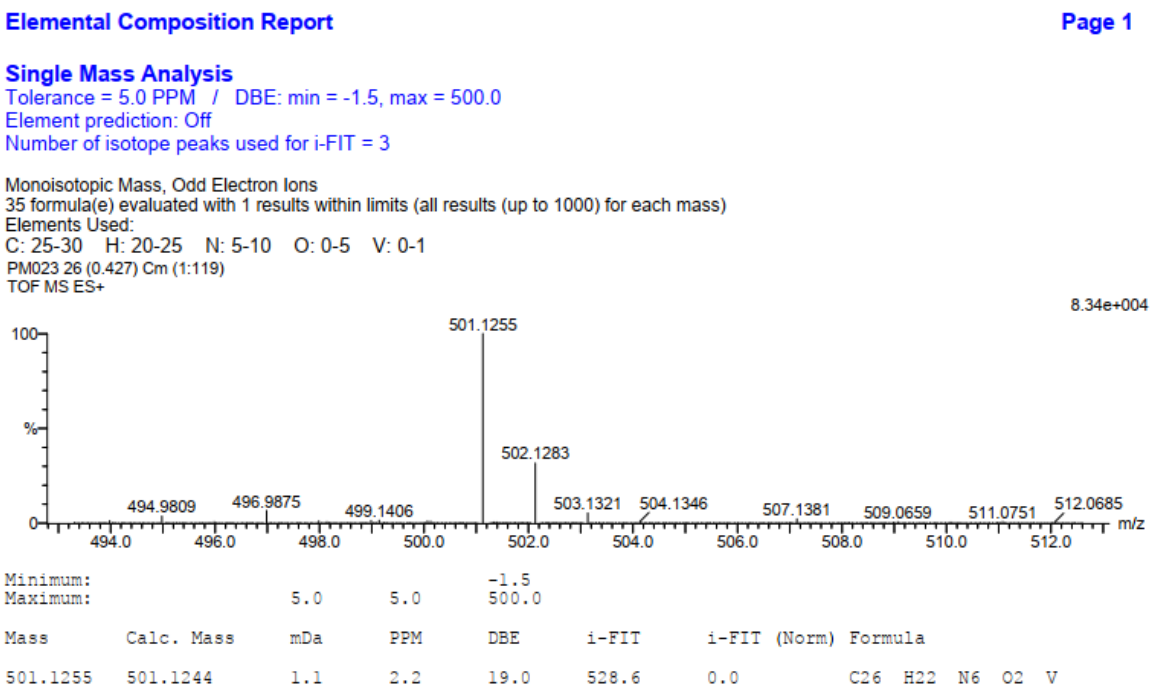

Figure 3.11: *Mass (ESI⁺-TOF) spectrum of the metal complex, cis-[VO_2(Hmpybz)(mpybz)] (**3**)*

Indicatively, the mass spectral analysis of **3** is characterized by a high intensity peak $[M]^+$ at *m/z* = 501.1255 amu, see **Fig**. 3.11 while its calculated mass is 501.1244 amu. The afore-mentioned MS spectral data corroborated the spectroscopic assignments made during the NMR and IR data discussion. Unlike the MS data, where gaseous ions are considered for analysis, the reported EA data and the calculated formulae correspond to their solid-state single crystals for **3** and **4**, respectively**.** and their corresponding solvent molecules of recrystallization are therefore included in the composition of each element. However, the drying process of **3** may have resulted in the removal of the co-crystallized pyridyl molecule, leaving two water molecules of recrystallization in the lattice of **3**.

*3.3.2 Crystal structures of **3** and **4***

The monomeric complexes (**3** and **4**) occupy the monoclinic unit cell in the same space group of $P2_{1/n}$. In particular, the asymmetric unit cell of **3** contains 8 molecules of **3**

where two sets of crystallographically-independent molecules coexist in an even distribution. In addition, pyridine and water molecules of recrystallization are found in respective 1:1 and 1:2 ratios with respect to **3**. In the case of **4**, four molecules are accompanied by eight water molecules of recrystallization are in the unit cell. Hydrogen-bonding occurring in the crystal lattice of **4** induces the formation of a unique supramolecular structure. More specifically, the molecules of **4** lie perpendicular to the [*a*]-axis which is supported by the following interactions: O4-H4B•••O3 = 1.933 Å, O4-H4A•••O5 = 1.914 Å and O5-H5A•••O2 = 1.985 Å while the resultant columns are reinforced by the residual intermolecular hydrogen bonds: O4-H3•••N3 = 1.999 Å, O5-H5B•••O4 = 2.038 Å. The two independent molecules render a metalorganic framework where they interact *via* the neutral Hmbzpy ligand of **3** and the deprotonated mbzpy chelated form of the neighbouring molecule: N12-H12A•••N10 = 1.719 Å. The bridging water molecules interlock the columns of 5 molecules through the following intermolecular hydrogen bonds: N7-H7•••O4 = 1.726 Å, O4-H4A•••N4 = 1.904 Å and O4-H4B•••O5 = 1.914 Å.

As the two independent molecules of **3** have nearly identical geometries and coordination modes, the geometrical parameters of molecule **A** will only be discussed, see Fig 3.12. The similarity between **A** and **B** is illustrated in the metal-to-oxo across the molecules (V1-O5 = 1.645(1) Å, V1-O2 = 1.623(1) Å for molecule **A**, V2-O2 = 1.630(1) Å, V2-O3 = 1.630(1) Å for molecule **B**). As shown in Fig. 3.13, the constrained five-membered chelate angles of **3** (N1-V1-N2 = 72.51(7)°, N5-V1-N13 = 73.68(7)°) induce deviations from linearity in the following angles: O5-V1-N2 = 161.12(8)° , N13-V1-N1 = 149.14(8)° and O1-V1-N5 = 164.90(8)°. Similarly, the constrained angle N2-V1-O1 = 83.87(5)°) in the structure of **4** induces a deviation of N2-V1-N1 = 165.80(5)°. In addition, the three O-V-O bond angles of **4** (O1-V1-O3 = 124.59(5)°, O3-V1-O2 = 109.38(6)° and O1-V1-O2 = 125.88(5)°) that constitute the equatorial plane differ from the ideal 120° of a classical trigonal pyramidal geometry, while the influence of the narrow bite angles of **3** extends its O-V-O (105.11(8)°) bond angle further apart from that of convectional equatorial bond angles.

Parity between the V=O bonds of **3** (V1-O5 = 1.645(1) Å, V1-O2 = 1.623(1) Å) and **4** (V1-O2 = 1.630(1) Å, V1-O3 = 1.633(1) Å) as well as the corresponding bonds of **1**[21] (V-

O1 = 1.621(3) Å, V-O2 = 1.638(1) Å) and **2**[22] (V-O1 = 1.625(1) Å) are clearly established based on the similar bond lengths. In fact, these V=O bonds are within the range of 1.594(3) to 1.661(3) Å reported for other dioxovanadium(V) complexes.[23-25] The single bond character of the V1-$O1_{(phenolate)}$ of **4** (1.905(1) Å) is evident by its longer V1O1 bond distance compared to other organovanadium(V) compounds.[26-28] As compounds **3** and **4** are isostructural to their corresponding parent compounds **1** and **2**, the remaining coordination bonds are comparable. In particular, the V-$N_{1/13(benzimidazole)}$ for the respective two coordinated N, N-bidentate ligands of **3** or **4** (2.078(2) Å, 2.041(2) Å for **3** and 2.032(2) Å, 2.092(2) Å for **1**) and V-$N_{pyridyl}$ (2.363(2) Å, 2.338(2) Å for **3** and 2.308(2) Å, 2.384(2) Å for **1**). These ligands exert a trans influence (elongation of the ground state bond lengths) on the ligands which are trans to the their bonds i.e. the oxo atoms (O1/5) experience it from the pyridyl ligands opposite to their bonds. The benzimidazole N donors are trans to each other,exert equal and mutual ground state effects. Thus, any difference in their (N donor atoms) bond distances to V is more likely due to the planar rigid structures and also the need to minimizes inter-ligands repulsions around the octahedral geometry, especially in the square plane where the N1N5N13O5 atoms are evidently non-co-planar as expected. The exert the same trans-influence base on the nucleophilicities of the benzimidazole Ns. Indicatively, the same phenomenon is observed in **2** and **4** where the analogous pyridyl nitrogens imposed a *trans*-effect on the neutral benzimidazole nitrogens (V-$N_{benzimidazole}$ (2.065(1) Å for **4** and 2.068(2) Å for **2**) and V-$N_{pyridyl}$ (2.174(1) Å for **4** and 2.191(2) Å for **2**). The afore-mentioned V-O coordination bonds are in agreement with other diamagnetic vanadium compounds with pyridyl benzimidazole chelators, *e.g.*: $[VO_2(Byim)]$.DMF (Byim = 2,6-*di*-(1*H*-benzimidazol-2-yl)pyridine): V-$N_{benzimidazole}$ = 2.075(2) Å, 2.032(2) Å and V-$N_{pyridyl}$ = 2.175(2) Å and $[VO_2(L)(L)]$ (L = 2-(2-pyridyl)benzimidazole):V-$N_{benzimidazole}$ = 2.035(3) Å, 2.097(2) Å and V-$N_{pyridyl}$ = 2.335(2) Å, 2.395(3) Å.[29, 30]

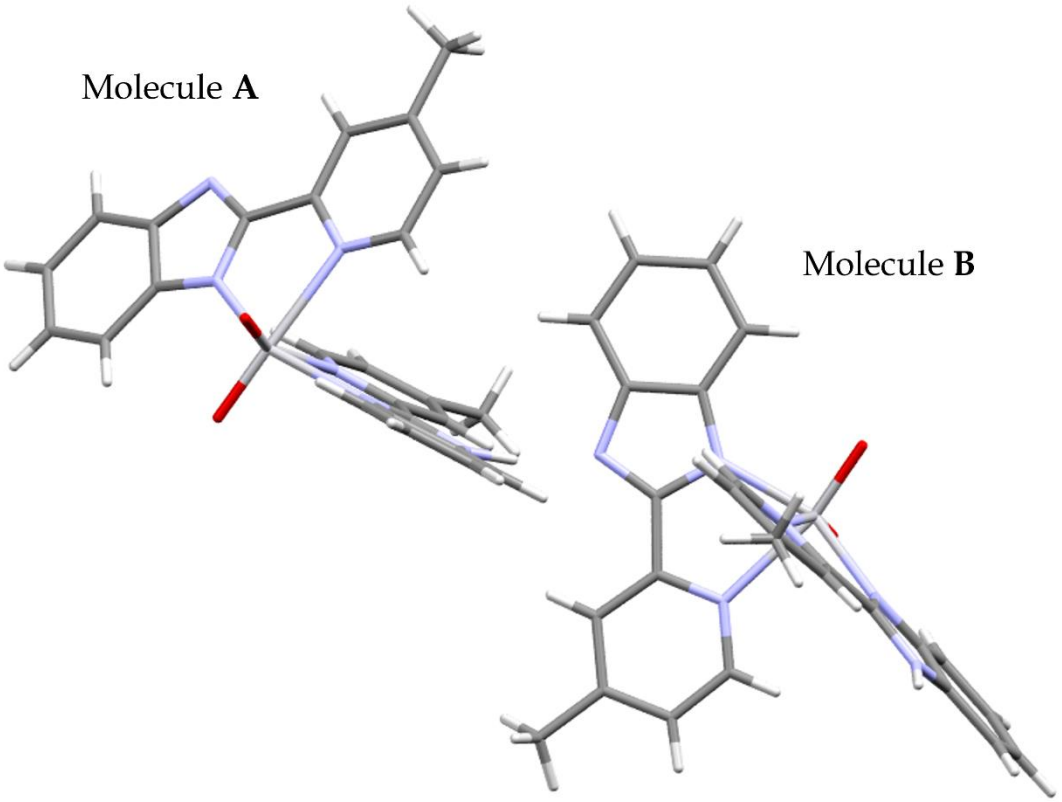

Figure 3.12: *An illustration of the two independent molecules of cis-[VO_2(Hmpybz)(mpybz)] entitled molecule **A** and molecule **B**.*

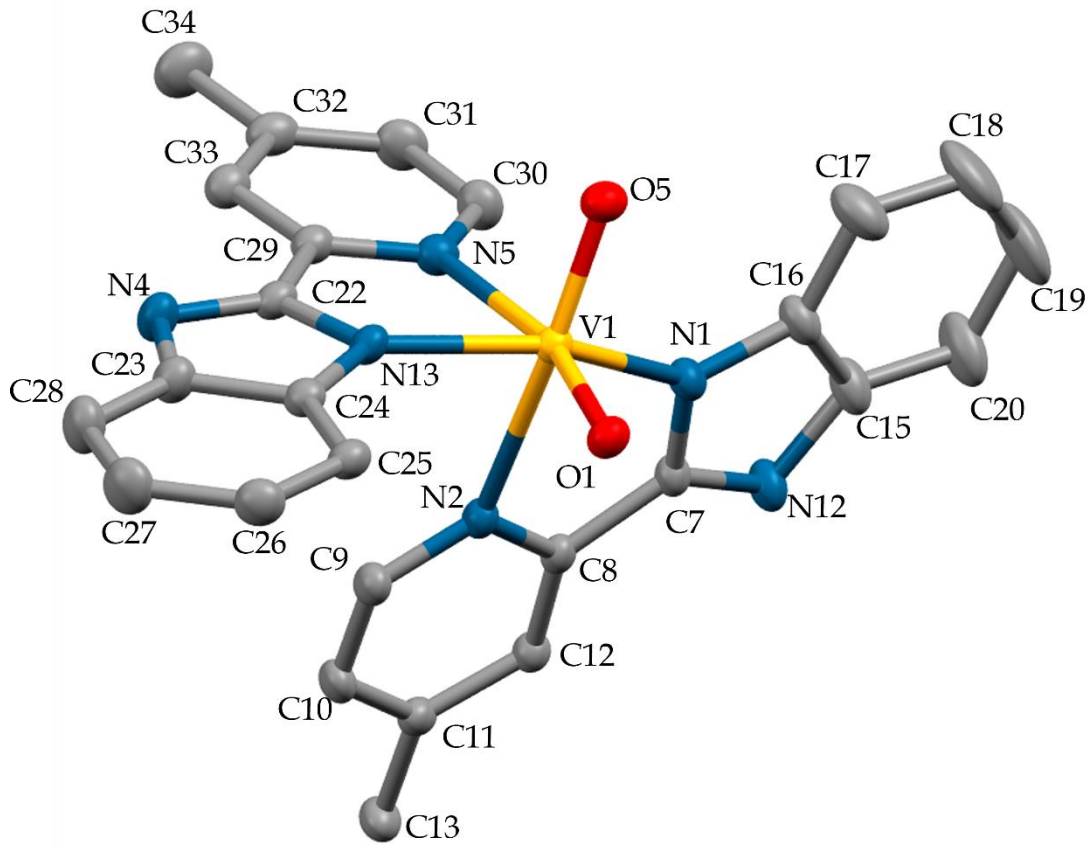

Figure 3.13: *Solid-state structure of cis-[VO_2(Hmbzpy)(mbzpy)] (**3**) (Hmbzpy = 2-(4-methylpyridine)-1H-benzimidazole). The second crystallographically-independent molecule of **3** along with two pyridines and one water molecule of recrystallisation has been omitted for the sake of clarity. Similarly, the protons are not shown.*

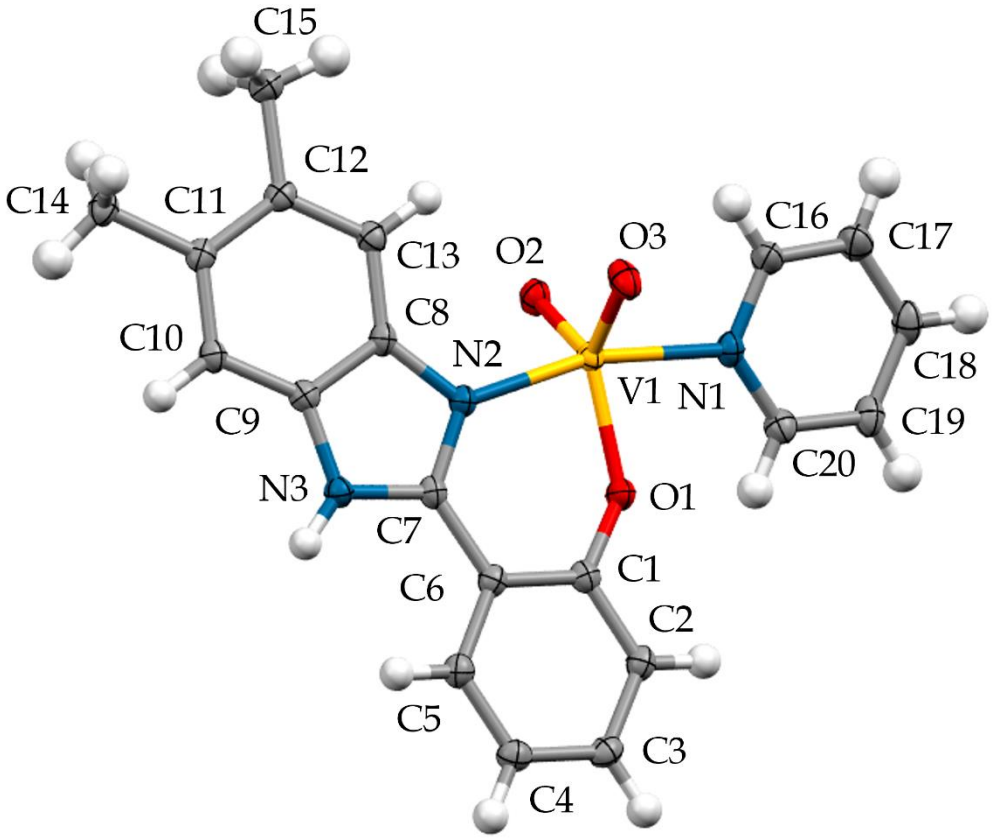

Figure 3.14: *Solid-state structure of cis-[VO_2H(mobz)(py)] (**4**) (Hmobz = 2-(5-6 dimethyl-2-pyridine)-1H-benzimidazolyl). The water molecules of recrystallization have been omitted for the sake of clarity.*

Table 3.1: *Crystallographic data for compounds* ***3*** *and* ***4****.*

	3	**4. 2(H_2O)**
Chemical formula	$C_{62}H_{54}N_{14}O_5V_2$	$C_{20}H_{18}N_3O_3V$
Formula weight	1177.07	435.34
Crystal system	monoclinic	monoclinic
Space group	$P2_{1/n}$	$P2_{1/n}$
Temperature (K)	100 K	100 K
Unit cell dimensions		
a(Å)	22.2654 (10)	14.5535 (7)
b(Å)	11.4396 (5)	7.5846 (4)
c(Å)	24.8417 (11)	17.7391 (9)
α (°)	90	90
β (°)	116.212 (2)	101.853 (2)
γ (°)	90	90
Crystal size (mm)	0.36 × 0.32 × 0.31	0.20 × 0.11 × 0.04
V ($Å^3$)	5676.7 (4)	1916.33 (17)
Z	4	4
Density calc. ($Mg.m^{-3}$)	1.377	1.509
Absorption coefficient (mm^{-1})	3.28	4.67
F(000)	2440	904
θ range for data collection (°)	4.4–68.1	4.4–71.8
Index ranges	-26 ≤ h ≤ 26	-17 ≤ h ≤ 17
	-13 ≤ k ≤ 13	-9 ≤ k ≤ 9
	-29 ≤ l ≤ 29	-21 ≤ l ≤ 21
Reflections measured	92759	39982
Observed reflections [I > 2σ(I)]	9418	3576
Independent reflections	10205	3742
Data/restraints/parameters	10205, 3, 766	3742, 0, 270
Goodness-of-fit on F^2	1.044	0.982
Observed R, wR^2	0.0479, 0.1187	0.031, 0.107
R_{int}	0.061	0.050

Table 3.2: *Selected bond lengths [Å] and bond angles [°] for* ***3*** *and* ***4****.*

	3	**4**
V1-O1	1.623(2)	1.905(1)
V1-O5	1.645(1)	-
V1-O2	-	1.633(1)
V1-O3	-	1.630(1)
V1-N1	2.078(2)	2.174(1)
V1-N5	2.338(2)	-
V1-N13	2.041(2)	-
V1-N2	2.363(2)	2.065(1)
N1-C7	1.336(3)	-

N13-C22	1.360(3)	-
N12-C7	1.342(4)	-
N4-C22	1.330(4)	-
N2-C7	-	1.342(2)
N3-C7	-	1.352(2)
O1-V1-N1	99.48(8)	82.12(5)
N1-V1-N2	72.51(7)	165.80(5)
N2-V1-N5	74.65(7)	-
N2-V1-N13	81.18(7)	-
O5-V1-N13	103.56(8)	-
N5-V1-N1	83.86(7)	-
O1-V1-O5	105.11(8)	-
N1-V1-O5	96.80(8)	-
N2-V1-O3	-	95.95(5)
N1-V1-O3	-	93.93(5)
O1-V1-O2	-	125.88(5)
O2-V1-O3	-	109.38(6)
O2-V1-N1	-	91.20(5)
O1-V1-N2	-	83.87(5)

3.4 **References**

1. Fernández, B.; Gómez-Vílchez, A.; Sánchez-González, C.; Bayón, J.; San Sebastián, E.; Gómez-Ruiz, S.; López-Chaves, C.; Aranda, P.; Llopis, J.; Rodríguez-Diéguez, A., Novel anti-diabetic and luminescent coordination compounds based on vanadium. *New Journal of Chemistry* **2016,** *40* (6), 5387-5393.
2. Szklarzewicz, J.; Jurowska, A.; Hodorowicz, M.; Kazek, G.; Głuch-Lutwin, M.; Sapa, J., Ligand role on insulin-mimetic properties of vanadium complexes. Structural and biological studies. *Inorganica Chimica Acta* **2021,** *516*, 120135.
3. Samart, N.; Althumairy, D.; Zhang, D.; Roess, D. A.; Crans, D. C., Initiation of a novel mode of membrane signaling: Vanadium facilitated signal transduction. *Coordination Chemistry Reviews* **2020,** *416*.
4. Crans, D.; Keramidas, A.; Drouza, C., Organic Vanadium Compounds - Transition State Analogy with Organic Phosphorus Compounds. *Phosphorus, Sulfur, and Silicon and the Related Elements* **1996,** *109* (1), 245-248.
5. Srivastava, A. K.; Mehdi, M. Z., Insulino-mimetic and anti-diabetic effects of vanadium compounds. *Diabet Med* **2005,** *22* (1), 2-13.
6. Rehder, D., Vanadium in health issues. *ChemTexts* **2018,** *4* (4).
7. Levina, A.; McLeod, A. I.; Kremer, L. E.; Aitken, J. B.; Glover, C. J.; Johannessen, B.; Lay, P. A., Reactivity-activity relationships of oral anti-diabetic vanadium complexes in gastrointestinal media: an X-ray absorption spectroscopic study. *Metallomics* **2014,** *6* (10), 1880-8.
8. Clark, T. A.; Deniset, J. F.; Heyliger, C. E.; Pierce, G. N., Alternative therapies for diabetes and its cardiac complications: role of vanadium. *Heart Fail Rev* **2014,** *19* (1), 123-32.
9. Gaba, M.; Mohan, C., Development of drugs based on imidazole and benzimidazole bioactive heterocycles: recent advances and future directions. *Medicinal Chemistry Research* **2015,** *25* (2), 173-210.
10. Vasava, M. S.; Bhoi, M. N.; Rathwa, S. K.; Jethava, D. J.; Acharya, P. T.; Patel, D. B.; Patel, H. D., Benzimidazole: A Milestone in the Field of Medicinal Chemistry. *Mini Rev Med Chem* **2020,** *20* (7), 532-565.
11. Mbatha, B.; Khathi, A.; Sibiya, N.; Booysen, I.; Mangundu, P.; Ngubane, P., Anti-hyperglycaemic effects of dioxidovanadium complex cis-[VO_2 (obz) py] avert kidney dysfunction in streptozotocin-induced diabetic male Sprague–Dawley rats. *Canadian Journal of Physiology and Pharmacology* **2021,** *99* (4), 402-410.
12. Mbatha, B.; Khathi, A.; Sibiya, N.; Booysen, I.; Mangundu, P.; Ngubane, P., Cardio-protective effects of a dioxidovanadium(V) complex in male sprague-dawley rats with streptozotocin-induced diabetes. *Biometals* **2021,** *34* (1), 161-173.
13. Sibiya, N. H. The effects of oxidovanadium complexes on glucose metabolism in liver and skeletal muscle cell lines. 2014.
14. Sibiya, S.; Msibi, B.; Khathi, A.; Sibiya, N.; Booysen, I.; Ngubane, P., The effect of dioxidovanadium complex (V) on hepatic function in streptozotocin-induced diabetic rats. *Canadian journal of physiology and pharmacology* **2019,** *97* (12), 1169-1175.
15. Ghorbanloo, M.; Jafari, S.; Bikas, R.; Krawczyk, M. S.; Lis, T., Dioxidovanadium (V) complexes containing thiazol-hydrazone NNN-donor ligands and their catalytic activity in the oxidation of olefins. *Inorganica Chimica Acta* **2017,** *455*, 15-24.

16. Maurya, M. R.; Bisht, M.; Kumar, A.; Kuznetsov, M. L.; Avecilla, F.; Pessoa, J. C., Synthesis, characterization, reactivity and catalytic activity of oxidovanadium (IV), oxidovanadium(V) and dioxidovanadium(V) complexes of benzimidazole modified ligands. *Dalton Transactions* **2011,** *40* (26), 6968-6983.
17. Maurya, M. R.; Chaudhary, N.; Avecilla, F.; Adão, P.; Pessoa, J. C., Oxidovanadium(IV) and dioxidovanadium(V) complexes of hydrazones of 2-benzoylpyridine and their catalytic applications. *Dalton Transactions* **2015,** *44* (3), 1211-1232.
18. Sheikhshoaie, I.; Ebrahimipour, S. Y.; Lotfi, N.; Mague, J. T.; Khaleghi, M., Synthesis, spectral characterization, X-ray crystal structure and antimicrobial activities of two cis dioxido-vanadium(V) complexes incorporating unsymmetrical dimalonitrile-based (NNO) Schiff base ligands. *Inorganica Chimica Acta* **2016,** *442*, 151-157.
19. Hlela, T.I., Oxidovanadium complexes with N-donor heterocyclic chelates (Doctoral dissertation, UKZN) **2013**.
20. Sutradhar, M.; Andrade, M. A.; Carabineiro, S. A.; Martins, L. M.; Guedes da Silva, M. d. F. C.; Pombeiro, A. J., Oxido-and Dioxido-Vanadium(V) Complexes Supported on Carbon Materials: Reusable Catalysts for the Oxidation of Cyclohexane. *Nanomaterials* **2021,** *11* (6), 1456.
21. Booysen, I. N.; Hlela, T.; Gerber, T. I.; Munro, O. Q.; Akerman, M. P., Novel vanadium compounds with 2-pyridylbenzimidazole. *Polyhedron* **2013,** *53*, 8-14.
22. Booysen, I. N.; Hlela, T.; Akerman, M. P.; Xulu, B., Mono-and polynuclear vanadium(IV) and-(V) compounds with 2-substituted phenyl/pyridyl heterocyclic chelates. *Polyhedron* **2015,** *85*, 144-150.
23. Ghorbanloo, M.; Bikas, R.; Jafari, S.; Krawczyk, M. S.; Lis, T., Synthesis, structural characterization and catalytic potential of oxidovanadium(IV) and dioxidovanadium(V) complexes with thiazole-derived NNN-donor ligand. *Journal of Coordination Chemistry* **2018,** *71* (10), 1510-1525.
24. Kurbah, S. D.; Asthana, M.; Syiemlieh, I.; Lywait, A. A.; Longchar, M.; Lal, R. A., New dioxido-vanadium(V) complexes containing hydrazone ligands: Syntheses, crystal structure and their catalytic application toward C H bond functionalization. *Journal of Organometallic Chemistry* **2018,** *876*, 10-16.
25. Kurbah, S. D.; Kumar, A.; Syiemlieh, I.; Lal, R. A., Crystal structure and biomimetic activity of homobinuclear dioxidovanadium(V) complexes containing succinoyldihydrazones ligands. *Polyhedron* **2018,** *139*, 80-88.
26. Miller-Shakesby, D. M.; Nigam, S.; Brookfield, A.; McInnes, E. J. L.; Prior, T. J.; Archibald, S. J.; Redshaw, C., Synthesis, structure, and cytotoxicity studies of oxidovanadium(IV and V) complexes bearing chelating phenolates. *Polyhedron* **2019,** *171*, 1-9.
27. Lotfi, N.; Sheikhshoaei, I.; Ebrahimipour, S. Y.; Krautscheid, H., Synthesis, characterization, crystal structure, and DFT studies of a cis dioxo -vanadium(V) complex containing a tridentate (NNO) Schiff base ligand. *Journal of Molecular Structure* **2017,** *1149*, 432-438.
28. A'Shidhani, S.; Al Bouromi, M.; Al Ameri, S.; Al Ghawi, S.; Jevtovic, V., Synthesis and Structural Analysis of a Dioxovanadium(V) Complex Incorporating

Pyridoxal-Thiosemicarbazone (PLTSC) Ligand. *American Journal of Chemistry* **2016,** *6* (1), 8-11.
29. Palmajumder, E.; Patra, S.; Drew, M. G. B.; Mukherjea, K. K., Vanadium bromoperoxidase (VBrPO) mimics: synthesis, structure and a comparative account of the catalytic activity of newly synthesized oxidovanadium and oxido-peroxidovanadium complexes. *New Journal of Chemistry* **2016,** *40* (10), 8696-8703.
30. Mal, S. K.; Chattopadhyay, T.; Fathima, A.; Purohit, C. S.; Kiran, M. S.; Nair, B. U.; Ghosh, R., Synthesis and structural characterization of a vanadium(V)-pyridylbenzimidazole complex: DNA binding and anticancer activity. *Polyhedron* **2017,** *126*, 23-27.

Chapter 4

An investigation into the binding interactions of the vanadium benzimidazole complexes with relevant biomolecules

4.1 Introduction

Elucidating the mechanistic action for vanadium-based anti-diabetic drug candidates requires insight into their *in vivo* stabilities and pharmacokinetics as well as affinities towards key biological targets.[1, 2] Organovanadium compounds that are designed to be orally-administered drugs, necessitate careful design into their hydrophobic and hydrophilic structural features to cater for optimal cell permeability as well as blood solubility.[3] The organic chelators of potential metallopharmaceuticals typically increase physiological compatibility and stability in the gastrointestinal (GI) tract.[4]

Generally, in aqueous media and at neutral pH, stability studies have revealed that numerous vanadium coordination compounds convert to the vanadate ions.[5] However, the structural integrity of vanadate is time-dependant where degradation of the latter can lead to toxic insoluble polyoxometalates. Thus, the pharmacokinetics for the conversion of the pro-drug, the original vanadium species to their active drug, vanadate is of importance. Owing to the fact that phosphate and vanadate are structural equivalents, the latter adopts bio-distribute similarly. Consequently, vanadate can inhibit auto-phosphorylation of the Protein Tyrosine Phosphatase (PTP)-1B which leads to the enhancement of insulin levels for glucose metabolism.[6, 7]

In this chapter, the binding affinities and modes of vanadium compounds **1** and **2** and the respective new structural analogues **3** and **4** towards CT-DNA and BSA were reported. Indicatively, the binding strengths of **1 - 4** with the PTP-1B were evaluated.

In addition, *in vitro* experiments were conducted in a kidney cell line to evaluate their glucose metabolism capabilities.

4.2 Experimental

4.2.1 DNA binding experiments

Binding affinities of the dioxidovanadium(V) compounds towards calf thymus (CT)-DNA were monitored in phosphate-buffered saline (PBS) using a fixed concentration of the metal complexes (20 μM). At a wavelength of 260 nm and 280 nm, the absorbances of the CT-DNA solution in PBS produced a ratio of 1.9: 1, implying that the CT-DNA was relatively free of protein. The solutions of the dioxovanadium(V) complexes (**1**-**4**) and CT-DNA at variable concentrations were incubated at 25 ^{o}C for 24 hours preceding any absorption titration. UV-Vis spectra of each metal complex before and after the additions of DNA concentrations ranging from 0 to 90 μM in PBS was collected. To determine the binding constant (K_b) the change in the absorbance of the respective charge transfer bands of the dioxovanadium(V) complexes **1**-**4** with increasing amounts of CT-DNA were monitored. Kb measures the binding strength of a pharmaceutical agent (the vanadium complex) at a complementary host molecule's bio-active sites or pockets. The electronic spectral data was then fitted to the following equation:

$$\frac{[DNA]}{(\varepsilon_a - \varepsilon_b)} = \frac{[DNA]}{(\varepsilon_b - \varepsilon_f)} + \frac{1}{K_b(\varepsilon_a - \varepsilon_f)} \qquad \text{(A)}$$

where [DNA] is the molar concentration of DNA in the base pairs, and ε_a, ε_f and ε_b refer to the corresponding apparent absorption coefficient ($A_{observed}$/ [**1**/**2**/**3**/**4**]), the extinction coefficient for the free dioxidovanadium complex and the extinction coefficient for the dioxidovanadium CT-DNA complex in the fully bound form, respectively. In the plots of [DNA]/ (ε_a-ε_f) versus [DNA] see **Figs.4.1- 4.4**, K_b is obtained by the ratio of the respective slopes to the intercepts.[8-10]

4.2.2 Fluorescence spectroscopic titrations

Interactions between the vanadium compounds and BSA was also analysed using fluorescence spectroscopy. The Stern-Volmer quenching constant (K_{SV}) was attained by using the Stern-Volmer relation (B):

$$\frac{I_0}{I} = 1 + K_{SV}\,[complex] \qquad (B)$$

where I and I_o are the emission intensities in the absence and presence of the Dioxovanadium(V) (**1-4**), respectively. The K_{SV} values were obtained from the slope of the derived plot.[11]

The quenching rate constant (k_q) was calculated from equation (C):

$$K_q = K_{SV} / \tau_0 \; (\tau_0 = 10^{-8}) \qquad (C)$$

Where τ_0 is the lifetime of the excited state of the protein (10^{-8} s) without the quencher. The binding constants (K_b) and the binding number (n) were then determined using equation (D):

$$Log\,(I_0 - I) / I = Log\,K_b + n\,Log\,[complex] \qquad (D)$$

where I_0 and I are the same as in equation (B), K_b is the binding constant of each metal complex **1-4** with BSA and n the number of binding sites per BSA molecule.[12]

"4.2.3 Cell culture

As per declaration I – plagiarism, the following subsection has been italicised and placed between quotation marks as it has been prepared by our collaborator, Dr Shantal Maharaj who has a PhD in biochemistry.

The HEK293T cell line was maintained in Dulbecco's Modified Eagle Medium (DMEM) supplemented with 10% (v/v) foetal bovine serum (FBS), 0.1% (v/v) PSA (100 U/ mL penicillin, 100 µg/ mL streptomycin, 12.5 µg/ mL amphotericin) and 0.1% Gentamycin at 37°C with 5% CO_2. Cell lysates were prepared by lifting a confluent T25 culture vessel with 0.25% trypsin and collecting cells in 1 mL of 1x phosphate-buffered saline (137 mM NaCl, 2.7 mM KCl, 10 mM Na_2HPO_4 and 1.8 mM KH_2PO_4). Cell pellets were stored at -20°C until

required and on the day of assay, cell pellets were thawed on ice. Collected cells were centrifuged at 13000 rpm for 15 minutes at room temperature and the supernatant was removed. Pellets were re-suspended in 0.5% Triton-X 100 in 1X assay buffer (0.5 M Tris-HCl, 0.01 M DTT, 0.1 M EDTA, 0.02 M β-mercaptoethanol, 1% protease inhibitor cocktail (PIC) (P8340, Sigma-Aldrich) and the supernatant containing the protein was analysed. Protein concentrations of cell lysates were measured using the Bradford's assay outlined below."

"4.2.4 Bradford's assay for protein determination

As per declaration I – plagiarism, the following subsection has been italicised and placed between quotation marks as it has been prepared by our collaborator, Dr Shantal Maharaj who has a PhD in biochemistry.

Bradford's assay was carried out according to literature using bovine serum albumin (BSA) as a standard. Various concentrations of BSA were used to generate standard curves which were carried out in triplicate. On a 96-well plate, 10 µL of BSA standards and 10 µL protein lysate were added to wells followed by 290 µL of Bradford's reagent (B6916, Sigma-Aldrich). The plate was incubated in the dark for ~20 minutes and absorbance were read at 595 nm.[13]"

"4.2.5 PTP-1B enzyme activity assay

As per declaration I – plagiarism, the following subsection has been italicised and placed between quotation marks as it has been prepared by our collaborator, Dr Shantal Maharaj who has a PhD in biochemistry.

The PTP-1B enzyme activity assays were carried out according to literature reported methods with slight modification.[14, 15] HEK293T cell lysates were used in proxy of purified enzyme. The assays were carried out in in 96-well microtiter plates using a 1x Tris assay buffer (0.5 M Tris-HCl, 0.01 M 1,4-dithiothreitol (DTT), 0.1 M ethylenediaminetetraacetic acid (EDTA), 0.02 M β-mercaptoethanol, 1% protease inhibitor cocktail (PIC) (P8340, Sigma Aldrich)[16]. For post-lysis assays, cell lysates with and without the addition of compounds of interest were plated and made up to 100 µL using 1x assay buffer followed by the addition of 200 µL of p-Nitrophenyl phosphate (pNpp) substrate (N7653-Sigma-Aldrich) solution to each well. This was allowed to develop for 30 minutes in the dark. The assays were carried out at 37°C.[16-18]

For the pre-lysis treatment, HEK293T cells were treated with compounds for 72 hours at indicated concentration. Lysates were then monitored for activity. pNpp dephosphorylation to pNp was measured at 405 nm using the SpectraMax ABS Plus microplate reader for 30-60 minutes. Sodium orthovanadate (Na_3VO_4) (Sigma Aldrich, S6508) was used as the positive control for PTP inhibition at 100 µM concentration in all instances. The activity was calculated using the equation below:

$$\frac{U}{mg} = \frac{\Delta E/min}{e.d.c} . \frac{vT}{vLys} = \frac{x/1{,}74x100}{mg\ protein} = \mu mol.min.mg\ (E)"$$

"4.2.6 Glycolytic flux assays

As per declaration I – plagiarism, the following subsection has been italicised and placed between quotation marks as it has been prepared by our collaborator, Dr Shantal Maharaj who has a PhD in biochemistry.

Glycolytic flux assays were carried out by measuring the lactate and glucose levels over time in the HEK293T cell lines using a lactate production and glucose import assay. Cells were seeded at 70% confluency in a T25 and allowed to adhere overnight. Cells were treated with compounds for 48 hours and initialization of the assay was carried out by replacing the media and taking spent media samples at 0, 2, 4, 8 and 24 hours. For the lactate assay, a lactate standard/calibration curve was carried out with 5 mM, 2.5 mM, 1.25 mM, 0.625 mM, 0.3125 mM, 0.1562 mM and 0.078 mM lactic acid (69775, Fluka Chemicals). The assay was carried out in a 96-well microtiter plate as follows: 10 µl of lactate standard and sample was pipetted into each well, 90 µl of assay cocktail (5 mM [w/v] NAD+ (N7004, Sigma-Aldrich), 1% [v/v] lactate dehydrogenase [LDH] (L2625, Sigma Aldrich), 2.5% [v/v] hydrazine in 1X PBS) was added to each well. The reaction was allowed to develop for 60 minutes and the absorbance due to the formation of NADH was read at 340 nm.

For glucose uptake, the glucose standard/calibration curve was carried out with 5 mM, 2.5 mM, 1.25 mM, 0.625 mM, 0.3125 mM, 0.1562 mM and 0.078 mM glucose (A2494001, Thermo Fisher). The glucose uptake assay was carried out in a 96-well microtiter plate as follows: 10 µl of glucose standard and sample was pipetted into each well, 90 µl of assay cocktail (5 mM [w/v] ATP, 5 mM [w/v] NADP+ (N3139, Sigma-Aldrich), 10 mM [w/v]

MgCl2, 0.8 mg/mL [w/v] hexokinase (H6380, Sigma Aldrich), 0.1% [v/v] glucose-6-phosphate dehydrogenase (G8404, Sigma-Aldrich) in 1X PBS) was added to each well. The reaction was allowed to develop for 90 minutes and the absorbance due to production of NADPH was read at 340 nm. The glucose import assay measures the conversion of glucose over time and the lactate production assay measures the level of lactic acid build up extracellularly over time. The lactate and glucose concentrations were calculated as a function of time and protein concentration using the equation:

$$\frac{Gradient\ (m)(mM.min^{-1})}{mg\ protein} x1000 = \mu mol.min.mg''$$

4.2.7 Binding study of vanadium complexes with PTP-1B

The fluorescence spectra of PTP-1B were recorded in the absence and presence of varying concentrations of vanadium complexes. PTP-1B solution was made up in a buffer solution (10 mM Tris at pH 7.5). Fluorescence emission spectra were recorded in the wavelength range of 250 – 400 nm by exciting the PTP-1B at 282 nm with the excitation and emission slit width of 5 nm. The fluorescence titrations were performed manually by adding incrementing concentrations of the vanadium metal complexes in a stepwise manner to the 2 mL of PTP-1B solution of 0.05 µM. The fluorescence quenching was calculated using equation (E).

$I_0/I = 1 + K_{SV}[Q] = 1 + K_q T_0 [Q]$ *(E)*

where, I_0 = fluorescence intensity of enzyme

I = Enzyme fluorescence intensity in the presence of the metal complex

K_{SV} = Stern-Volmer quenching constant

[Q] = Concentration of quencher (metal complex)

K_q = bimolecular quenching rate constant of enzyme

τ_0 = average lifetime of the biomolecules in absence of quencher.

The K_{SV} values were obtained from the slope of the graph I_0/ I *vs* [Q]. Quenching rate constant $K_q = K_{SV} / \tau_0$ ($\tau_0 = 10^{-8}$, average lifetime of PTP-1B without quencher). The double logarithmic plots between Log [Q] *vs* Log $(I_0-I)/I$ was used to obtain binding

constant, Log K_b (*y* intercept) and the value of the slope is taken as the number of binding sites in enzyme.

4.3 Results and discussion

4.3.1 CT-DNA UV-Visible absorption titrations

To assess the toxicity of anti-diabetic metal-based compounds, it is imperative to gauge the tendency of the metal complexes to interact with DNA, see **Figs.** 4.1 – 4.4.[19] Therefore, the propensities of the metal complexes to form adducts with CT-DNA were monitored. Common UV-Vis spectral trends for metallo-intercalators were monitored. The hypochromic spectral changes were observed for **1**, **3** and **4**. In contrast, compound **2**'s *pi to pi** intra-ligand transition undergoes hypochromism accompanied with a well-defined isosbestic point indicating a single binding mode. The level of hypochromism is generally correlated to the strength of binding interaction.[20] The spectral changes of **1 - 4**, upon gradual increments of CT-DNA, affirm that they interact with CT-DNA *via* stacking between their corresponding aromatic chromophores and the DNA base pairs. The intrinsic binding constants (K_b) values obtained for complexes **1 - 4** were 8×10^3 M^{-1}, 4.3×10^3 M^{-1}, 3×10^3 M^{-1} and 1.3×10^2 M^{-1}, respectively. Consequently, the lower K_b values of **1** and **2** than other cytotoxic metal-based DNA intercalators ($K_b > 10^6$ M^{-1}) could justify their low *in vitro* and *in vivo* toxicities, respectively.[21-23]

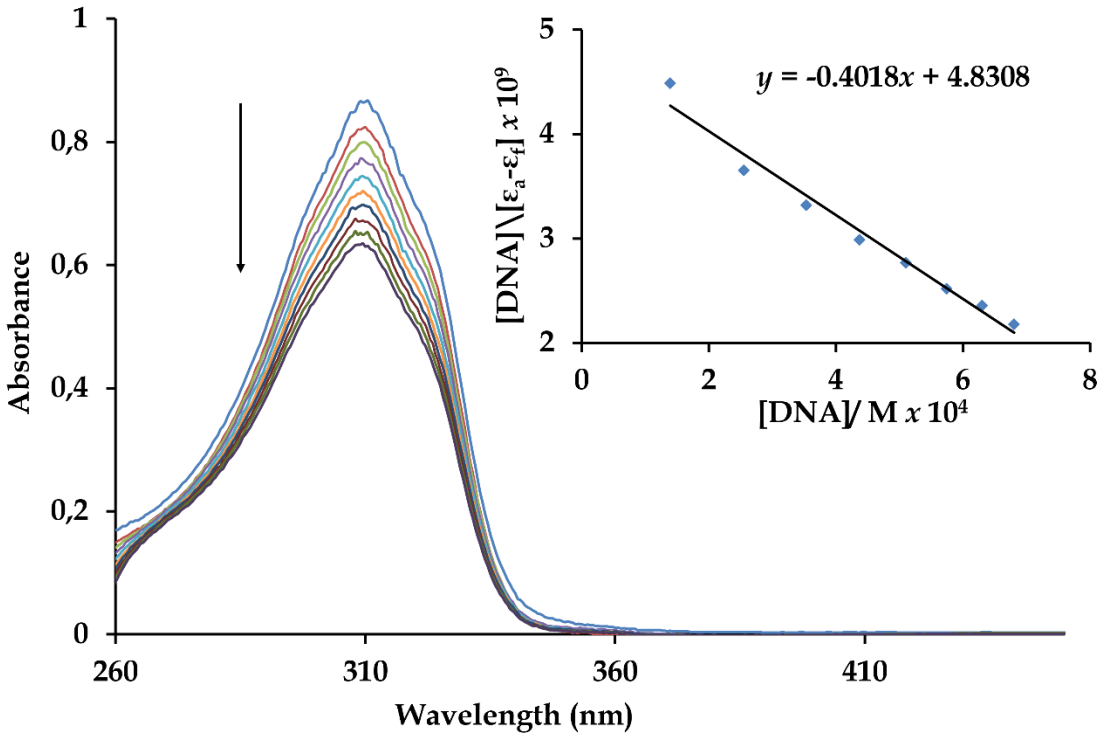

Figure 4.1: *Absorption spectra of cis-[VO_2(Hpybz)(pybz)] (**1**) in PBS buffer upon addition of 0.05 µM calf thymus DNA. Arrow shows the absorbance change upon increasing DNA concentrations.* **The insert** *is the respective [DNA]/(εa - εf) vs. [DNA] plot. Binding constant K_b = 4 x 10^6 M^{-1}. (R = 0.9903 for 8 points).*

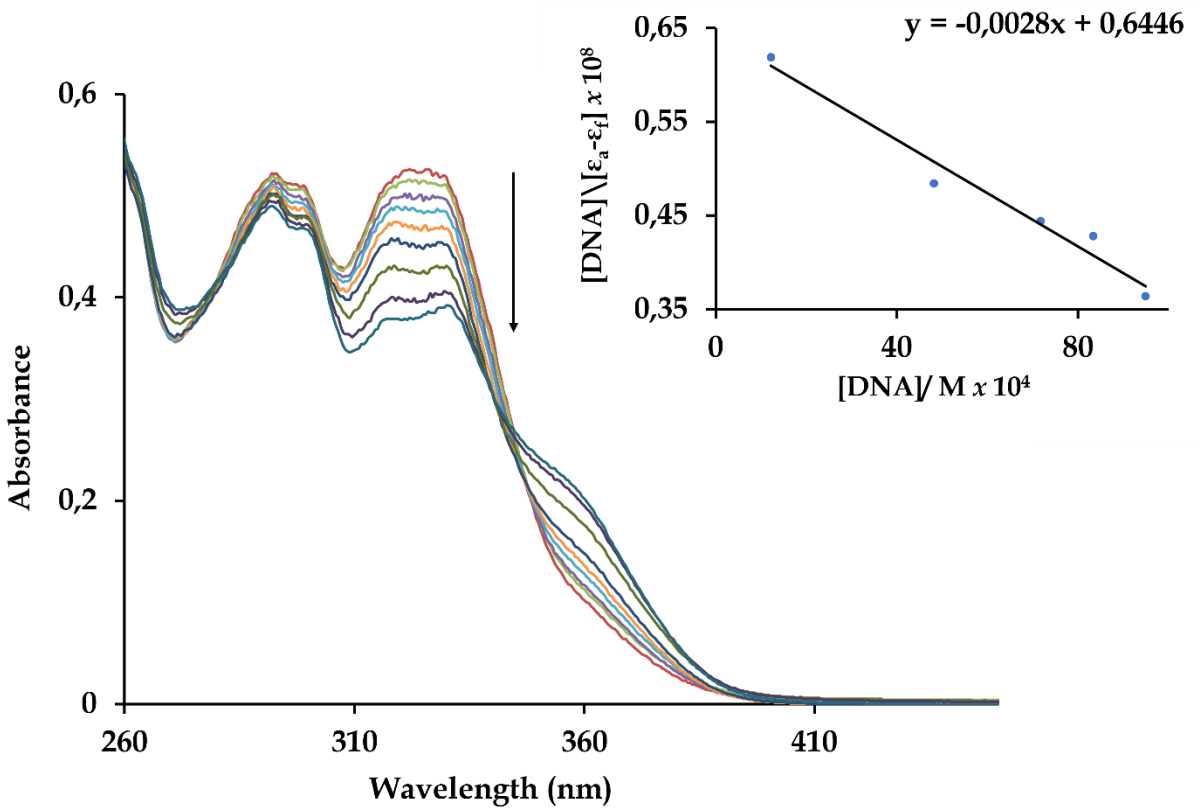

Figure 4.2: *Absorption spectra of cis-[VO_2(obz)py] (**2**) in PBS buffer upon addition of calf thymus DNA. The arrow shows the absorbance change upon increasing DNA concentrations.*

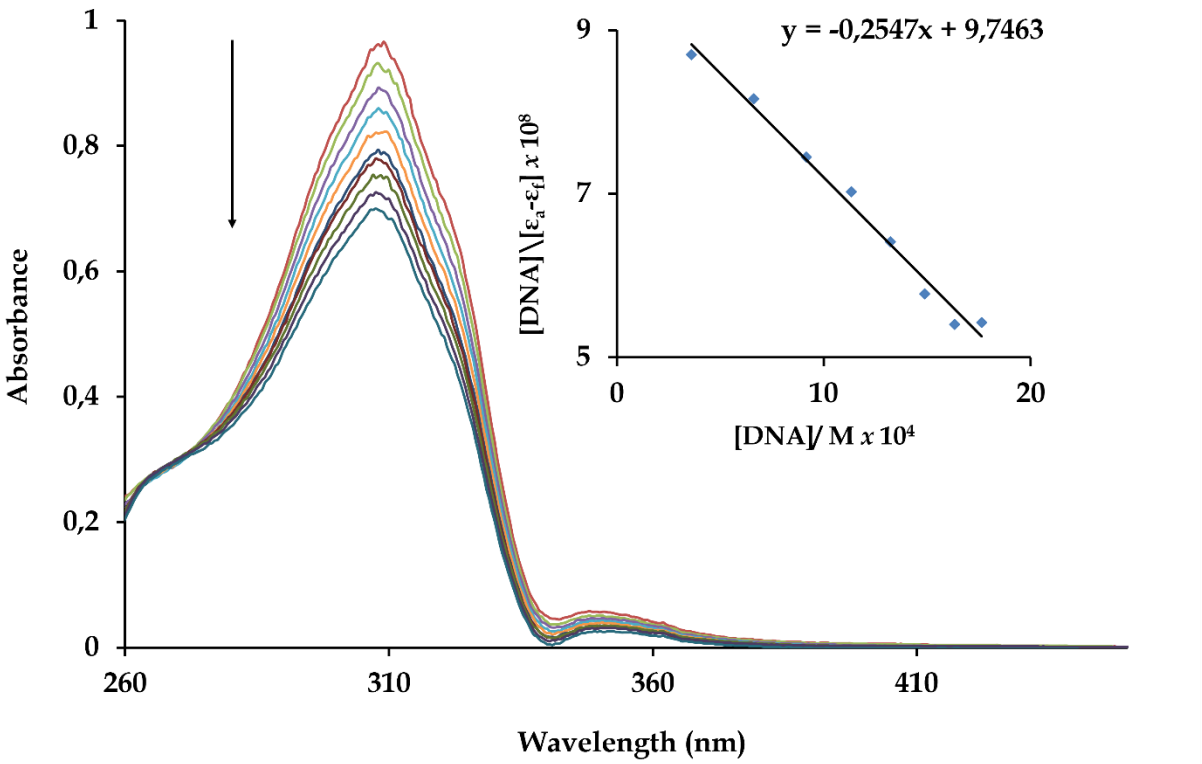

Figure 4.3: *Absorption spectra of cis-[VO_2(Hmpybz)(mpybz)] (**3**) in PBS buffer upon addition of 0.05 µM calf thymus DNA. Arrow shows the absorbance change upon increasing DNA concentrations.*

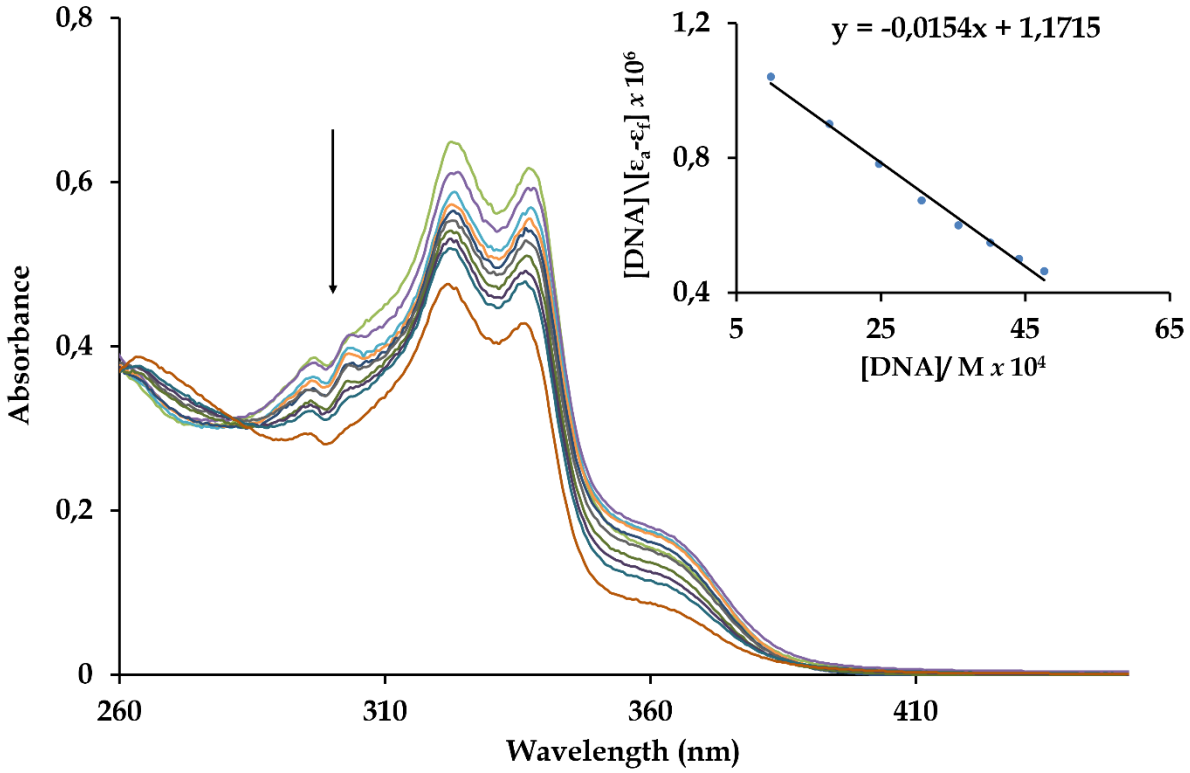

Figure 4.4: *Absorption spectra of cis-[VO_2(mobz)(py)] (**4**) in PBS buffer upon addition of 0.05 µM calf thymus DNA. Arrow shows the absorbance change upon increasing DNA concentrations.*

4.3.2. BSA emission spectroscopic titrations:

The reversible uptake and release of a drug by serum proteins such as human serum albumin (HSA) is an indicator of its capability to exhibit an optimal *in vivo* biodistribution route.[24] Bovine Serum Albumin (BSA) is often used as a credible model to assess the affinities between HAS, because of the close resemblance between the structures of two macro molecules. Metal complexes can occupy one of three domains I – III which are further subdivided into subdomains A and B. BSA-metal complex adduct formation is typically governed by the stereo-electronic properties of the metal complex.

BSA is a highly fluorescent protein due to the strong photochemical emissions of some of its tryptophan amino acids. Hence, distortion in the protein micro-environments through the binding of a metal complex is reflected by quenching of the intense BSA emission peak. To ensure limited or no degradation of **1 - 4**, the experiments were conducted with fresh solutions of metal complexes prepared in DMSO. Upon sequential additions of the respective metal complex solutions, the BSA emission band at 287 nm was gradually quenched due to the interaction of the corresponding metal complexes with the BSA protein, see **Figs.** 4.5 - 4.8. No noticeable shifts in the BSA emission bands were observed which implies that the metal complexes largely interacted with BSA through hydrophobic van der Waals bonding.[25, 26] However, well-defined isosbestic points at 302, 309, 298 and 301 nm occurring within the relating BSA titration profiles for **1 – 4**. This suggests that each metal complex adopts a single binding mode.[12] Evidentially, the number of binding sites per BSA molecule (n) were all close to 1 which were determined from equation (D).

Furthermore, K_{SV} values of the metal complexes **1 – 4** were found to be 1.76×10^5 M^{-1}, 9.3×10^4 M^{-1}, 5.3×10^4 M^{-1} and 6.0×10^4 M^{-1}, and comparable with other moderate BSA binders, refer to **Table 1**.[27-29] Also, the high quenching rate constants ($k_q > 10^{12}$ M^{-1} s^{-1}) were attained which shows that the interactions between the respective metal complexes and BSA is governed by a static mechanism. The binding constants of **1 – 4** ranges from 10^4 M^{-1} to 10^6 M^{-1} which are comparable to those of other oxidovanadium(IV) and (V) compounds with BSA: [VO(L^1)(1,10-phen)], where L^1 is [(Z)-3-((2-hydroxybenzylidene)amino)dibenzo [b,d]furan-2-ol], [$V^{IV}O(L^4)$(bipy)] (3-hydroxy-2-naphthoic hydrazide = H_2L^4) and [VO(dios)$(OH)_3$]$Na_5.6H_2O$(VOdios), where Diosmin is (3′,5,7-trihydroxy-4′-methoxyflavone 7-rutinoside) have the following K_b values 3.7×10^6 M^{-1}, 5.0×10^5 M^{-1} and $55,3 \times 10^4$ M^{-1}, respectively.[30-32]

Table 4.1. Stern-Volmer, quenching rate constant, binding constants and number of binding sites for the interactions of BSA with various dioxovanadium(V) complexes from fluorescence spectroscopy.

Metal Complex	K_{sv} (M^{-1})	K_q (M^{-1} s^{-1})	K_b (M^{-1})	n
1	1.76×10^5	3.5×10^{13}	1.7×10^6	1
2	9.3×10^4	1.9×10^{13}	9.2×10^4	1
3	5.3×10^4	1.1×10^{13}	2.4×10^4	1
4	6.0×10^4	1.2×10^{13}	6.7×10^4	1

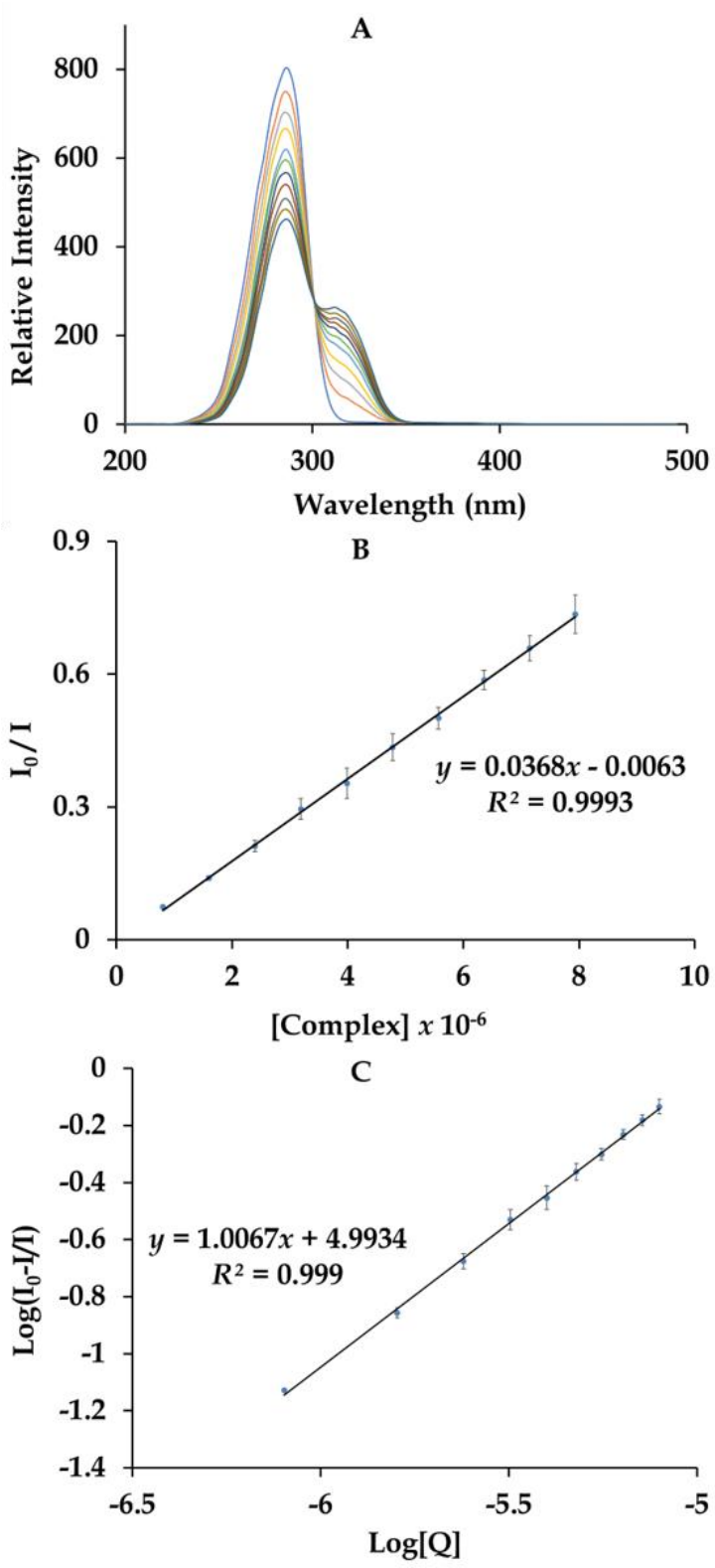

Figure 4.5: *(**A**) The fluorescence titration of BSA with cis-[VO_2(Hpybz)(pybz)] (**1**), (**B**) the corresponding Stern-Volmer plot and (**C**) the linear regression plot of Log(I_0-I/I) vs Log[complex]. The relative standard addition of each data points (n = 3) where all below 5%.*

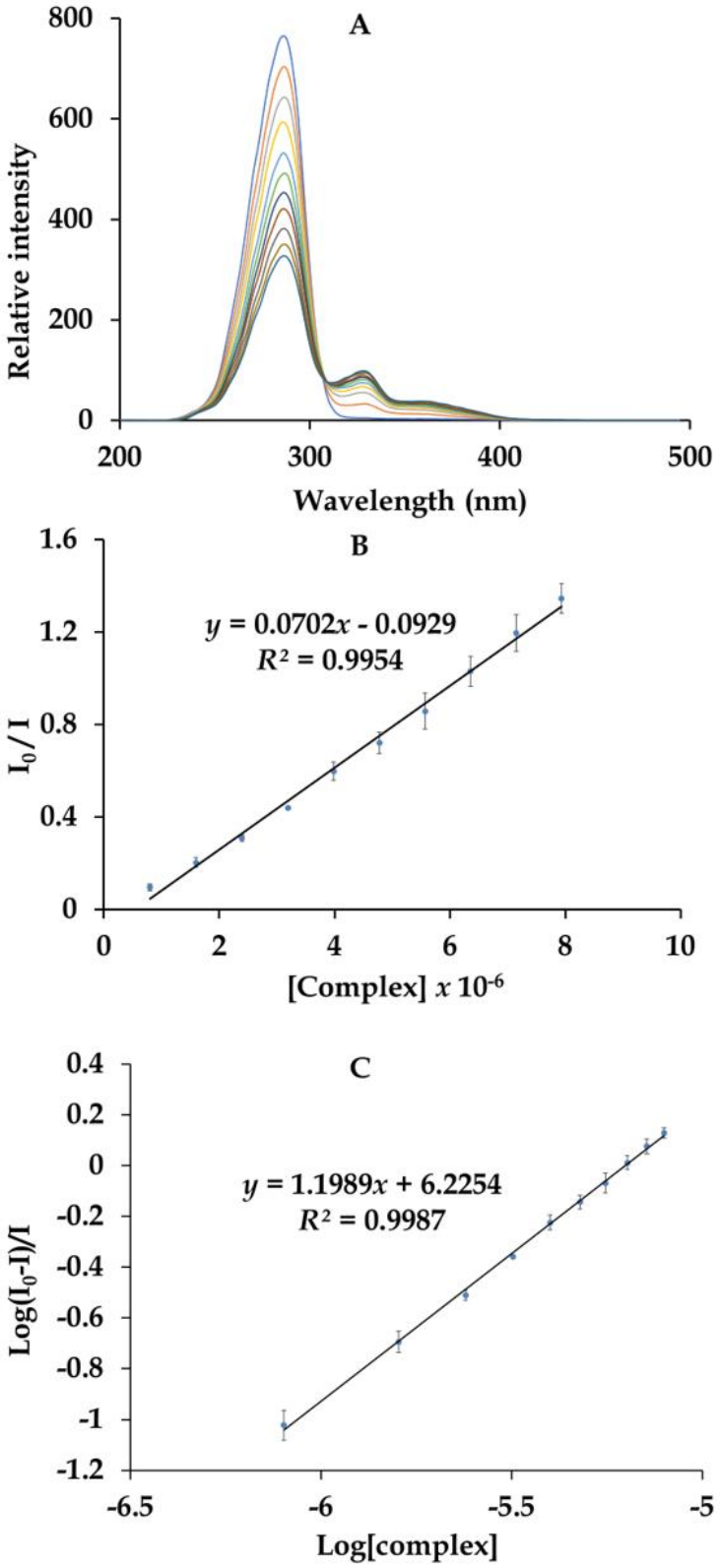

Figure 4.6: *(**A**) The fluorescence titration of BSA with cis-[VO_2(obz)(py)] (**2**), (**B**) the corresponding Stern-Volmer plot and (**C**) the linear regression plot of Log(I_0-I/I) vs Log[complex]. The relative standard addition of each data points (n = 3) where all below 5%.*

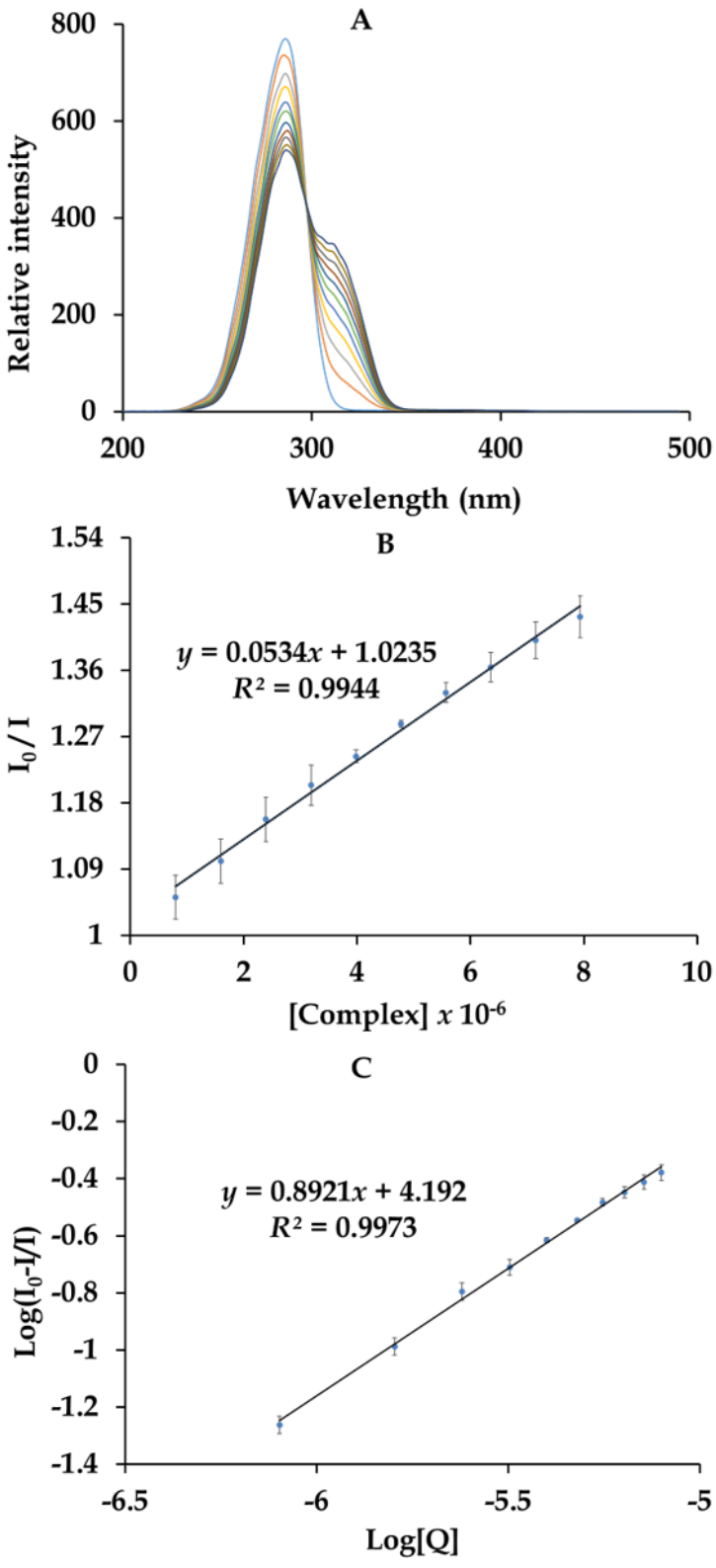

Figure 4.7: *(**A**) The fluorescence titration of BSA with cis-[VO_2(Hmpybz)(mpybz)] (**3**), (**B**) the corresponding Stern-Volmer plot and (**C**) the linear regression plot of Log(I_0-I/I) vs Log[complex]. The relative standard addition of each data points (n = 3) where all below 5%.*

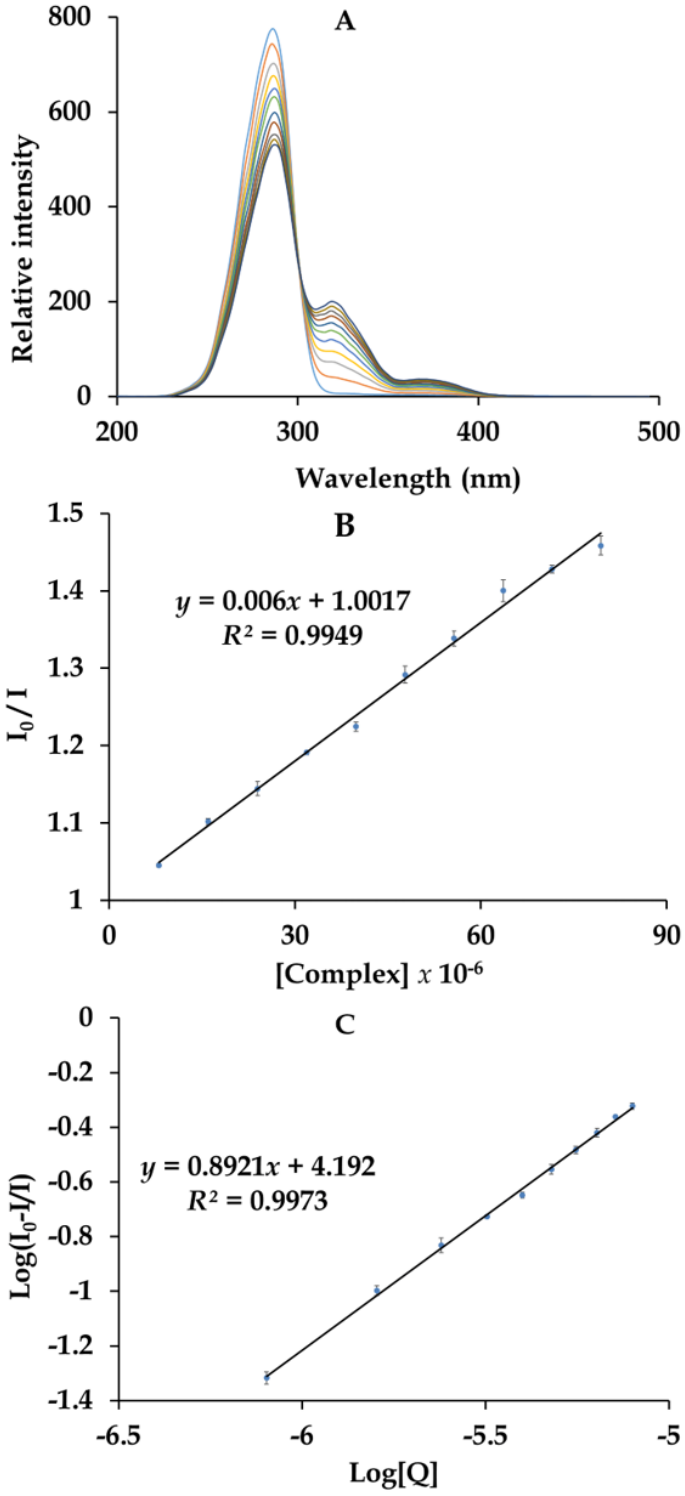

Figure 4.8: *(A) Fluorescence titration of BSA with cis-[VO_2(mobz)(py)] (**4**), (**B**) the corresponding Stern-Volmer plot and (**C**) the linear regression plot of Log(I_0-I/I) vs Log[complex]. The relative standard addition of each data points (n = 3) where all below 5%.*

4.3.3 PTP Inhibition by plate reading assay

As per declaration I – plagiarism, selected paragraph in the following subsection has been italicised and place between quotation marks as these have been prepared by our collaborator, Dr Shantal Maharaj who has a PhD in biochemistry.

"To evaluate the potential for the PTP-1B inhibition activities of the synthesized dioxidovanadium(V) benzimidazole compounds, the PTP-1B enzyme activity in HEK293T cells were analysed in response to 100 mM (post-lysis) treatment of the derivatives as well as 10 mM, 72-hour treatment of compounds ***1*** *-* ***4****. Relative to the basal activity of PTP-1B, compounds* ***2*** *and* ***4*** *proved to exhibit no significant inhibition of the enzyme activity at 100 mM whereas compounds* ***1*** *and* ***3*** *significantly decreased the enzyme activity 25% and 75% respectively, see* ***Fig. 4.9****. This suggests that the addition of the methyl groups to the derivative compound results in inhibitory activity against PTP-1B.*

The potentially active compounds ***1*** *and* ***3*** *were further investigated for their inhibitory activity against PTP-1B by measuring the activity over a range of concentrations post-lysis. Relative to the basal, compound* ***1*** *exhibited only a significant reduction in activity at 100 mM and compound* ***3*** *displayed a significant reduction in activity at the 100 mM concentration whereas both compounds displayed no significant activity at the lower concentrations. Due to post-lysis inhibition occurring at high compound concentrations, we aimed to assess whether a prolonged treatment at a lower concentration of the compounds would exhibit PTP-1B inhibitory activity. To this end, HEK293T cells were treated with compounds* ***1*** *and* ***3*** *at 10 mM for 72 hours before lysis. At a lower concentration it was discovered that compound* ***1*** *showed a significant reduction in activity (~50%) relative to the DMSO treated cells, whereas compound* ***3*** *showed no significant reduction in activity at the lower concentration. Sodium orthovanadate, a known phosphatase inhibitor was used as the positive control.*[33] *This data suggest that compound* ***1*** *has potential inhibitory activity against PTP-1B even at lower concentrations whereas a very high concentration of compound* ***3*** *is necessary for a significant reduction of PTP-1B activity."*

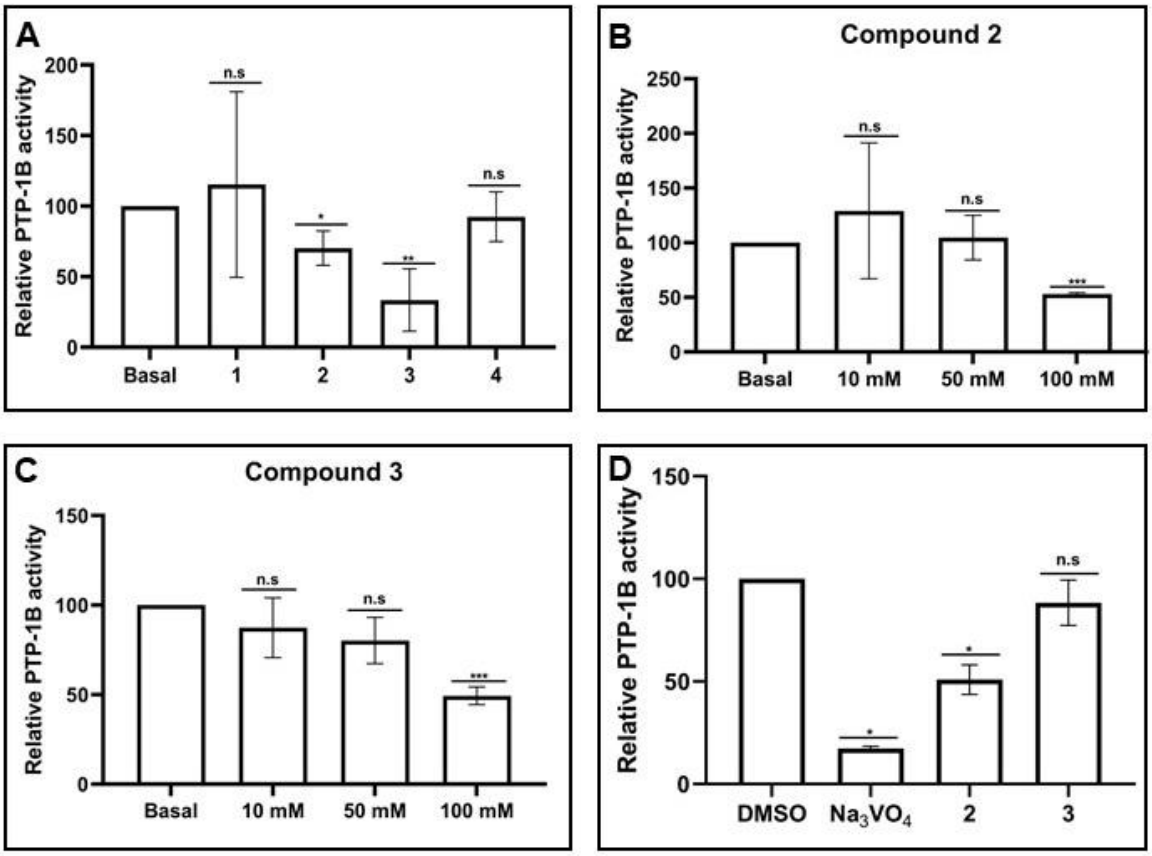

Figure 4.9: *Relative PTP1B activity assay of compounds* ***1*** *–* ***4****. Enzyme assays were carried out in HEK293T cells. (A) Compounds* ***1****-* ***4*** *at 100 mM post-lysis. (B) Compound* ***1*** *10-100 mM post-lysis (C).* ***3*** *10-100 mM post-lysis. (D) 10 mM, 72 hour treatment. Basal=untreated.* Na_3VO_4 *= sodium orthovanadate (positive control). Values are averaged. Statistical analyses carried out using students t-test. n.s=non-significant, *p-value<0.05, **p-value<0.01, ***p-value<0,001.*

Degradation rates of vanadium complexes to the active drug, vanadate is a significant factor which influence their relative *in vitro* PTP-1B inhibitory activities.[34, 35] In fact, *bis*(5,6,7-trihydroxyflavone)oxovanadium (BBOV) illustrated time dependent PTP-1B inhibitory activities where the latter increased as the metal complex degrades. Therefore, the *in vitro* inhibitory activities of **1** and **3** in contrast to the of benign **2** and **4** could be tentatively accounted to the faster degradation of the former in aqueous media as opposed to the latter. It should also be noted that longer times were used when the dioxovanadium compound **2** was administered to STZ-diabetic rats during

some reported *in vivo* studies.[21, 36-38] Although, the pharmacokinetic parameters and biodistribution of this metal complex have not been fully established, it is hypothesized that it had sufficient time to undergo hydrolysis to vanadate and this process might have been catalysed through interactions with other bio-entities.[39]

As compound **3** induced significant lowering of the *in vitro* PTP-1B enzymatic activity, its direct binding affinity towards the enzyme was determined. The tryptophan residues of the pure enzyme characteristically fluoresce at a wavelength of 284 nm. The fluorescence spectral titration profile shows combined dynamic and static quenching ($K_D K_S$ = 9.0 × 10^{-9} μM^{-1} s^{-1}) of the emission intensity as derived from the neo-quadratic plot (**Fig 4.11**) as expressed on the polynomial equation (E). Furthermore, increasing distortions of the emission band were observed which is attributed to the metal complex altering the enzyme's microenvironment upon binding.

The spectral data also indicates that the metal complex adopts a single binding mode since the number of binding sites (n = 0.7938) is approaching unity. Furthermore, the PTP-1B binding strength (K_b = 3.9 × 10^3 M^{-1}) of **3** are essentially half of those reported for other octahedral oxidovanadium(IV) compounds with K_b values in the order of 10^6 M^{-1}.[40] This comparative analysis suggests that **3** is a moderate binder but the pharmacokinetics of the metal complexes have not been considered.

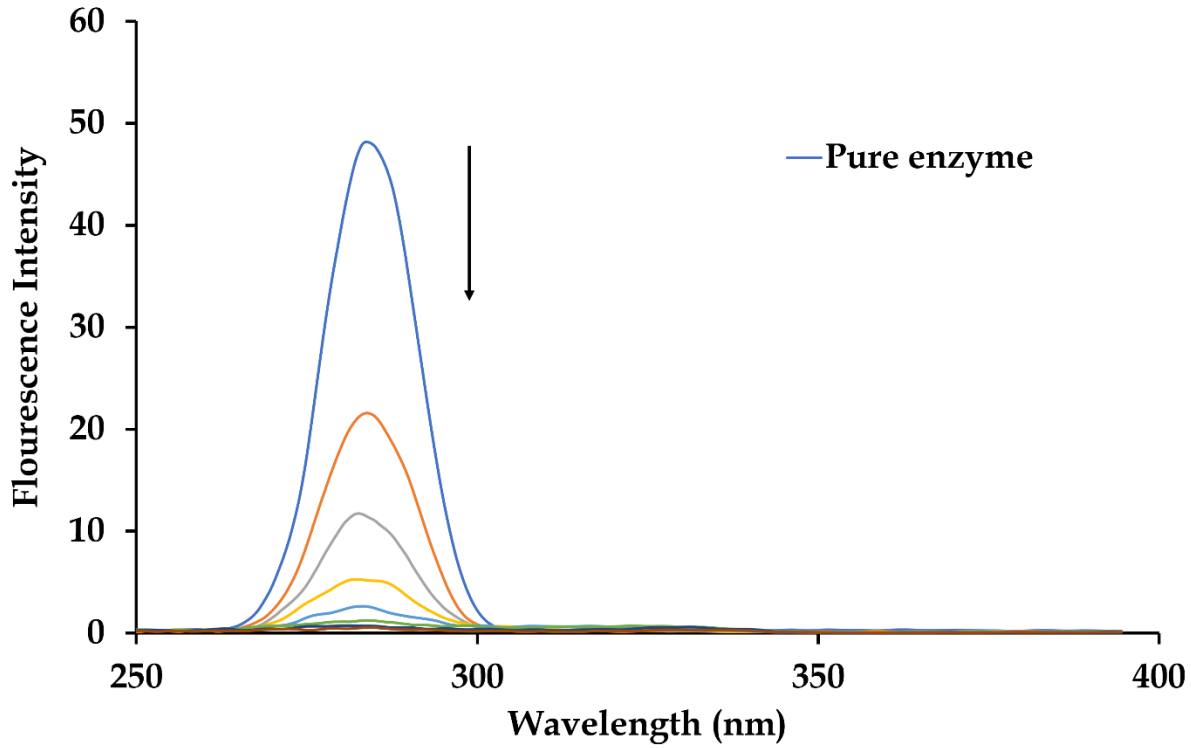

Figure 4.10: *Fluorescence emission spectra of PTP-1B in the absence and presence of different concentrations of cis-[VO_2(Hmpybz)(mpybz)] (**3**).*

Table 2. *The various parameters associated with the interactions of PTP-1B with compound **3** obtained from fluorescence spectroscopy.*

Metal Complex	K_{sv} (M^{-1})	K_q (M^{-1} s^{-1})	K_b (M^{-1})	n
3	9.0×10^4	9.0×10^{12}	3.9×10^3	0.7938

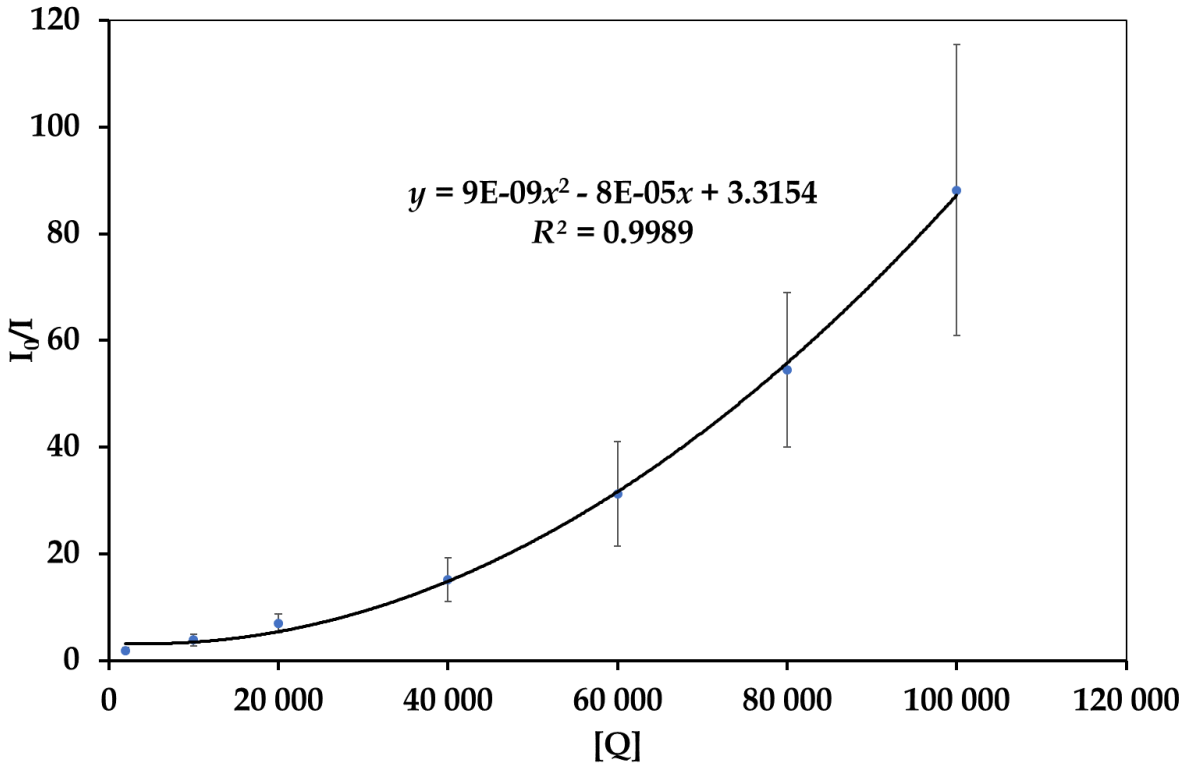

Figure 4.11: *Stern-Volmer curve for the binding of cis-[VO_2(Hmpybz)(mpybz)] (**3**) onto PTP-1B.*

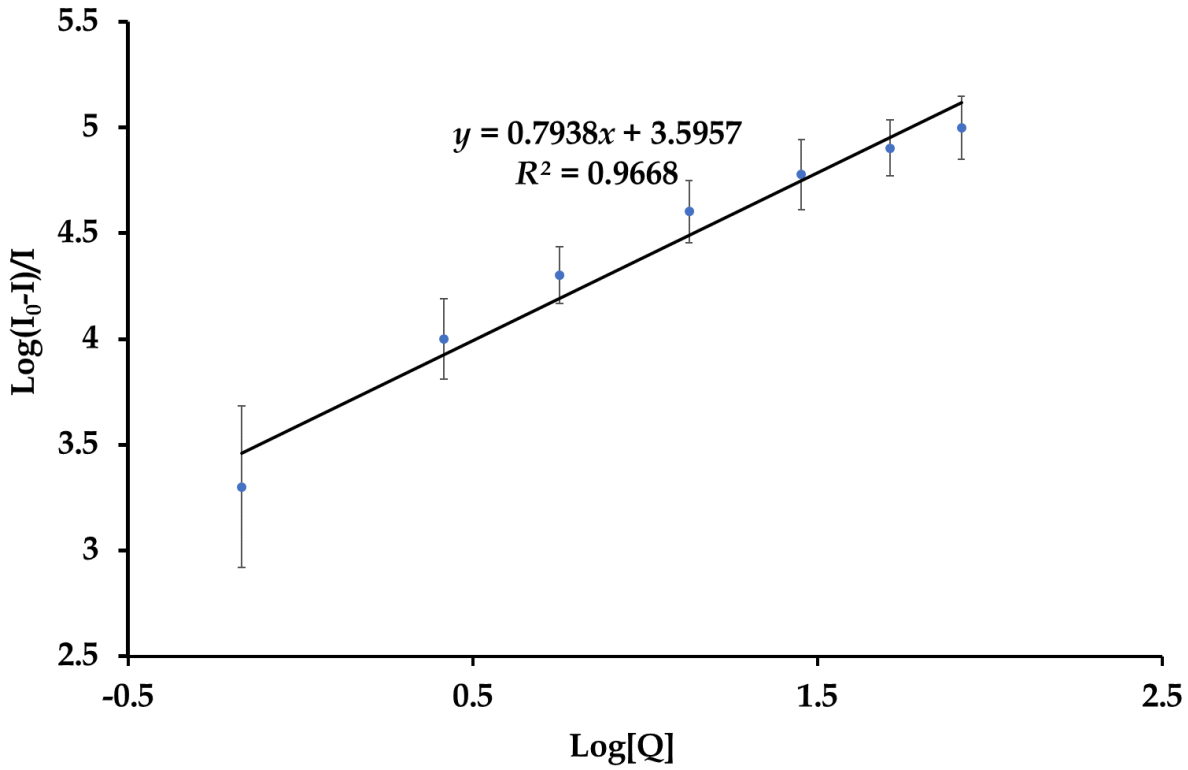

Figure 4.12: *The double logarithmic plots for the binding of cis-[VO_2(Hmpybz)(mpybz)] (**4**) on to PTP-1B.*

"4.3.4 In vitro glucose metabolism

As per declaration I – plagiarism, the following subsection has been italicised and place between quotation marks as it has been prepared by our collaborator, Dr Shantal Maharaj who has a PhD in biochemistry.

*As we observed a potential reduction in PTP-1B activity upon treatment with compounds **1** and **3**, we sought to enquire whether these compounds will have a likely impact on glycolytic flux. To this end, the level of lacate production as well as glucose consumption in HEK293T cells were measured. The lactate assays displayed a ~90% reduction in lactate production upon treatment with the positive control Na_3VO_4. There is also a significant reduction in the lactate production upon treatment with both compounds **1** (~50%) and **3** (~50%) see, **Fig. 4.13**. The glucose assays revealed a four-fold increase in the glucose consumption upon treatment with the Na_3VO_4 positive control, whereas there was no significant change in the glucose consumption upon treatment with the dioxidovanadium(V) compounds, see, **Fig. 4.13**. Overall, this data suggest that compounds **1** and **3** inhibit the rate of glycolysis based on the*

rate of lactate being produced. The glucose consumption assays also reveal that via the potential inhibition of PTP-1B, glucose turnover is increased in HEK293T cells.

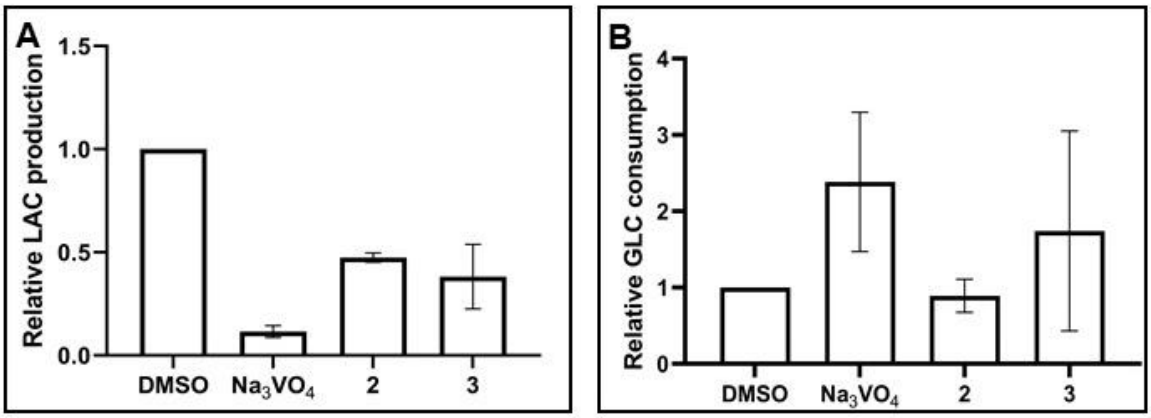

Figure 4.13*: Glycolytic flux assays in response to PTP1B inhibition. Flux assays were carried out in HEK293T cells. (A) Relative lactate production in response to 10mM of compounds **1** and **3**. (B) Relative glucose consumption in response to 10 mM of compounds **1** and **3**. Na3VO4=sodium orthovanadate (positive control). Values are averaged. Statistical analyses carried out using students t-test. n.s=non-significant, *p-value<0.05, **p-value<0.01, ***p-value<0,001."*

4.4 References

1. Jakusch, T.; Kiss, T., In vitro study of the antidiabetic behavior of vanadium compounds. *Coordination Chemistry Reviews* **2017,** *351*, 118-126.
2. Del Carpio, E.; Hernández, L.; Ciangherotti, C.; Coa, V. V.; Jiménez, L.; Lubes, V.; Lubes, G., Vanadium: History, chemistry, interactions with α-amino acids and potential therapeutic applications. *Coordination Chemistry Reviews* **2018,** *372*, 117-140.
3. Thompson, K. H.; Lichter, J.; LeBel, C.; Scaife, M. C.; McNeill, J. H.; Orvig, C., Vanadium treatment of type 2 diabetes: a view to the future. *Journal of Inorganic Biochemistry* **2009,** *103* (4), 554-558.
4. Gundhla, I. Z.; Walmsley, R. S.; Ugirinema, V.; Mnonopi, N. O.; Hosten, E.; Betz, R.; Frost, C. L.; Tshentu, Z. R., pH-metric chemical speciation modeling and studies of in vitro antidiabetic effects of bis [(imidazolyl) carboxylato] oxidovanadium (IV) complexes. *Journal of Inorganic Biochemistry* **2015,** *145*, 11-18.
5. Lima, L. M.; Belian, M. F.; Silva, W. E.; Postal, K.; Kostenkova, K.; Crans, D. C.; Rossiter, A. K. F.; da Silva Júnior, V. A., Vanadium(IV)-diamine complex with hypoglycemic activity and a reduction in testicular atrophy. *Journal of Inorganic Biochemistry* **2021,** *216*, 111312.
6. Li, M.; Ding, W.; Baruah, B.; Crans, D. C.; Wang, R., Inhibition of protein tyrosine phosphatase 1B and alkaline phosphatase by bis (maltolato) oxovanadium (IV). *Journal of Inorganic Biochemistry* **2008,** *102* (10), 1846-1853.
7. Irving, E.; Stoker, A. W., Vanadium Compounds as PTP Inhibitors. *Molecules* **2017,** *22* (12).
8. Gramni, L.; Vukea, N.; Chakraborty, A.; Samson, W. J.; Dingle, L. M. K.; Xulu, B.; de la Mare, J.-A.; Edkins, A. L.; Booysen, I. N., Anticancer evaluation of ruthenium(III) complexes with N-donor ligands tethered to coumarin or uracil moieties. *Inorganica Chimica Acta* **2019,** *492*, 98-107.
9. Karami, K.; Mehri Lighvan, Z.; Farrokhpour, H.; Dehdashti Jahromi, M.; Momtazi-borojeni, A. A., Synthesis and spectroscopic characterization study of new palladium complexes containing bioactive O, O-chelated ligands: evaluation of the DNA/protein BSA interaction, in vitro antitumoural activity and molecular docking. *Journal of Biomolecular Structure and Dynamics* **2018,** *36* (13), 3324-3340.
10. Maikoo, S.; Chakraborty, A.; Vukea, N.; Dingle, L. M. K.; Samson, W. J.; de la Mare, J.-A.; Edkins, A. L.; Booysen, I. N., Ruthenium complexes with mono-or bis-heterocyclic chelates: DNA/BSA binding, antioxidant and anticancer studies. *Journal of Biomolecular Structure and Dynamics* **2020**, 1-12.
11. Kondaparthy, V.; Shaik, A.; Reddy, K. B.; Manwal, D. D., Studies on interaction of vanadium metal complexes with bovine serum albumin-Fluoremetric and UV–visible spectrophotometric studies. *Chemical Data Collections* **2019,** *20*, 100203.
12. Maikoo, S.; Chakraborty, A.; Vukea, N.; Dingle, L. M. K.; Samson, W. J.; de la Mare, J. A.; Edkins, A. L.; Booysen, I. N., Ruthenium complexes with mono- or bis-heterocyclic chelates: DNA/BSA binding, antioxidant and anticancer studies. *J Biomol Struct Dyn* **2021,** *39* (11), 4077-4088.
13. Kielkopf, C. L.; Bauer, W.; Urbatsch, I. L., Bradford assay for determining protein concentration. *Cold Spring Harbor Protocols* **2020,** *2020* (4), pdb. prot102269.
14. Song, Y. H.; Uddin, Z.; Jin, Y. M.; Li, Z.; Curtis-Long, M. J.; Kim, K. D.; Cho, J. K.; Park, K. H., Inhibition of protein tyrosine phosphatase (PTP1B) and α-

glucosidase by geranylated flavonoids from Paulownia tomentosa. *Journal of Enzyme Inhibition and Medicinal Chemistry* **2017,** *32* (1), 1195-1202.
15. Fang, L.; Cao, J.; Duan, L.; Tang, Y.; Zhao, Y., Protein tyrosine phosphatase 1B (PTP1B) and α-glucosidase inhibitory activities of Schisandra chinensis (Turcz.) Baill. *Journal of Functional Foods* **2014,** *9*, 264-270.
16. van Ameijde, J.; Overvoorde, J.; Knapp, S.; den Hertog, J.; Ruijtenbeek, R.; Liskamp, R. M., A versatile spectrophotometric protein tyrosine phosphatase assay based on 3-nitrophosphotyrosine containing substrates. *Analytical Biochemistry* **2014,** *448*, 9-13.
17. Yuan, C.; Lu, L.; Gao, X.; Wu, Y.; Guo, M.; Li, Y.; Fu, X.; Zhu, M., Ternary oxovanadium(IV) complexes of ONO-donor Schiff base and polypyridyl derivatives as protein tyrosine phosphatase inhibitors: synthesis, characterization, and biological activities. *JBIC Journal of Biological Inorganic Chemistry* **2009,** *14* (6), 841-851.
18. Ma, L.; Lu, L.; Zhu, M.; Wang, Q.; Li, Y.; Xing, S.; Fu, X.; Gao, Z.; Dong, Y., Mononuclear copper(II) complexes with 3, 5-substituted-4-salicylidene-amino-3, 5-dimethyl-1, 2, 4-triazole: synthesis, structure and potent inhibition of protein tyrosine phosphatases. *Dalton Transactions* **2011,** *40* (24), 6532-6540.
19. Adam, M. S. S.; Elsawy, H., Biological potential of oxo-vanadium salicylediene amino-acid complexes as cytotoxic, antimicrobial, antioxidant and DNA interaction. *Journal of Photochemistry and Photobiology B: Biology* **2018,** *184*, 34-43.
20. Lu, J.; Guo, H.; Zeng, X.; Zhang, Y.; Zhao, P.; Jiang, J.; Zang, L., Synthesis and characterization of unsymmetrical oxidovanadium complexes: DNA-binding, cleavage studies and antitumor activities. *Journal of Inorganic Biochemistry* **2012,** *112*, 39-48.
21. Xulu, N.; Ngubane, P.; Khathi, A.; Booysen, I.; Sibiya, N., Heamanetic Effects of a Dioxidovanadium (V) Complex in STZ-Induced Diabetic Male Sprague Dawley Rats. *Diabetes, Metabolic Syndrome and Obesity: Targets and Therapy* **2021,** *14*, 4321.
22. Mbatha, B.; Khathi, A.; Sibiya, N.; Booysen, I.; Mangundu, P.; Ngubane, P., Cardio-protective effects of a dioxidovanadium(V) complex in male sprague–dawley rats with streptozotocin-induced diabetes. *BioMetals* **2021,** *34* (1), 161-173.
23. Jarman, P. J.; Noakes, F.; Fairbanks, S.; Smitten, K.; Griffiths, I. K.; Saeed, H. K.; Thomas, J. A.; Smythe, C., Exploring the Cytotoxicity, Uptake, Cellular Response, and Proteomics of Mono- and Dinuclear DNA Light-Switch Complexes. *J Am Chem Soc* **2019,** *141* (7), 2925-2937.
24. Chubarov, A.; Spitsyna, A.; Krumkacheva, O.; Mitin, D.; Suvorov, D.; Tormyshev, V.; Fedin, M.; Bowman, M. K.; Bagryanskaya, E., Reversible Dimerization of Human Serum Albumin. *Molecules* **2020,** *26* (1).
25. Ali, M. S.; Muthukumaran, J.; Al-Lohedan, H. A., Molecular interactions of ceftazidime with bovine serum albumin: Spectroscopic, molecular docking, and DFT analyses. *Journal of Molecular Liquids* **2020,** *313*.
26. Feizi-Dehnayebi, M.; Dehghanian, E.; Mansouri-Torshizi, H., A novel palladium(II) antitumor agent: Synthesis, characterization, DFT perspective, CT-DNA and BSA interaction studies via in-vitro and in-silico approaches. *Spectrochim Acta A Mol Biomol Spectrosc* **2021,** *249*, 119215.

27. Zhai, S.; Guo, Q.; Dong, J.; Xu, T.; Li, L., An oxovanadium (IV) complex of an l-serine Schiff base and 1, 10-phenanthroline: synthesis, crystal structure, and DNA and albumin-binding properties. *Transition Metal Chemistry* **2014,** *39* (3), 271-280.
28. Islas, M. S.; Naso, L. G.; Lezama, L.; Valcarcel, M.; Salado, C.; Roura-Ferrer, M.; Ferrer, E. G.; Williams, P. A., Insights into the mechanisms underlying the antitumor activity of an oxidovanadium(IV) compound with the antioxidant naringenin. Albumin binding studies. *Journal of Inorganic Biochemistry* **2015,** *149*, 12-24.
29. Kondaparthy, V.; Shaik, A.; Reddy, K. B.; Manwal, D. D., Studies on interaction of vanadium metal complexes with bovine serum albumin - Fluoremetric and UV–visible spectrophotometric studies. *Chemical Data Collections* 20 (**2019**) 100203.
30. Majumder, M.; Das, T.; Sepay, N.; Rajak, K. K., A study of DNA/BSA interaction and catalytic potential of oxidovanadium(V, IV) complexes incorporating dibenzofuran based O^ N^ O ligand. *Journal of Organometallic Chemistry* **2021**, 122244.
31. Banerjee, A.; Dash, S. P.; Mohanty, M.; Sanna, D.; Sciortino, G.; Ugone, V.; Garribba, E.; Reuter, H.; Kaminsky, W.; Dinda, R., Chemistry of mixed-ligand oxidovanadium(IV) complexes of aroylhydrazones incorporating quinoline derivatives: Study of solution behavior, theoretical evaluation and protein/DNA interaction. *J Inorg Biochem* **2019,** *199*, 110786.
32. Naso, L.; Martinez, V. R.; Lezama, L.; Salado, C.; Valcarcel, M.; Ferrer, E. G.; Williams, P. A. M., Antioxidant, anticancer activities and mechanistic studies of the flavone glycoside diosmin and its oxidovanadium(IV) complex. Interactions with bovine serum albumin. *Bioorg Med Chem* **2016,** *24* (18), 4108-4119.
33. Gordon, J. A., [41] Use of vanadate as protein-phosphotyrosine phosphatase inhibitor. *Methods in Enzymology* **1991,** *201*, 477-482.
34. Scibior, A.; Pietrzyk, L.; Plewa, Z.; Skiba, A., Vanadium: Risks and possible benefits in the light of a comprehensive overview of its pharmacotoxicological mechanisms and multi-applications with a summary of further research trends. *J Trace Elem Med Biol* **2020,** *61*, 126508.
35. Duan, L.; Ye, J.; Sun, W.; Wang, S.; Gong, W.-t.; Dong, Y.; Ning, G., A novel PTP1b inhibitor vanadium-flavone complex: synthesis and pharmacodynamic evaluation in streptozotocin-induced diabetic mice. *Medicinal Chemistry Research* **2017,** *26* (9), 1863-1870.
36. Sibiya, S.; Msibi, B.; Khathi, A.; Sibiya, N.; Booysen, I.; Ngubane, P., The effect of dioxidovanadium complex(V) on hepatic function in streptozotocin-induced diabetic rats. *Canadian Journal of Physiology and Pharmacology* **2019,** *97* (12), 1169-1175.
37. Trevino, S.; Diaz, A.; Sanchez-Lara, E.; Sanchez-Gaytan, B. L.; Perez-Aguilar, J. M.; Gonzalez-Vergara, E., Vanadium in Biological Action: Chemical, Pharmacological Aspects, and Metabolic Implications in Diabetes Mellitus. *Biol Trace Elem Res* **2019,** *188* (1), 68-98.
38. Trevino, S.; Diaz, A., Vanadium and insulin: Partners in metabolic regulation. *J Inorg Biochem* **2020,** *208*, 111094.
39. Pessoa, J. C.; Santos, M. F.; Correia, I.; Sanna, D.; Sciortino, G.; Garribba, E., Binding of vanadium ions and complexes to proteins and enzymes in aqueous solution. *Coordination Chemistry Reviews* **2021,** *449*, 214192.
40. Shaik, A.; Kondaparthy, V.; Aveli, R.; Vijjulatha, M.; Kanth, S. S.; Manwal, D. D., Interaction of vanadium metal complexes with protein tyrosine phosphatase-1B

enzyme along with identification of active site of enzyme by molecular modeling. *Inorganic Chemistry Communications* **2021,** *126*, 108499.

Chapter 5

Conclusion and future work

5.1 Conclusion

The introductory chapter highlights the importance of the fundamental coordination chemistry of dioxidovanadium compounds in relation to its applied bio-inorganic chemistry in Diabetes Mellitus therapy. In addition, the main research objective of the research study is introduced and appropriately motivated with relevant literature. An emphasizes was also placed to gain an enhanced understanding on how this series of diamagnetic vanadium(V) benzimidazole compounds can act as insulin-enhancing agents.

In chapter 3 of this report the synthesis and spectra of *cis*-[VO_2(Hpybz)(pybz)] (**1**) and *cis*-[VO_2(obz)py] (**2**) is discussed. Spectral characterization data of *cis*-[VO_2(Hmpybz)(mpybz)]py (**3**) and *cis*-[VO_2(mobz)py] (**4**), including their single crystal X-ray and elemental analyses is described and discussed. The two dioxovanadium(V) were synthesized from respective methods described for *cis*-[VO_2(Hpybz)(pybz)]py (**1**) and *cis*-[VO_2(obz)py] (**2**).[1, 2] The coordination modes of the bidentate heterocyclic chelators of **3** and **4** were identical to the chelating benzimidazoles of the corresponding complexes **1** and **2**.

In chapter 4, CT-DNA was titrated with complexes, **1 - 4**, and the non-covalent interactions were monitored using UV-Vis spectrophotometry. The titration spectral data revealed that these metal complexes exhibit low binding affinities toward CT-DNA with intrinsic binding constants (Kb) in the order 10^3 M^{-1}. Emission spectroscopic titration data for the BSA with complexes **1-4** gave calculated apparent association constants and quenching constants (K_a and K_{SV} > 10^6 M^{-1}) were attained. The respective monomeric compounds occupy one binding site each, which are regarded as strong BSA binders as the K_{SV} and K_b values are higher than 10^4 M^{-1}.

The binding strengths of the individual metal complexes were evaluated towards one of the key enzyme, Protein Tyrosine Phosphate (PTP)-1B which is involved in insulin production. The *in vitro* inhibitory activities of 1 and 4 were classed as non-significant since they afforded relatively low PTP-1B inhibitory activities relative to the untreated enzyme (viz. Basal). Compounds **2** and **3** showed significant PTP-1B inhibition activity when compared to the Basal. However, compound **3** exhibited the most significant lowering of the in vitro PTP-1B enzymatic activity with binding strength ($Kb = 3.9 \times 10^3\ M^{-1}$) and affinity ($Ksv = 9.0 \times 10^4\ M^{-1}$). Glycolytic flux assays affirmed that the compounds **2** and **3** supresses the rate of glycolysis which can directly be related to the lactate production. In addition, the glucose consumption assays also reveal that, via the potential inhibition of PTP-1B, glucose turnover is increased in HEK293T cells

5.2 Future work

Intravenous injections of aqueous solutions of these drug candidates can be regarded as tedious and uncomfortable oppose to oral-administration and transdermal patches, which offer more facile administration of drugs.[3] Future work will entail the fabrication of bio-degradable electrospun nanofibers of four vanadium benzimidazole complexes *via* electrospinning. These nanoconjugates will be characterized by electron microscopy and powder X-ray diffraction while the mechanical properties will be investigated using thermal analysis techniques. Dissolution kinetics will be evaluated with the aid of UV-Vis spectrophotometry and photoluminescence methods.

5.3 References

1. Booysen, I. N.; Hlela, T.; Gerber, T. I.; Munro, O. Q.; Akerman, M. P., Novel vanadium compounds with 2-pyridylbenzimidazole. *Polyhedron* **2013,** *53*, 8-14.
2. Booysen, I. N.; Hlela, T.; Akerman, M. P.; Xulu, B., Mono-and polynuclear vanadium (IV) and-(V) compounds with 2-substituted phenyl/pyridyl heterocyclic chelates. *Polyhedron* **2015,** *85*, 144-150.
3. Thakkar, S.; Misra, M., Electrospun polymeric nanofibers: New horizons in drug delivery. *European Journal of Pharmaceutical Sciences* **2017,** *107*, 148-167.